N73-31498

WANL-M-FR-72-005

FEBRUARY, 1973

CASE FILE COPY

FINAL REPORT

MECHANICAL PROPERTY DETERMINATION OF HIGH CONDUCTIVITY METALS AND ALLOYS

BY

D. L. HARROD, E. VANDERGRIFT, AND L. FRANCE

WESTINGHOUSE ASTRONUCLEAR LABORATORY

CONTRACT NAS 7-725

prepared for

NATIONAL AERONAUTICS AND SPACE ADMINISTRATION

NASA PASADENA OFFICE

PASADENA, CALIFORNIA

W. B. POWELL, TECHNICAL MANAGER LIQUID PROPULSION,

JET PROPULSION LABORATORIES

Request for copies of this report should be referred to

National Aeronautics and Space Administration
Scientific and Technical Information Facility
P. O. Box 33
College Park, Maryland 20740

FOREWORD

The work described herein was done at the Astronuclear Laboratory, Westinghouse Electric Corporation, under NASA Contract NAS 7-725 with the NASA Pasadena Office. The Technical Manager for the contract was Mr. Walter B. Powell, Member of the Technical Staff, Liquid Propulsion Section, Jet Propulsion Laboratories, California Institute of Technology.

TABLE OF CONTENTS

TABLE OF CONTENTS (Continued)

LIST OF ILLUSTRATIONS

LIST OF ILLUSTRATIONS (Continued)

LIST OF ILLUSTRATIONS (Continued)

ABSTRACT

Pertinent mechanical properties of three high conductivity metals and alloys; namely, vacuum hot pressed grade S-200E beryllium, OFHC copper and beryllium-copper alloy No. 10 were determined. These materials were selected based on their possible use in rocket thrust chamber and nozzle hardware. They were procured in a form and condition similar to that which might be ordered for actual hardware fabrication.

The mechanical properties measured include (1) tension and compression stress strain curves at constant strain rate, (2) tensile and compressive creep, (3) tensile and compressive stress-relaxation behavior and (4) elastic properties. Tests were conducted over the temperature range of from 75°F to 1600°F. The resulting data is presented in both graphical and tabular form.

1.0 INTRODUCTION

Rocket thrust chambers and nozzles are subjected to transient and steady state stress distributions during firing and usually residual stresses following shutdown. The stress analysis of this problem requires a knowledge of the time dependent creep and stress relaxation properties of the chamber-nozzle material, as well as the stress-strain behavior in the elastic and plastic ranges of deformation - all as a function of temperature throughout the operating temperature range. In support of the stress analysis program, the present program was initiated to measure the desired mechanical properties on select candidate thrust chamber-nozzle materials.

Three materials were studied: (1) beryllium, (2) copper and (3) a beryllium-copper alloy.

The mechanical properties measured included (1) stress-strain curves at constant strain rate, (2) creep, (3) stress relaxation, and (4) elastic properties. For each type of property, tests were run in both tension and compression at temperatures ranging from room temperature to 1600°F.

The materials are characterized in Section 2. In Section 3, the experimental techniques are described and the test results are summarized in graphical form in Section 4. Tabulations of the data are given in the Appendices. Section 5 presents a general discussion of the experimental data.

2.0 MATERIALS

The intent in purchasing the test materials was to obtain each of them in a form and condition similar to what might be ordered for the actual fabrication of a rocket thrust chamber and nozzle.

2.1 Beryllium

The beryllium was purchased from the Brush Beryllium Co. as Grade S-200-E, Type II. This is a vacuum hot pressed powder metallurgy product. It was obtained in the form of a rectangular block measuring 5" x 5 5/8" x 15" which was cut out of a much larger pressing as shown by the sketch in Figure 1.

The vendor test report gave the following information:

- Lot No. 6044
- Density: 1.85 g/cc
- Composition: (wt/%)

Be	-	98.8 (Assay)
BeO	-	1.5
C	-	0.07
Fe	-	0.10
Al	-	0.05
Mg	-	0.04
Si	-	0.04
Mn	-	0.01
Other Metallics	-	0.04 max. each

- Radiographic Inspection per MIL-STD-453 - Acceptable
- Penetrant Inspection per MIL-I-6866 - Acceptable
- Tensile Properties (Transverse to pressing direction)

Ultimate Strength	58.0 and 57.8 ksi
0.2% Offset Yield Strength	42.8 and 43.3 ksi
% Elongation	3.2 and 2.7%

The specimens were tested in the as-received, as-hot pressed condition, i.e., they were not heat treated. It is noted that the composition of this block of S-200-E beryllium is within the composition range for so-called brake grade beryllium. In particular, the iron to aluminum ratio is high, being 2.0. Brake grade beryllium is sometimes heat treated (e.g., 72 hrs. at 1375°F) for the purpose of tieing up any free aluminum which might be present at grain boundaries as an iron-aluminum-beryllide. Because of the large size of the pressing from which the present material was taken, the cooling rate was probably slow enough to allow this reaction to go nearly to completion during cooling of the pressing.

The microstructure of the as-vacuum hot pressed material is shown in Figure 2. The average grain diameter (linear intercept) measured about 6×10^{-4} in. and was not noticeably changed by 1 hr exposures at 1600°F. The density, measured by determining the weight and volume of the dynamic modulus specimen, was 0.066 lb/in^3. The room temperature hardness measured 70 DPH for a 10 kg load.

2.2 OFHC Copper

The pure copper (certified OFHC) was obtained from AMPCO Metal, Inc. It was processed from a continuous casting measuring about 10" in diameter. The casting was 3-way hot forged in the temperature range 1500° to 1300°F and water quenched. The final as-forged size measured 5" x 5-5/8" in cross-section by 15-1/2" long.

The vendor test report gave the following information:

- Material Designation: Ampcoloy 900, Certified OFHC Copper
- Heat No. E-0313: This is the heat number supplied by American Metal, the manufacturer of the continuous casting.
- Composition: Certified to be 99.99+ %Cu; no actual chemical analysis was made.
- A room temperature tensile test run on a sample cut from the end of the forging showed these results:

Tensile Strength	31,000 psi
0.5% Offset Yield Strength	13,000 psi
% Elongation in 2"	57%

- Measured Conductivity: 99%

One end of the as-received, as-hot forged billet was macroetched to reveal the grain structure. The grain size (diameter) was estimated to vary from about 0.002 - 0.01 in. The grain structure was reasonably uniform, although it was somewhat coarser at the center and corners than at the edges at mid-face. For a hot forging of this size the grain structure looked very good.

Samples of the as-received hot forged material were annealed for 1 hour in argon at temperatures ranging from 800° to 1600°F. The grain structure was about the same for all the heat treatments and was the same as the as-hot forged material. Thus, the hot forged block was well recrystallized and the grain structure was stable with respect to 1 hour exposures up to 1600°F. Based upon these results it was decided to anneal all mechanical test specimens for 1 hour at 1000°F in an argon atmosphere to provide a definitive reference condition. The average grain size determined by the linear intercept method measured ~0.003 in.

The microstructure is shown in Figure 3. The hardness measured 60 DPH (5 kg load) and the density measured 0.322 lb/in^3 (determined by measuring the weight and volume of the dynamic modulus test specimen).

2.3 Beryllium-Copper Alloy

The beryllium-copper alloy, designated Alloy 10, was obtained from Kawecki Berylco Industries, Inc. The billet was hot forged from a 9" diameter cast ingot to a 2:1 reduction ratio in the longitudinal axis. Forging was done in air in the temperature range 1700°F (starting) to 1200°F (finishing). Following forging, the billet was solution annealed for 2 hours at 1700°F and water quenched. This was the condition of the as-received 5" x 5 5/8" x 15" billet.

The test report supplied by Kawecki Berylco contained the following information:

• Designation:	Alloy 10, Heat No. 92-218
• Composition:	0.61% Be, 2.70% Co, Bal. Cu
• Properties:	Solution Annealed Condition: 48.4 ksi Tensile Strength 30% Elongation B38 Hardness
	After Aging 3 Hrs/900°F: 102 ksi Tensile Strength 20% Elongation B92 Hardness 47.5% IACS Conductivity

This alloy is a precipitation hardenable alloy. Hence the question arose as to the optimum heat treatment for the intended application. A number of samples were heat treated to assess the microstructure and aging response and the following are results of hardness measurements:

Condition	R_B Hardness
Solution Treated 2 hrs/1700°F and water quenched (as-received)	47, 41
ST + Aged 3 hrs/900°F	97
ST + 3 hrs/900°F + 1 hr/1600°F	37
ST + 1 hr/1600°F	39

The usual heat treatment for optimum low temperature mechanical properties is to solution treat and age 3 hrs at 900°F. This gives a slightly overaged condition. The microstructure for this condition as well as that for the solution treated condition is shown in Figure 4. There is still some evidence of the as-cast structure. For the present program, the decision was made to use the standard heat treatment. Thus, the test specimens were machined from the as-received solution treated block and then aged in an argon atmosphere for 3 hrs at 900°F and furnace cooled.

Dimensional measurements were made on the dynamic modulus specimen to assess the dimensional changes due to aging that accompanied heat treatment, i.e., the dimensions of the specimen (nominally 15" long by 1" by 1" in cross section) were measured before and after aging. In both cases the specimen was housed for 24 hrs in a temperature controlled (68.1°F) instrumentation laboratory prior to making the measurements. The specimen length decreased by 0.00696 inch which gives $\Delta L/L_o$ = -0.046% contraction. Measurements made at five positions along the length gave contractions of -0.034%, -0.033%, -0.049%, -0.014% and -0.026%.

3.0 EXPERIMENTAL PROCEDURES

3.1 Test Specimens

The layout of the test specimens within the as-received block is shown in Figure 5. The same layout was used for each of the three test materials.

The tension specimen design for the copper and beryllium-copper alloy is shown in Figure 6. Figure 6a shows the constant strain rate, creep and stress relaxation specimen while Figure 6b shows the special specimen design (flat gage section) used for some of the elastic properties tests. The beryllium tension specimen design is shown in Figure 7.

The compression specimen design and the dynamic moduli specimen design were the same for all three materials and are shown in Figures 8 and 9, respectively.

The copper and beryllium copper specimens were finished-machined prior to heat treatment. To remove the slight tarnish which developed during heat treatment, the specimens were bright cleaned by immersing for ten minutes in a 25% sulfuric acid-water solution at 160°F followed by dipping for 20 seconds in a 30% nitric acid-water solution at room temperature.

The as-machined beryllium specimens were chemically etched at room temperature in a solution consisting of 250 ml deionized water, 50 g chromic acid, 35 ml phosphoric acid and 2.5 ml sulphuric acid. Three mils (0.003") per surface were removed at a rate of about 0.2 mils/min.

3.2 Elevated Temperatures

Elevated temperatures were obtained with a resistance heated nichrome wound furnace. The heating rate was generally 10 degrees per minute, with the specimen being held at test temperature for 20 minutes to assure thermal stability prior to loading. Three chromel-alumel thermocouples were tied to the gage length of each sample to monitor temperatures. Temperature control during the test was $\pm 2^{\circ}$F with a maximum gradient over the gage length of $\pm 4^{\circ}$F.

An inert gas environment was used in all elevated temperature tests. Commercially pure helium was fed into the work zone from the top of the furnace and evacuated from the bottom through a copper tube which terminated in a glass contained oil bath. This bath served as a catch-all for any debris emanating from the furnace (a safety feature in the case of tests on beryllium) as well as an indicator of the flow rate, which had to be controlled to facilitate temperature control.

3.3 Constant Strain Rate Tests *

The tension tests were run in a 20,000 lb capacity Instron screw driven machine and the compression tests were run in a Wiedemann Mark "G" 60,000 lb screw driven machine. Depending upon the load range required, a variety of load cells were used ranging from 0-500 lb to 0-60,000 lb. The load measurements were accurate to within 0.1% of the load cell capacity. The strain rate was nominally 0.05 in/in/min as based upon the constant crosshead rate (0.10 in/min for tension and 0.05 in/min for compression) and the initial gage length (2" for tension and 1" for compression).

Strain (elongation) was measured by a combination of two procedures. A strip chart record of crosshead motion versus load gave a reasonably good measure of the plastic deformation, particularly for strains beyond 1-2%. An electro-mechanical averaging extensometer (ASTM Class B-1) was also used which recorded strains out to 5-10%. The sensing element in this extensometer was a dual strain gaged cantilever beam assembly currently manufactured by SATEC Systems, Inc. The extensometer and load cell outputs were recorded simultaneously on an X-Y recorder.

Young's modulus was measured during each of the constant strain rate tests using the electro-mechanical extensometer. Three runs were made at each test temperature at low stress levels prior to running the complete stress-strain curve. Since the extensometer was attached to the shoulders of the tensile specimens and to the compression platens in the compression tests it

* A summary of the parameters for each type of test and a schematic of each test setup is in Appendix I.

was necessary to define an effective gage length upon which to base strain. This was done by comparing the elongation, e, indicated by the extensometer to the strain, ϵ, indicated by strain gages, thus:

$$l(\text{effective gage length}) \equiv \frac{e}{\epsilon}$$

The effective gage length is discussed in greater detail in Appendix II.

In the room temperature tensile tests the sensing element was attached directly to the shoulders of the test specimen. In the elevated temperature tests two pairs of inconel rods attached to the shoulders of the tensile specimen transmitted the motion (elongation) out of the furnace to the sensing element.

The compression specimens were loaded between two parallel ground inconel platens using the test fixture shown in Figure 10. With this fixture the crossheads actually move apart. The platens were coated with molybdenum disulfide to minimize end friction effects. In the compression tests the electro-mechanical extensometer was attached to the inconel platens. This fixture could only be used up to loads of about 12,000 lb. If the load during testing exceeded this limit then the test was stopped and the fixture was removed. The test was then continued by loading the specimen between inconel platens attached to the crossheads which then moved together and the strain measurements were taken from the crosshead motion.*

3.4 Creep Tests

Constant load (dead weight) creep tests were run in SATEC lever arm machines. These machines have a nominal lever arm ratio of 20:1. The exact ratio is verified annually by calibration with a proving ring traceable to the National Bureau of Standards. For tests at 1600°F the loads were too low to use the lever arm loading and in these tests the specimens were loaded directly by means of a weight pan suspended from the specimen itself.

* Occurred for only one test.

Creep strain was measured using the electro-mechanical extensometer described in Section 3.3 The outputs of the extensometer and one of the measuring thermocouples were recorded autographically as a function of time. Creep strain was also measured by means of a dial gage fixed to the frame of the machine which measured the deflection of the weight pan.

3.5 Stress Relaxation Tests

Stress relaxation tests were run in Baldwin "spring" machines. These machines are so-named because a heavy duty bar spring serves as a dynamometer for the system. These bars have a spring constant of about 500 pounds per 1 mil deflection.

One of two Baldwin SR 4 load cells (500 lbs or 10,000 lbs capacity, having deflections of 5 mils full range) was linked in series with the test specimen. The specimen was loaded manually by means of a crank to the initial stress at a rate of approximately 500 pounds per second. The output of the load cell was plotted as a function of time along with temperature. An effort was also made to run true strain-control stress relaxation by using an electro-mechanical extensometer to monitor strain. This is discussed in greater detail in Appendix III.

Each test system was evaluated for system relaxation; in tension by substitution for the test specimen of a 3/4 inch diameter bar of Inconel 718 having approximately the same length as the sample and in compression by running the two platens together with no specimen. Test conditions such as load, rate of load application and temperature were duplicated.

3.6 Elastic Properties Tests

Elastic properties were measured as a function of temperature using both static and dynamic methods.

3.6.1 Static Measurements

In the static tests strain was measured by means of resistance strain gages bonded to the specimen gage section and also by means of the electro-mechanical extensometer described in Section 3.3.

Four high temperature platinum free-filament strain gages (Type BLH HT1212-5b) were mounted on each of the flat gage-section specimens shown in Figures 6b, 7b and 8b. Two gages were mounted on opposing surfaces of the specimen with their strain measuring axis parallel to the load axis (longitudinal strain) and two were mounted on opposing surfaces so as to measure transverse strains. In each case the two opposing gages were wired in series so as to average out any slight differences in strain due to bending or non-axial loading. The procedure for mounting these gages was as follows:

1. Grit blast specimen surface with No. 80 silicon carbide.
2. Clean surface with acetone, then with alcohol. After this step, the sample is handled with rubber surgical gloves.
3. Precoat sample with Allen H. T. Cement.
   a. Cure 30 minutes at room temperature.
   b. In vacuum heat to and hold for one hour each at 200, 400 and 600°F.
4. Apply gage package.
   a. Apply cement through mask.
      a.1 Cure at 150°F for 10 minutes.
   b. Remove mask.
      b.1 Cement remainder of gage.
   c. Cure at 150°F for 10 minutes.
   d. Air dry at room temperature for 1 hour.
   e. Repeat step 3b.

The specimens were tested in a SATEC lever arm machine with a 10,000 pound Baldwin load cell placed in series with the specimen. The specimens were tested at room temperature then at successively higher temperatures until the gages burned out. Three runs were made at each temperature at stress levels less than about 60% of the proportional limit at the test temperature. The strain gages were compensated in Wheatstone bridge circuits with precision wound variable resistors. The gage factor was corrected to take into account the lengths of nichrome ribbon lead wire required to make the hookup. The outputs of the load cell, longitudinal and transverse gages were recorded on an XYY' recorder. A number of tests were also run at room temperature using BLH Type A7 and Dentronic strain gages.

3.6.2 Dynamic Measurements

Dynamic measurements of the elastic constants were made by the pulse-echo technique using a Sperry Reflectoscope, Type 5NRF. A barium titanate crystal was used to transmit longitudinal waves and a Y-cut quartz crystal was used to transmit shear waves. The crystals were coupled to the test specimen (Figure 9) with high viscosity vacuum grease. The beryllium was tested at a frequency of 5 MHz while the copper and beryllium-copper alloy were tested at a frequency of 1MHz.

The specimen was mounted in a vycor chamber which held a dynamic atmosphere of helium gas. The "test portion" of the specimen (the 2" length between the hole and the end of the specimen) was heated by RF heating. Chromel-alumel thermocouples were used to control the test temperature within $\pm 5^{\circ}$F. The end of the specimen opposite the "test portion" passed through a water cooled lead pot. Thus the transmission crystals were maintained at room temperature.

Two separate temperature excursions were made starting at room temperature, one using the longitudinal crystal and one using the shear crystal. The important response signals were displayed on an oscilloscope and photographed for measurements of the pulse lengths. The longitudinal and transverse velocities were calculated as follows:

$$\text{Velocity} \equiv V = \frac{\text{Specimen Length}}{K_t \times \text{Pulse Length}}$$

where the time constant K_t was determined for the given settings on the reflectoscope using an aluminum calibration specimen as follows:

$$K_t = \frac{\text{Al Specimen Length}}{\text{Long. Vel. of Al} \times \text{Pulse Length of Al}}$$

From the measured longitudinal velocity, V_L, and shear velocity, V_S, the elastic constants were calculated as follows:

G = Shear Modulus = $(V_s)^2$ x density, gms/cc, x $1.45 \times 10^{-5} \text{psi}/\text{dyne/cm}^2$

$$E = \text{Youngs Modulus} = \left(\frac{3V_L^2 - 4V_s^2}{V_L^2 - V_s^2}\right) G$$

$$\nu = \text{Poissons Ratio} = 0.5\left(\frac{V_L^2 - 2V_s^2}{V_L^2 - V_s^2}\right)$$

4.0 EXPERIMENTAL RESULTS

This section summarizes the experimental data in graphical form. A complete tabulation of the data is presented in Appendix IV.

4.1 Beryllium

4.1.1 Constant Strain Rate Tests

True stress-true strain* curves for beryllium as a function of temperature are shown in Figures 11 and 12 for tension and compression, respectively. Upper and lower yield points were observed at test temperatures up through 750°F. In the compression tests the yield drops were manifested as inflections in the load-deflection curves. Beyond the yield points, i.e., after a few percent strain, the tension and compression curves are in reasonably good agreement. The tension curves at 1250°F and 1600°F are dashed to indicate that the specimens necked-down very early in the tests. The conventional engineering properties (yield strength, elongation, etc.) are given in Table A-1 of Appendix IV.

The fracture appearances of the tensile specimens changed in an unusual way with increasing temperature as shown in Figure 13. The light grey areas represent cleavage fracture typical

---

* The method of calculating true stresses and true strains is described in Appendix V.

of beryllium tested at low temperatures. The dark grey or black areas are difficult to describe. Optical and scanning electron microscopy failed to identify the microstructural nature of these areas but did show them to have a sponge-like morphology. Note also the elliptical cross section of the specimens tested at 500°F and 750°F. This result is presumably due to preferred orientation.

4.1.2 Creep Tests

Creep tests at various stress levels were run at 500°F, 1000°F and 1600°F. The beryllium tension creep curves are shown in Figure 14-16 and the compression creep curves are shown in Figures 17-19.

The creep behavior at 500°F was unusual as shown in Figure 14. There was virtually no strain on loading. At the lowest stress level (35 ksi) the creep rate was low out to 60 minutes, the duration of the test. The same creep curve was obtained for the two higher stress levels out to a point where there was a "burst" of deformation followed by a higher creep rate. This behavior is similar to that for niobium-oxygen alloys as reported by Stoop and Shahinian(1). In the compression tests this behavior was manifested as inflections in the creep curves as shown in Figure 17. The stress levels in these creep tests were in the range of the lower yield stress determined in the constant strain rate tests. Undoubtedly, this unusual creep behavior and the upper and lower yield points are due to the same metallurgical phenomenon.

The creep curves were normal at 1000°F and 1600°F, and the tension and compression curves were in reasonable agreement, considering the inherent difference between tension and compression deformation at constant load.

4.1.3 Stress Relaxation Tests

Stress relaxation tests were run at 500°F, 1000°F and 1600°F. The tension stress relaxation curves are shown in Figures 20-22 and the compression curves are shown in Figures 23-25. The strain-control tests were not generally successful because the specimen could not be unloaded with sufficient speed and accuracy to maintain the specimen length constant. Hence, unless otherwise noted on the figures the curves are for constant crosshead displacement. This is discussed in greater detail in Appendix III.

The sudden drop after about 17 minutes in the curve for the highest stress level at 500°F (Figure 20) is probably real and due to the yield point phenomenon described in the constant strain rate tests and creep tests at 500°F.

4.1.4 Elastic Property Tests

The elastic properties of beryllium are shown in Figure 26 as a function of temperature. No distinction is made here between tension and compression modes of loading as this is included in the tabulation of the data in Table A-8 of Appendix IV. The dynamic values of E appear quite high compared with the generally accepted static value of 40-45 x 10^6 psi at room temperature. No source of error could be isolated to account for the high dynamic values. However, it is noted that the formulas used to calculate the dynamic moduli are based on isotropic behavior. The extensometer data are for tensile loading only and are based on the actual gage length, i.e., not a corrected or effective gage length. The extensometer was found to be inadequate in the compression tests on beryllium.

4.2 OFHC Copper

4.2.1 Constant Strain Rate Tests

True stress-true strain curves for OFHC copper as a function of temperature are shown in Figures 27 and 28 for tension and compression loading, respectively. The conventional engineering properties as determined in tension are shown in Figure 29 as a function of temperature. The decrease in ductility with increasing temperature was accompanied by an increased tendency towards intercrystalline (grain boundary) fracture as shown by the photograph of the fractured tensile specimens in Figure 30.

The stress-strain curves in tension and compression were in reasonable agreement. Figure 31 shows the flow stress for tension and compression as a function of temperature for strains of 0.2% (yield stress) and 10%.

4.2.2 Creep Tests

Creep curves for OFHC copper as a function of stress at 500°F, 1000°F and 1600°F are shown in Figures 32-34 for tension loading and in Figures 35-37 for compression loading. The tension and compression creep curves are in reasonable agreement if the difference in prevailing true stresses for otherwise similar test conditions are taken into account.

4.2.3 Stress Relaxation Tests

Stress relaxation curves for OFHC copper at various initial stress levels at 500°F, 1000°F and 1600°F are shown in Figures 38 and 39 for tension and compression loading, respectively.

4.2.4 Elastic Property Tests

The elastic properties of copper are shown in Figure 40 as a function of temperature. These data are tabulated in Table B-8 of Appendix IV. The tension extensometer values are based on an effective gage length of 2.5" as compared with the nominal gage length of 2.0". The low dynamic values of Poisson's ratio led to a cursory check on preferred orientation. A sample cut from the as-received block was heat treated and examined by means of x-ray diffraction on three mutually perpendicular faces. The qualitative evaluation of the results was that there was insufficient texturing to account for the low values of Poisson's ratio. Thus, for $\nu = 0.3$ the dynamic ratio E/G would be in error by about 20%, assuming isotropy.

4.3 Beryllium-Copper Alloy No. 10

4.3.1 Constant Strain Rate Tests

True stress-true strain curves for beryllium-copper Alloy No. 10 are shown as a function of temperature in Figures 41 and 42 for tension and compression loading, respectively. The tensile specimens tested at 750°F and 1000°F broke in the threads prior to the onset of detectable plastic strain. The photograph of the fractured tensile specimens shown in Figure 43 suggests that there is a ductility minimum in this temperature range. Further, the compression curves show a peak in the flow stress in the 500°F-750°F temperature range. Figure 44 shows some of the conventional strength and ductility parameters as a function of temperature. The peak in the compression flow stress curve suggests that additional precipitation, perhaps strain induced, occurred during testing. The differences between the tension and compression flow stresses at the lower temperatures is probably due to differences in heat treatment response, either response to solution treatment or to aging treatment.

4.3.2 Creep Tests

Creep tests were run at various stress levels at temperatures of 500°F, 1000°F and 1600°F. The tension creep curves are shown in Figures 45-47 and the compression creep curves are shown in Figures 48-50. The tension specimens tested at 500°F fractured in the threads after relatively small creep strains. To eliminate thread failure the specimens tested at 1000°F were tested with a reduced gage section diameter. In these tests the specimens tested at the higher stress levels fractured in the gage section again after relatively small creep strains. The differences in the strains on loading between the tension and compression creep tests at 500°F and the tensile creep fractures are generally consistent with the constant strain rate test results.

4.3.3 Stress Relaxation

The stress relaxation curves for the beryllium-copper Alloy No. 10 at 500°F, 1000°F and 1600°F are shown in Figures 51 and 52 for tension and compression loading, respectively. Note that the tensile specimen loaded to an initial stress of 40 ksi at 1000°F fractured in the gage section after 72 seconds under decreasing stress.

4.3.4 Elastic Property Tests

The elastic properties of beryllium-copper Alloy 10 are shown in Figure 53 as a function of temperature and tabulated in Table C-8 of Appendix IV. The tension extensometer values are based on an effective gage length of 2.5" as discussed in Appendix II.

5.0 DISCUSSION

5.1 Literature Review and Data Comparison

Prior to and during the testing phase of this program a literature review was conducted on the three materials being studied. The results of this survey are summarized in the following sections.

5.1.1 Beryllium (S200-E)

The literature, for example references 2 and 3 presents mechanical property data for numerous types of beryllium, but the quantity of data on any one type of material is generally not extensive. The survey was limited to QMV hot pressed block, specifically the grades S-200C, D and E. The data for C and D are included since only meager data is available on the E grade.

Before a detailed comparison with literature data is attempted, it must be realized that a number of variables affect the mechanical properties of beryllium, such as, date of material production i.e. grade S200 C, D, E, hot pressing size, grain size, BeO content, and testing techniques such as specimen design, surface finish, strain rate, etc.[2,3,4] Frequently, it is not possible to make direct comparisons with literature values and only interpretive comparisons are possible because of the influence of one or more of the previously mentioned variables.

The room temperature properties of S200E grade beryllium which represent some 303 individual tests are presented in reference 4 and tabulated in Table 1. The agreement with this data is remarkably good when the fact that only two specimens were tested at RT in this program is considered. The distribution and range of tensile properties at room temperature are presented in reference 5 and thus will not be detailed here.

The tensile properties of beryllium tested in this study as a function of temperature are presented in Figures 54, 55, and 56 together with selected literature data for hot pressed block. The rather large spread of literature data should be noted as well as the relation of the data generated in this study to the literature data.

A comparison of the compressive yield data for beryllium from this study with literature data is shown as a function of temperature in Figure 57 while the comparison of modulus data is shown in Figure 58.

Comparison of tensile creep data with literature values is complicated by the fact that the vast majority of literature work is concerned only with stress rupture life. Thus the stress levels studied are not the same as those evaluated in this investigation. Creep rate versus stress at 1000°F for several literature values and present data are shown in Figure 59.

The review of the beryllium literature did not reveal any significant data concerning compressive creep, tensile stress relaxation or compressive stress relaxation.

5.1.2 Oxygen Free High Conductivity Copper

There is a scarcity of data in the literature on the mechanical properties of OFHC annealed copper above 400°F. This is understandable due to the very limited commercial utilization of pure copper above that temperature.

The comparison of tensile yield strength and ultimate tensile strength with the data generated in this study are shown in Figure 60. Tensile elongation as a function of test temperature up to 400°F is in substantial agreement with the literature values and ranges between 50 and 60 percent. The rather abrupt drop in ductility between 400 and 500°F is also in good agreement.

No reliable compressive properties for OFHC annealed copper were found.

Young's modulus data is compared to literature values in Figure 61.

Tensile creep data that exists in the literature, for example reference 11, has generally been established at temperatures lower than 500°F. The limited available data at 500°F is plotted together with the data from this study in Figure 62. In the case of compressive creep data, and stress relaxation at 500°F and higher no data was found that could be compared to data from this work.

5.1.3 Beryllium Copper Alloy 10

The data available in the literature for beryllium copper alloy 10 (CA175) is primarily restricted to rather low temperature since the main applications are those requiring high strength coupled with high electrical conductivity at temperatures of from RT to perhaps 150°C. The principle form used is strip rather than the wrought form evaluated in this study and generally the strip is evaluated in the "HT" condition rather than the "AT" heat treatment used for this program.

The comparison of tensile test data generated during this program with literature values is presented in Figures 63 thru 65. It will be noted that relative good agreement is demonstrated for these data. The generally accepted room temperature modulus for this alloy is 17.5×10^6 psi and this value compares well with the average value of 17.6×10^6 psi determined using an extensometer. The stress rupture times (1000°F tests) are plotted in Figure 66 together with data from reference 19. Additional comparable creep data was either not available or not found during the literature survey.

Comparable data for the other properties evaluated in this study were not located during the limited literature review conducted as part of this program.

5.2 Constant Strain Rate Tests and Elastic Properties

The stress-strain behavior is the same in tension and compression for the materials and conditions evaluated, i.e., no strength differential between tension and compression was observed. Hence, the tension and compression curves can be averaged to give a single uniaxial stress-strain curve for monotonic loading at constant strain (crosshead) rate. However, the effect of strain rate is unknown since only one strain rate was employed. Also, it is recalled that the beryllium exhibited yield points at the lower temperatures, and the Alloy 10 showed low ductility at the intermediate temperatures.

The elastic property data obtained with the electromechanical extensometer are probably the least accurate of the elastic property measurements. The strain gage data are probably the most accurate, particularly at the lower temperatures. Based upon the beryllium data the dynamic values appear to be high, although they might be the best measure of the temperature dependence of the elastic constants. The data for pure copper and the beryllium-copper Alloy 10 might be averaged: the assumption that they have the same elastic properties would appear to be consistent with the accuracy of the experimental measurements.

5.3 Creep and Stress Relaxation

Allowing for the fact that the creep tests were run at constant load and not at constant stress, the creep behavior of the materials studied is the same in tension and compression within the accuracy of the experimental data. Similarly, the stress relaxation behavior is the same in tension and compression.

Experimental methods of measuring stress relaxation and the correlation of stress relaxation with creep are discussed in Appendix III.

6.0 REFERENCES

1. J. Stoop and P. Shahinian, "Effect of Oxygen on Creep-Rupture of Niobium," High Temperature Refractory Metals, Part 2, AIME Metallurgical Society Conference, Volume 34, 1966, pp. 407-432.

2. A. G. E. Darwin and J. H. Buddery eds. Beryllium New York, Academic Press, 1960.

3. B. D. W. White and J. H. Burke eds., The Metal Beryllium, Cleveland, American Society for Metals, 1955.

4. B. King, "New Grades of Beryllium - Their Meaning and Use," The Brush Beryllium Company, October 1967.

5. H. Hausner ed., Beryllium Its Metallurgy and Properties, Los Angeles, University of California Press, 1965, p. 219.

6. R. F. Crawford and A. Bruce Burns, "Strength, Efficiency and Design Data for Beryllium Structures," ASD TR61-692, February 1962.

7. J. M. Beeston, "Beryllium Metal as a Neutron Moderator and Reflector Material," Nuclear Eng. and Design 2 of 14, 1970, p. 445.

8. O'Rourke, Hurd, Wilke and Beaner, "Mechanical Properties of Reactor Grade Beryllium at Elevated Temperatures," AEC Rep. C00-312, August 1956.

9. Brush Beryllium Company, "Beryllium Structures, Aero/Space Applications Data," Preliminary Release, May 1961.

10. J. Williams, Metallurgy Rev. 3, 1, 1958, CU-OFHC.

11. C. Upthegrove and H. L. Burghoff, "Elevated-Temperature Properties of Copper and Copper-Base Alloys," ASTM Special Tech. Pub. No. 181, ASTM, Philadelphia, 1956.

12. R. P. Caneker and W. Rittibland Jr., "Tensile Deformation of High Purity Copper as a Function of Temperature Strain Rate and Grain Size," Acta Met. Vol. 1, 1953, p. 654.

13. L. R. Jackson, A. M. Hall and A. D. Schwope, "Comparative Properties of Several Types of Commercial Coppers, as Cold Worked and as Recrystallized," AIME Tech Pub 2274, 1947.

14. W. D. Jenkins and T. G. Diggs, "Creep of Annealed and Cold-Drawn High-Purity Copper," Journ. Res. Nat. Bur. Stand. Vol. 47, 1951, p. 272.

15. Anom., "Technical Survey OFHC Brand Copper," American Metals Company, Ltd. 1957.

16. N. D. Benson, J. McKeown and D. N. Mends, "The Creep and Softening Properties of Copper for Alternator Rotor Windings," J. Chist. Metals Vol. 80, 1951-52, p. 131.

17. Brush Beryllium Copper Rod, Bar, Plate and Wire, Data Sheet from The Brush Beryllium Company, Cleveland, Ohio.

18. J. T. Richards, "Conductive Materials for Elevated Operating Temperatures," Electrical Manufacturing, June 1951.

19. K. G. Wikle, "ASK Product Concept Applied to Beryllium Copper Alloys," Metallurgical Report No. M-44, The Brush Beryllium Company, September 1965.

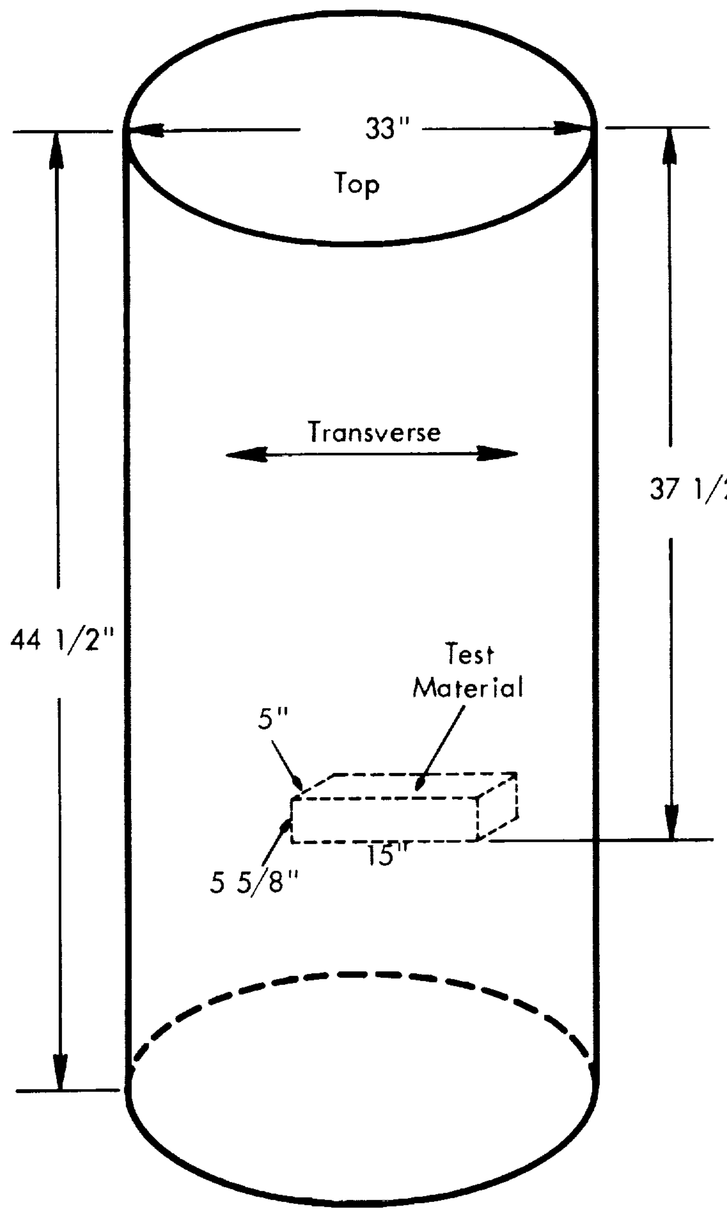

FIGURE 1 - Sketch showing approximate location and orientation of beryllium test material within the original large pressing

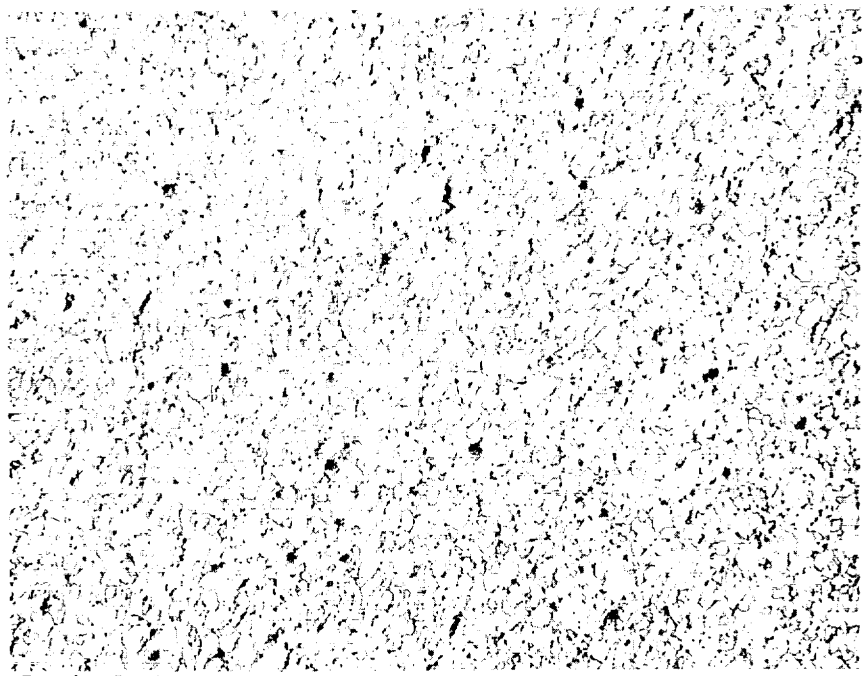

Bright Field 100X

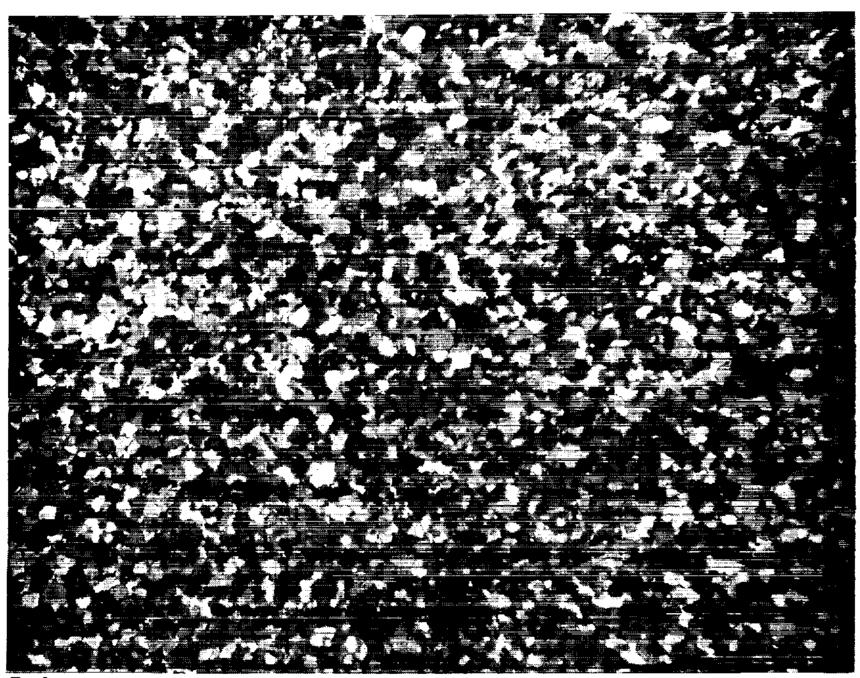

Polarized Light 100X

FIGURE 2 - Microstructure of As-VHP S-200E beryllium

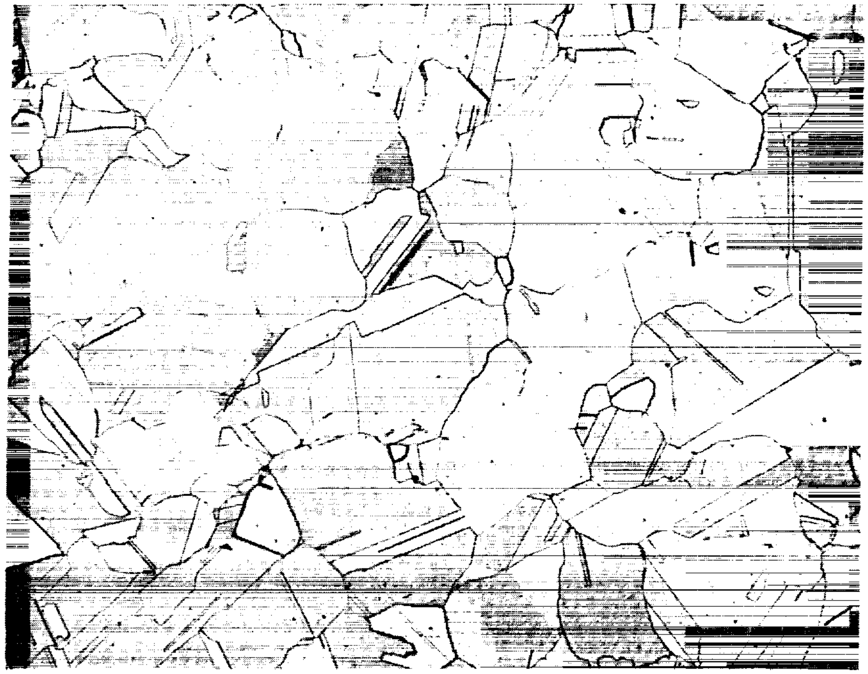

100X

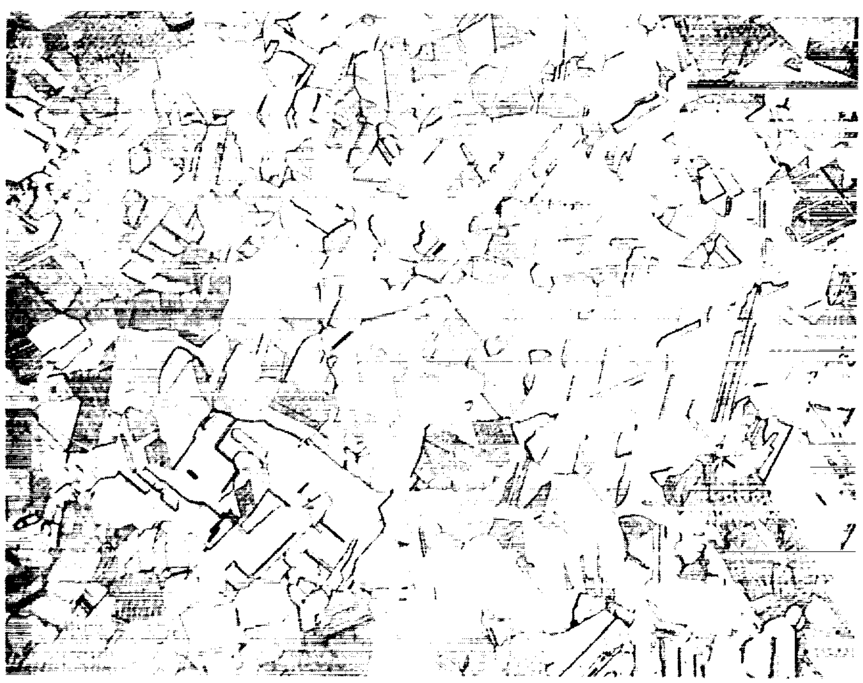

50X

FIGURE 3 - Microstructure of OFHC Copper. Hot forged plus annealed 1 hr. at 1000°F

ST

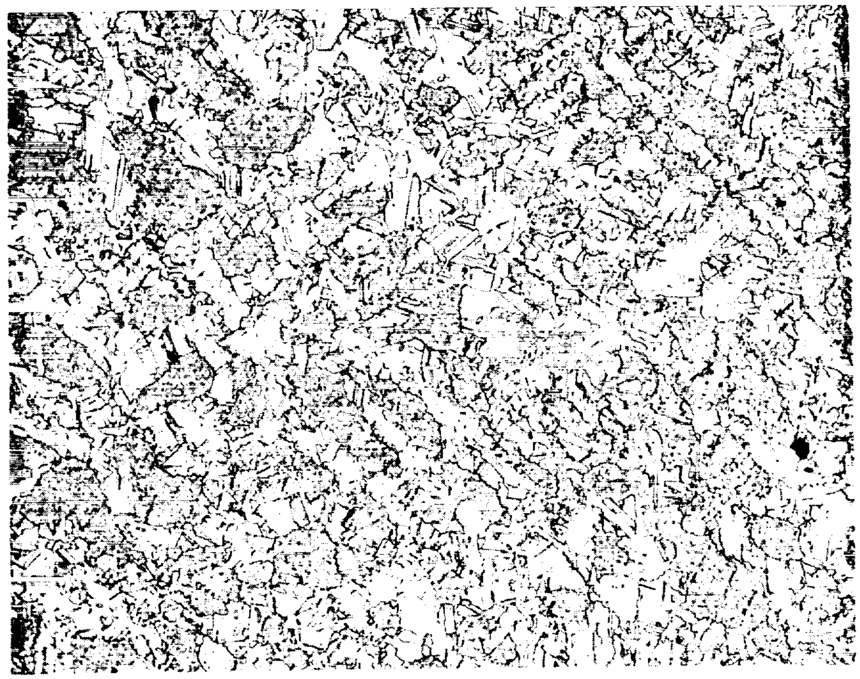

100X

ST & Aged
3 hr/900°F

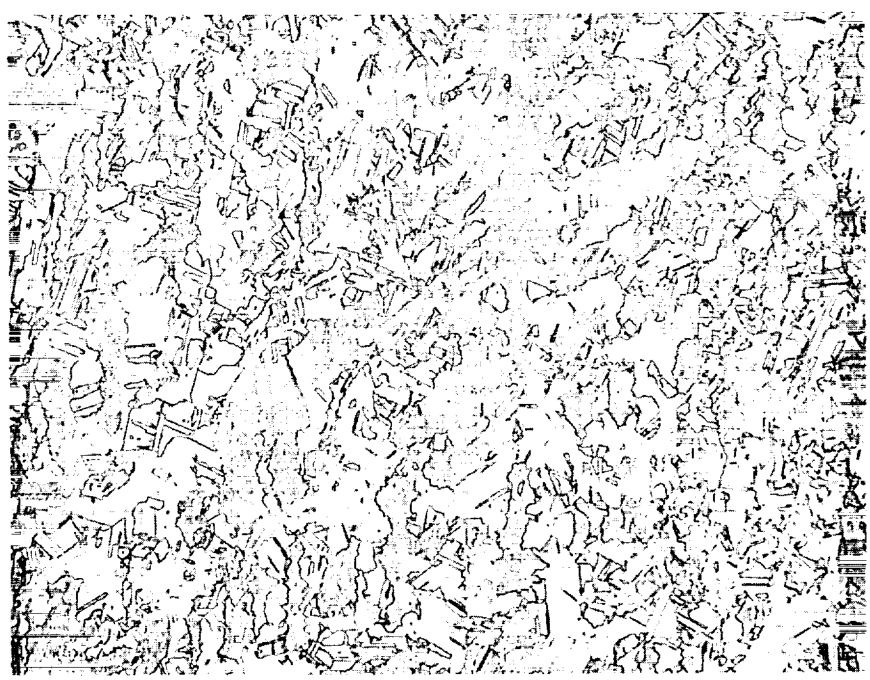

100X

FIGURE 4 - Microstructure of beryllium-copper alloy No. 10

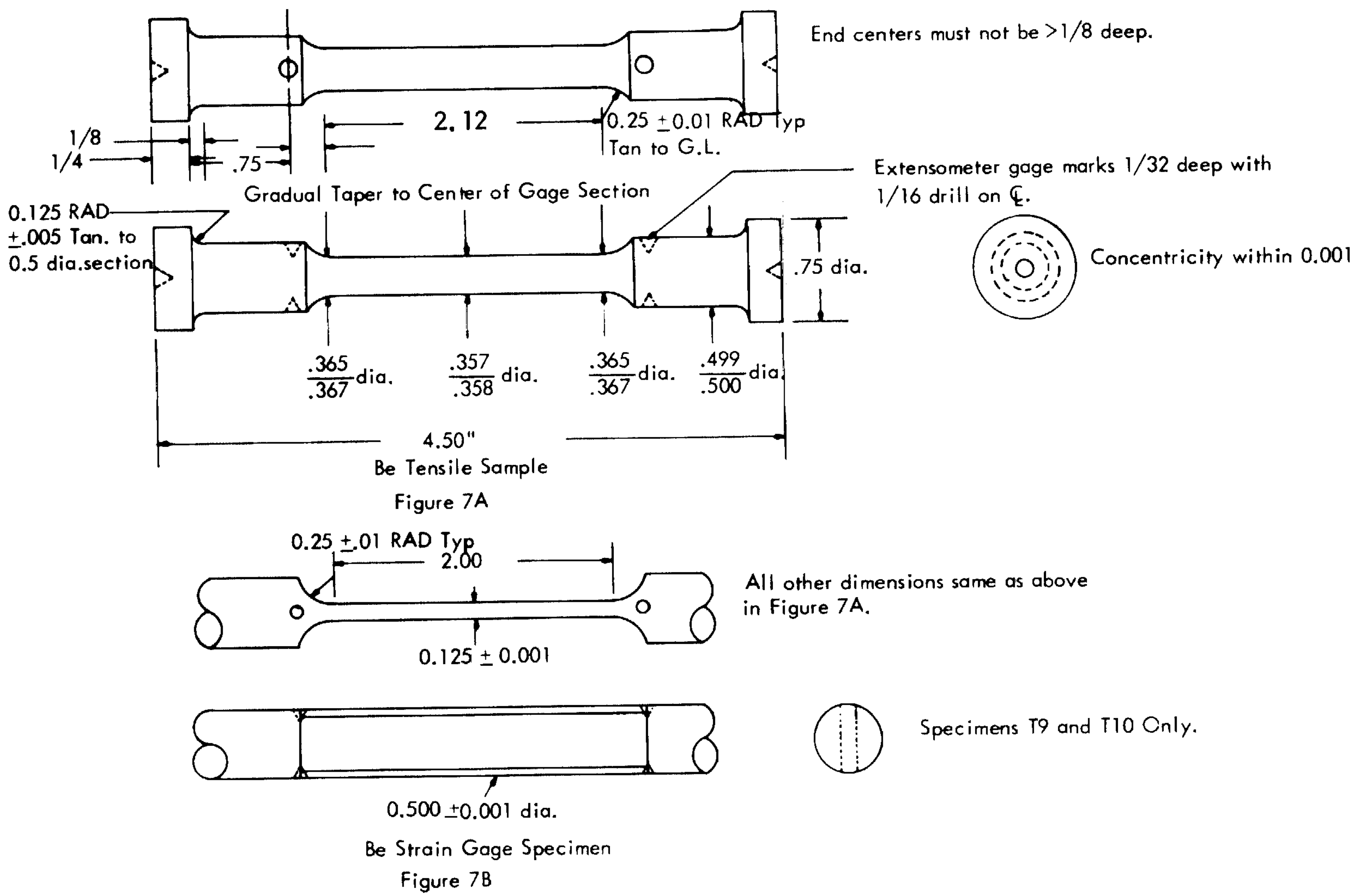

Figure 7. Tensile Specimen Design for Beryllium.
(A) Constant strain rate, creep and stress relaxation specimen.
(B) Elastic property test specimen

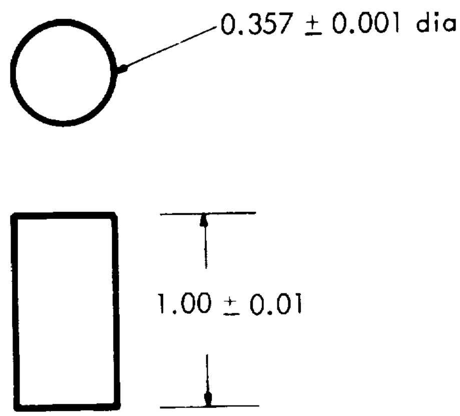

Compressive Load Sample

Figure 8A

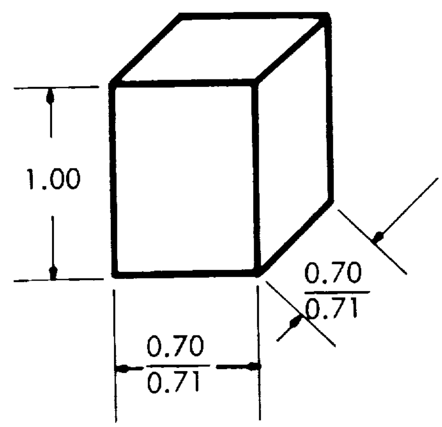

Compressive Modulus Sample

Specimens C2 and C3 Only

Figure 8B

Figure 8. Compression Test Specimen Design
(A) Constant strain rate, creep and stress relaxation specimen.
(B) Elastic property test specimen.

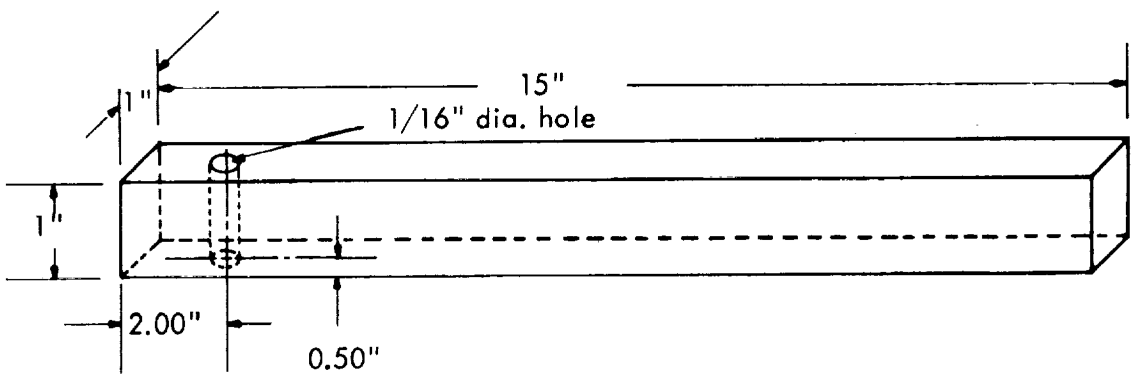

Specimen D1

Sonic Modulus Sample

FIGURE 9 - Dynamic moduli specimen design

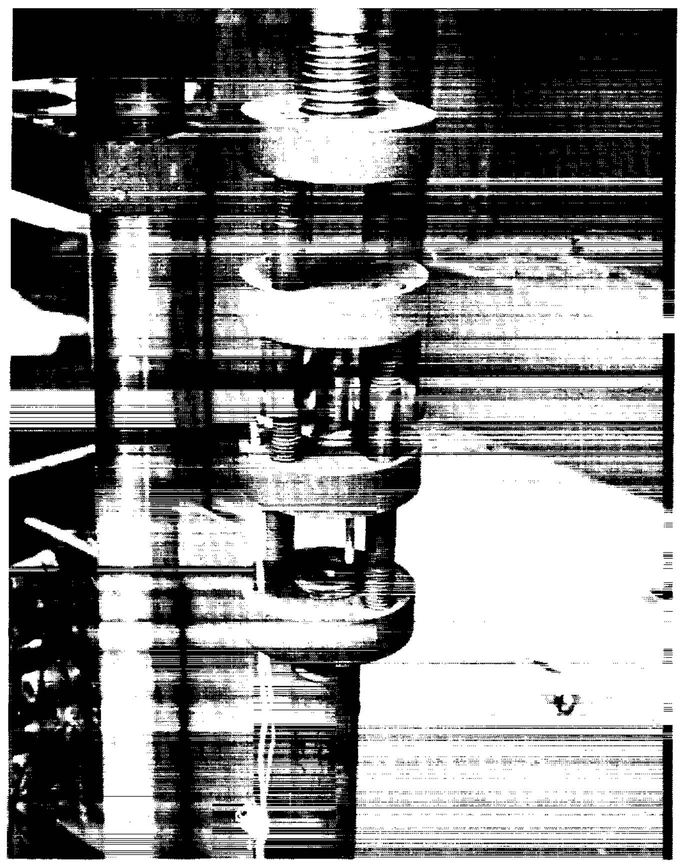

FIGURE 10 - Compression Fixture

(Calculated Using Data in Table A-2, GL_{eff} = 2.12")

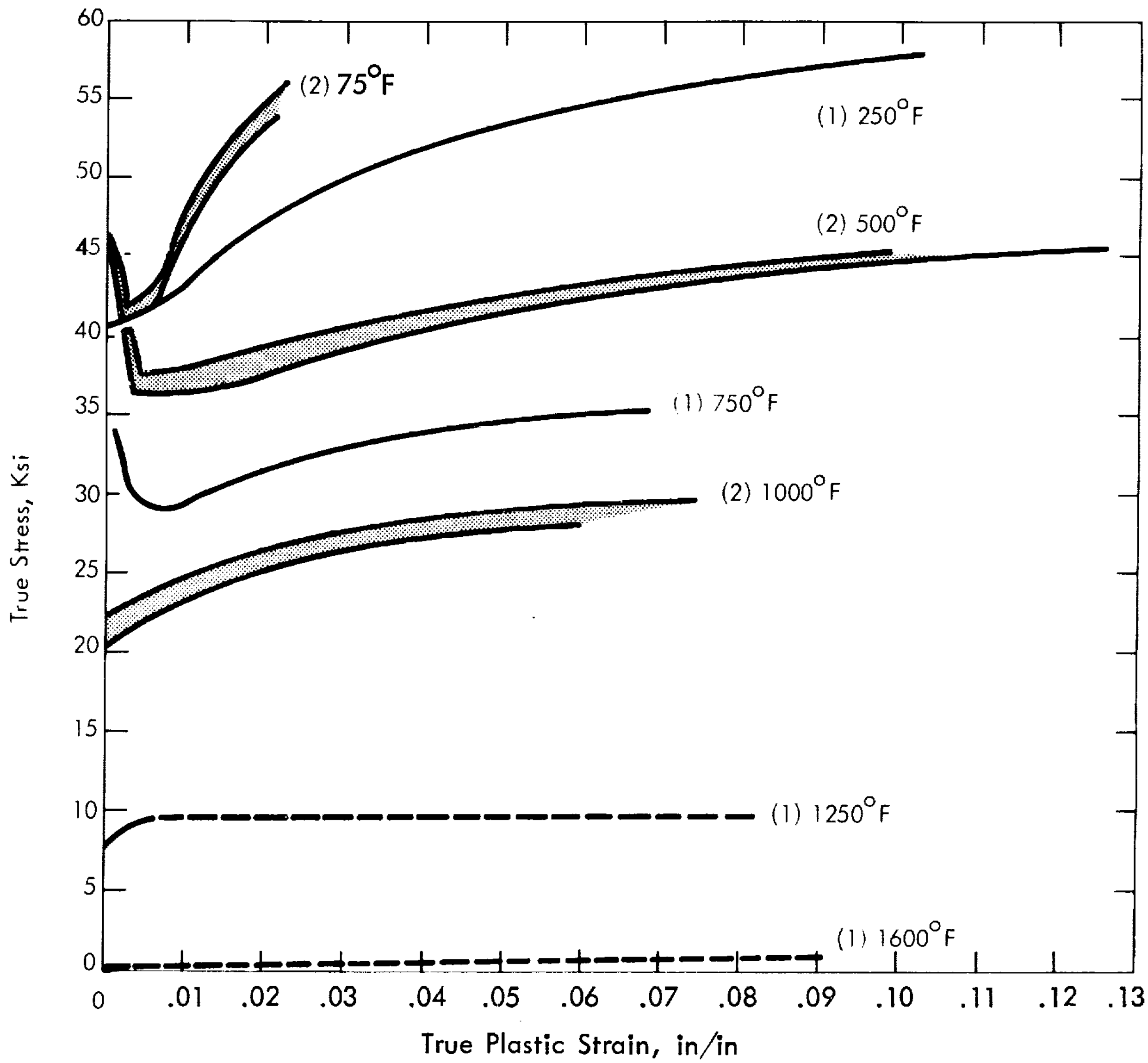

FIGURE 11 - Tensile True Stress-True Strain Curves for S-200 Beryllium as a Function of Temperature. Numbers in Parentheses Refer to Number of Tests

(Calculated Using Data in Table A-3; $GL_{eff} = 1.0"$)

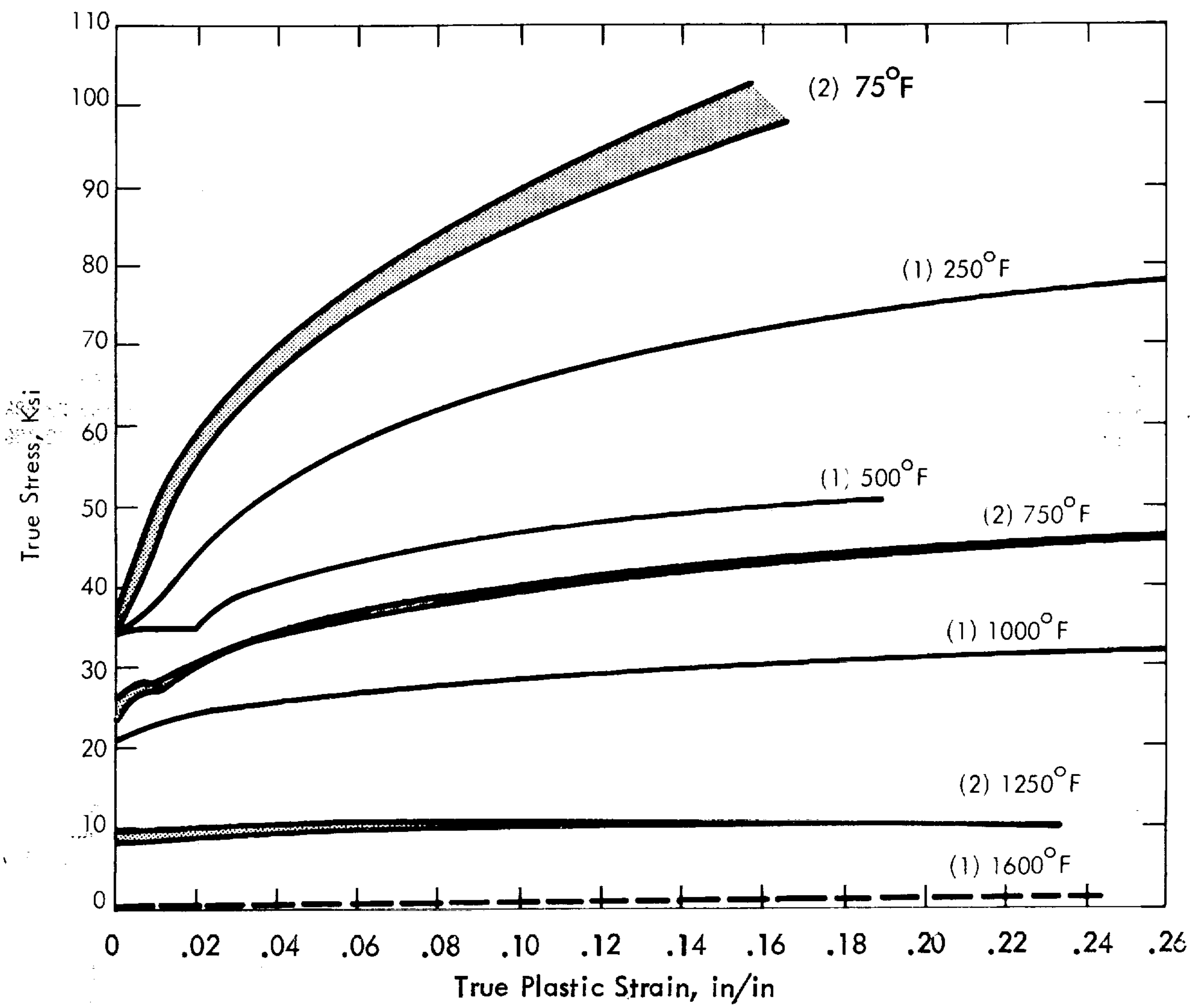

FIGURE 12 - Compression True Stress-True Strain Curves for S-200 Beryllium as a Function of Temperature. Numbers in Parentheses Refer to Number of Tests

75°F
Elong.2.3%
R.A. 2.1%

250°F
Elong.11.0%
R.A. 9.4%

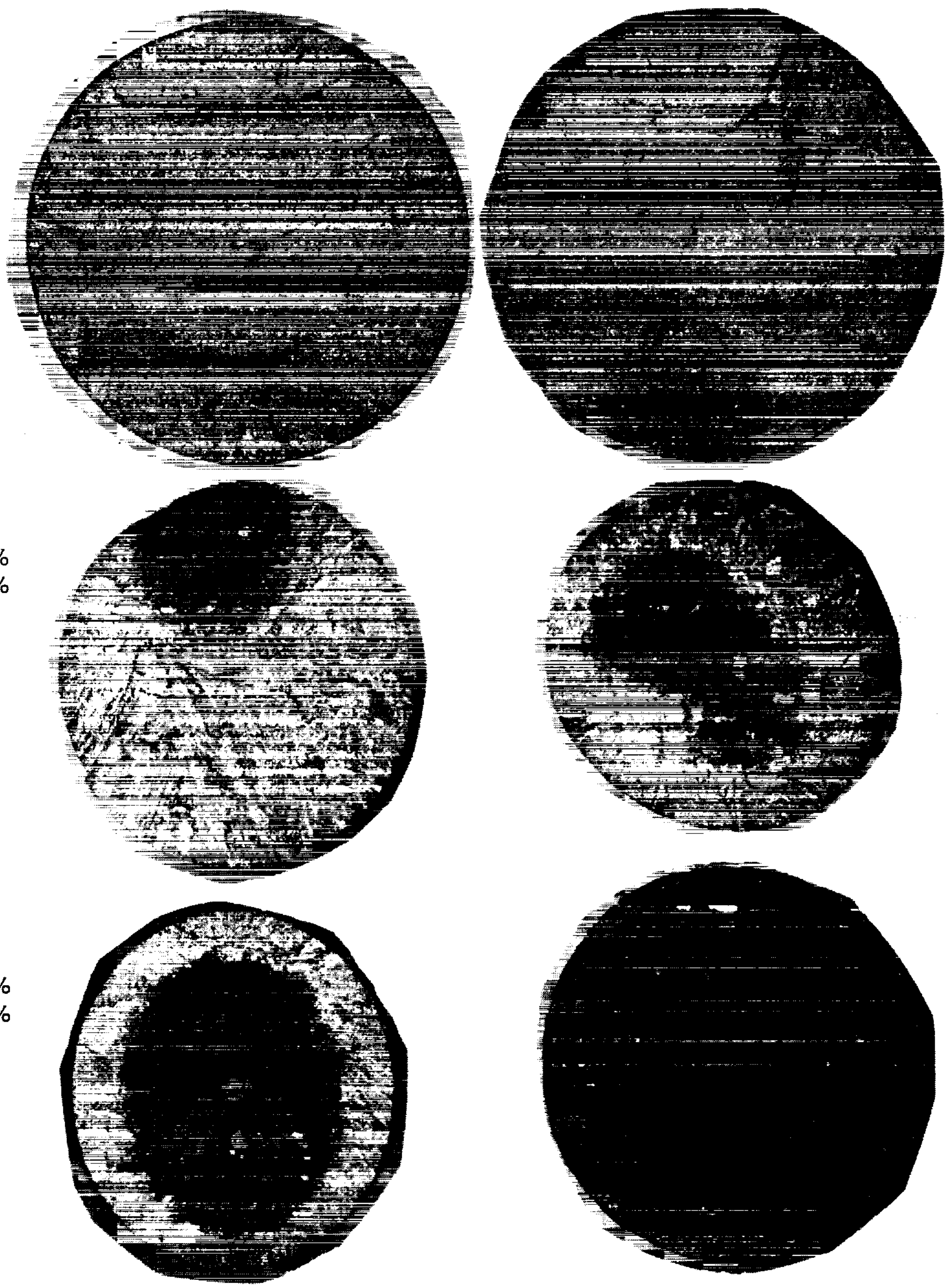

500°F
Elong.21.6%
R.A. 39.6%

500°F
Elong.23.6%
R.A. 48.1%

750°F
Elong.14.1%
R.A. 49.1%

1000°F
Elong.15.1%
R.A. 30.3%

FIGURE 13 - Fracture appearance of beryllium tensile specimens

(Calculated Using Data in Table A-4; GL_{eff} = 2.12)

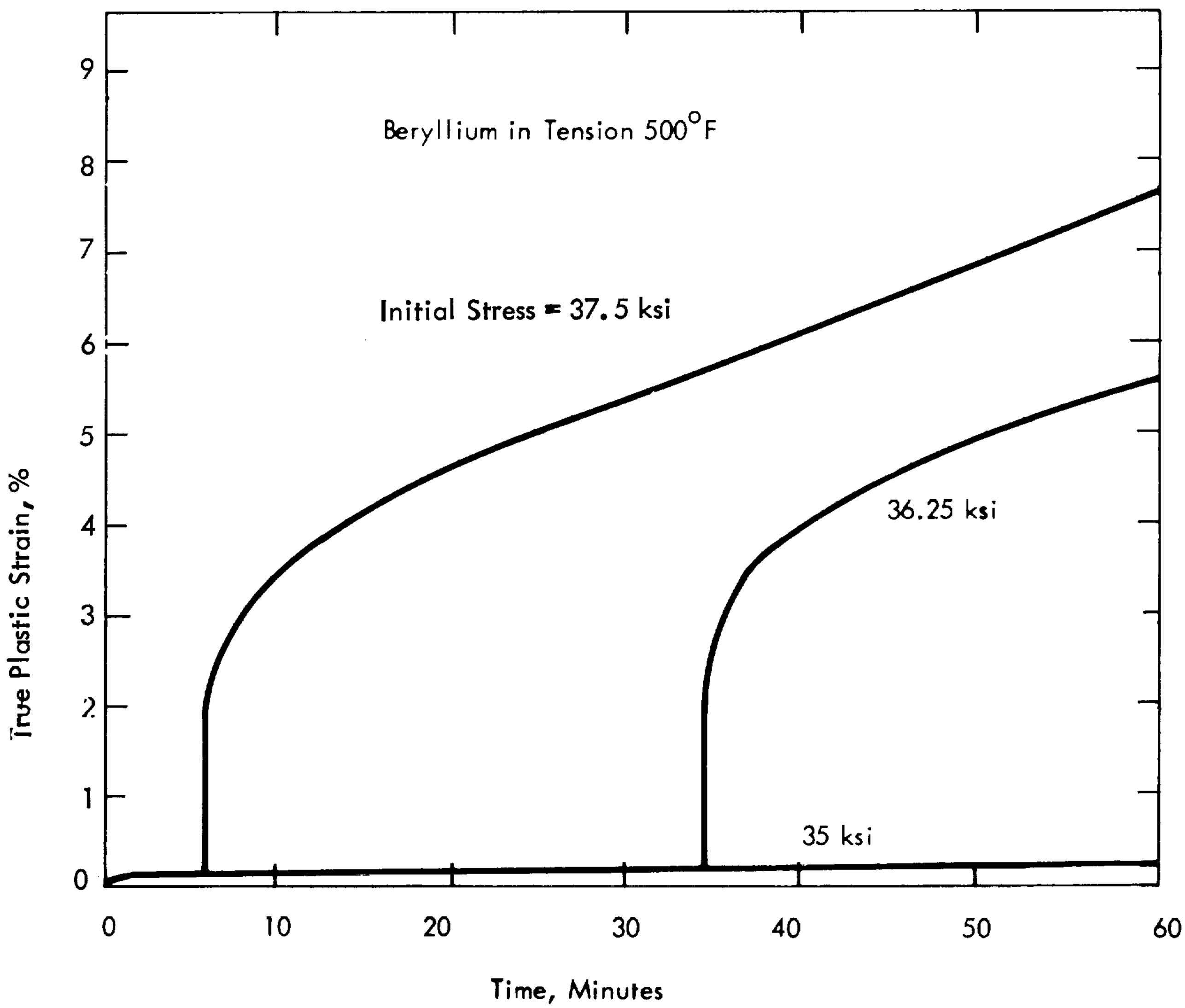

FIGURE 14. Tensile Creep Curves for Beryllium at 500°F

(Calculated Using Data in Table A-4; $GL_{eff} = 2.12''$)

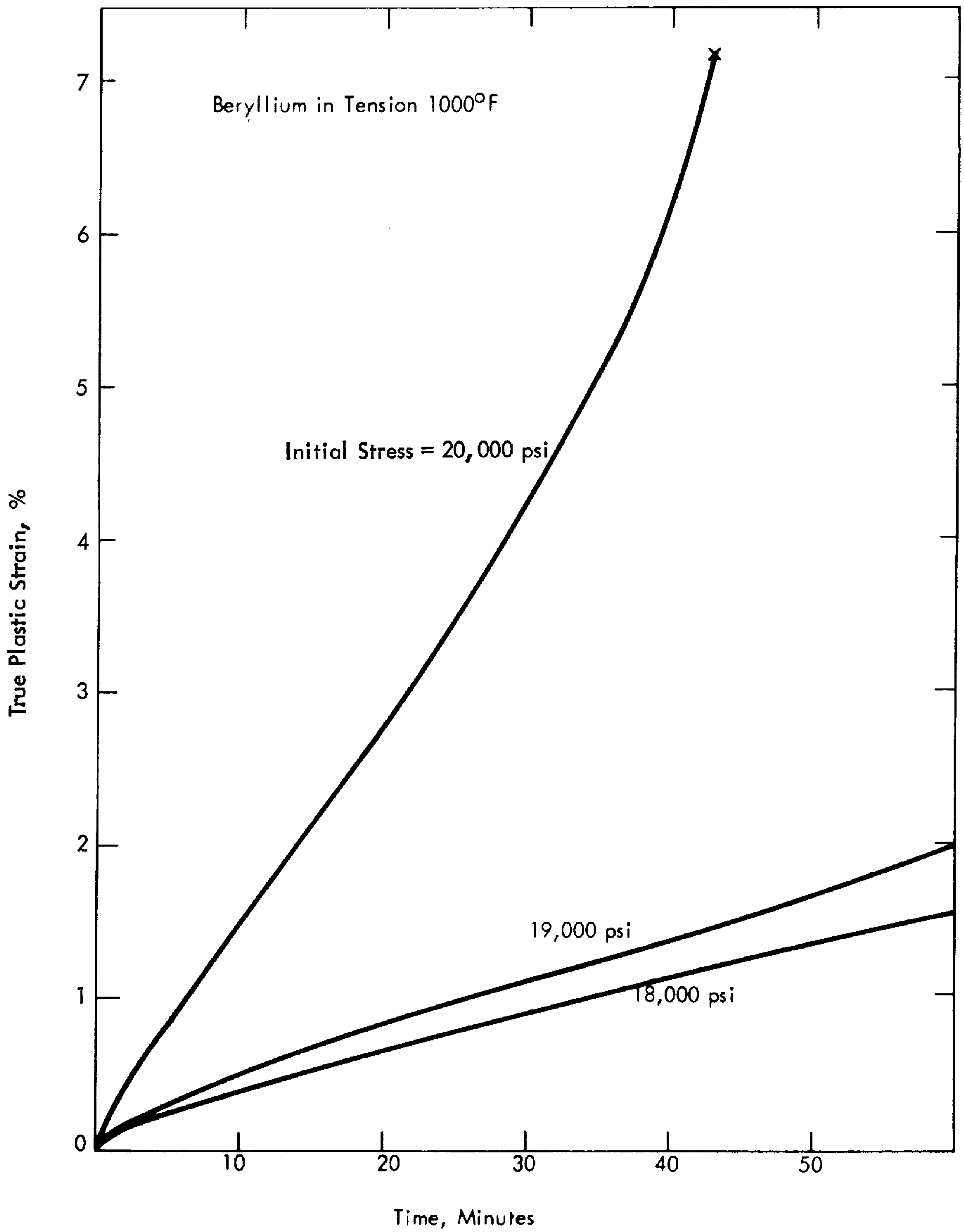

FIGURE 15. Tensile Creep Curves for Beryllium at 1000° F

(Calculated Using Data in Table A-4; $GL_{eff} = 2.12''$)

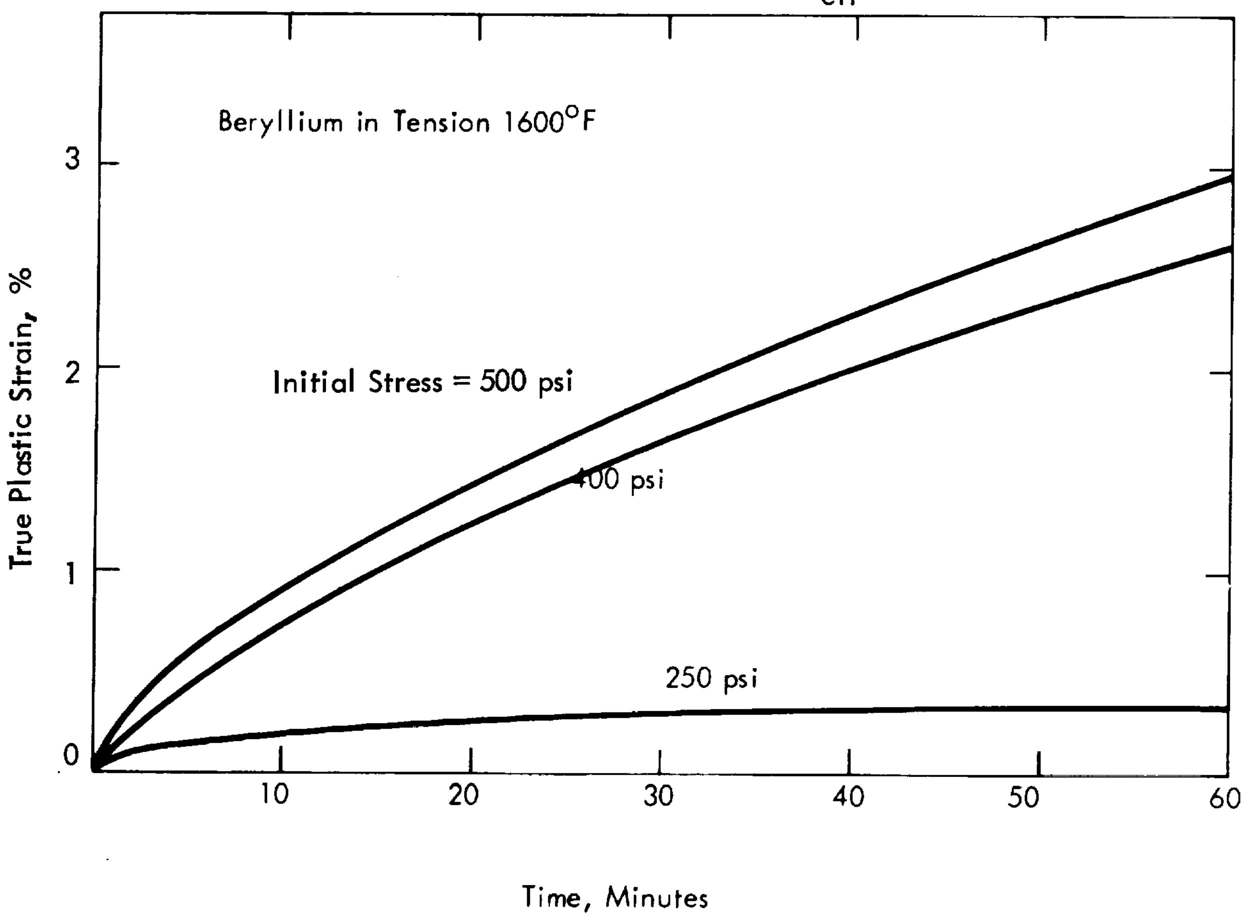

FIGURE 16. Tensile Creep Curves for Beryllium at 1600°F

(Calculated Using Data in Table A-5, GL_{eff}= 1.0")

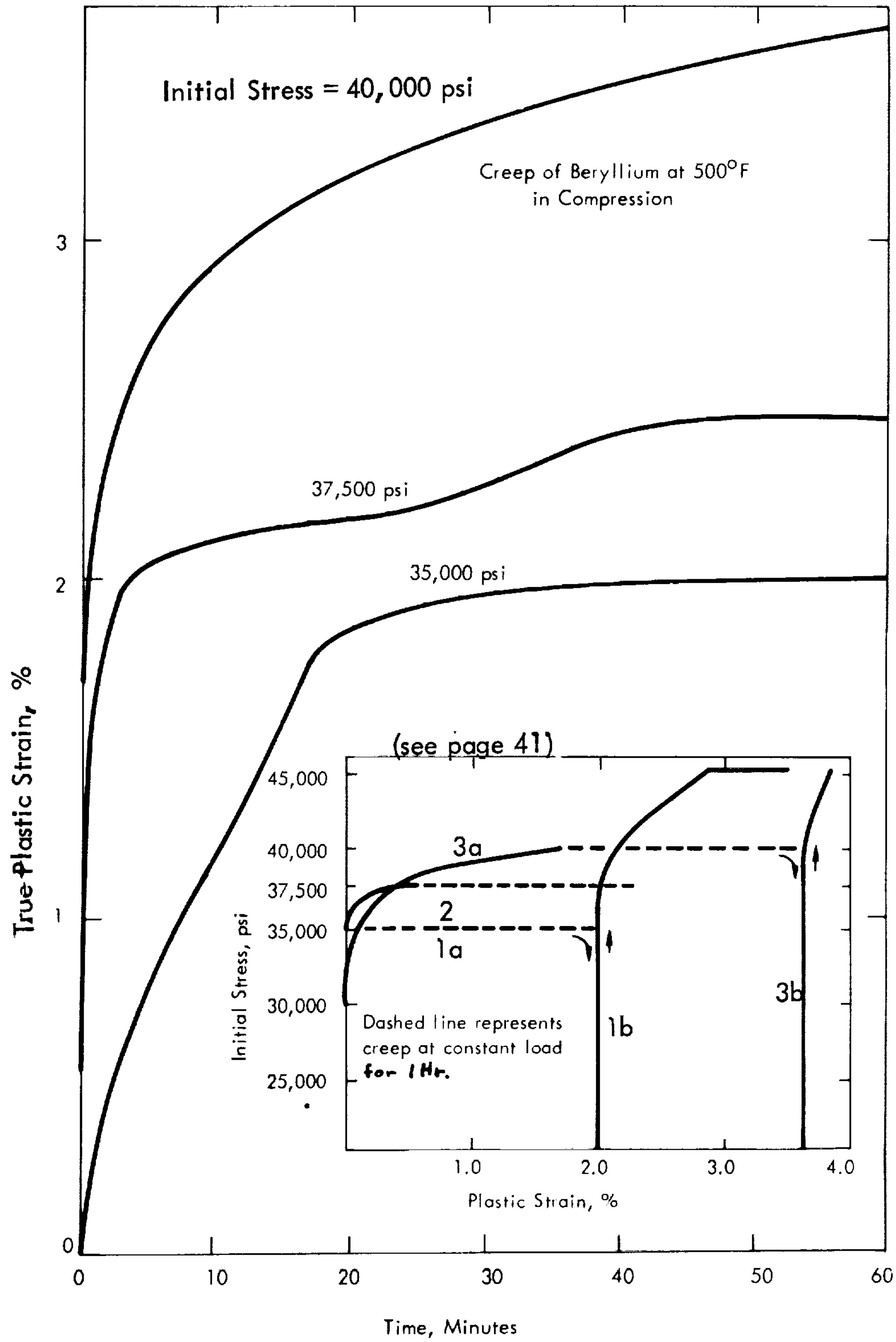

FIGURE 17. Compression Creep Curves for Beryllium at 500°F

The explanation of the "insert" in Figure 17 is as follows: Curve 1a is for the specimen creep tested at an initial stress of 35 ksi. No strain occurred on loading. The dashed curve shows that it crept to 2% strain in 60 minutes. The specimen was unloaded and then reloaded as in a compression test (Curve 1b) out to a stress of 45 ksi and cumulative strain of about 2.8%. It was then crept at that stress out to a cumulative strain of about 3.5%.

Curve 2 shows the specimen that was creep tested at 37.5 ksi. It showed about 1/2% strain on loading (solid portion of curve) and then crept to about 2-1/4% strain (dashed). This specimen was not retested in a compression test.

Curve 3a shows the strain on loading to a creep stress of 40 ksi (solid) and the creep strain at that initial stress (dashed). The specimen was unloaded and then reloaded in a compression test (Curve 3b).

The purpose of these tests was to compare the yield stress of the virgin samples with that of the samples after creep straining, and the result is evident in the figure.

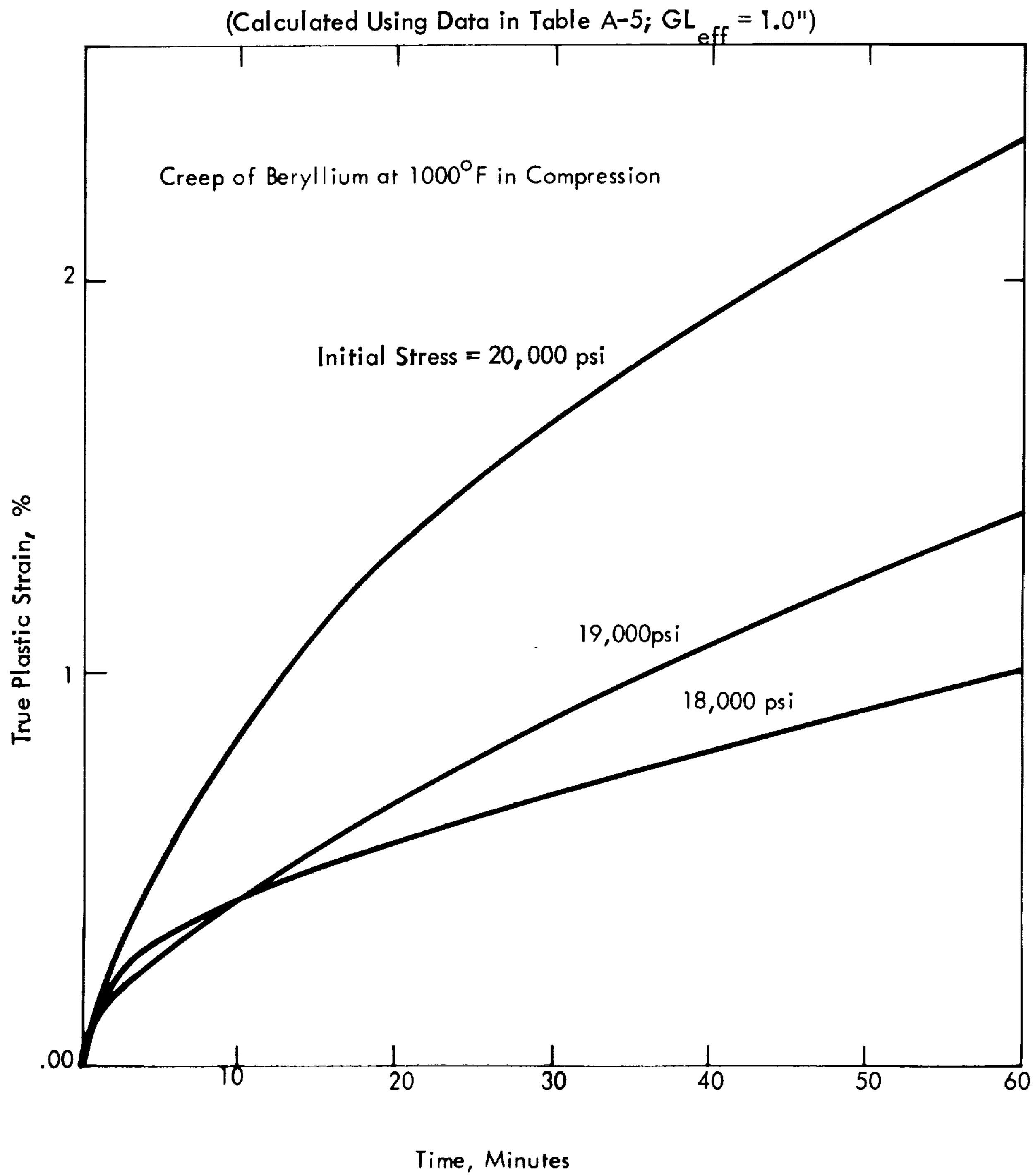

FIGURE 18. Compression Creep Curves for Beryllium at 1000°F

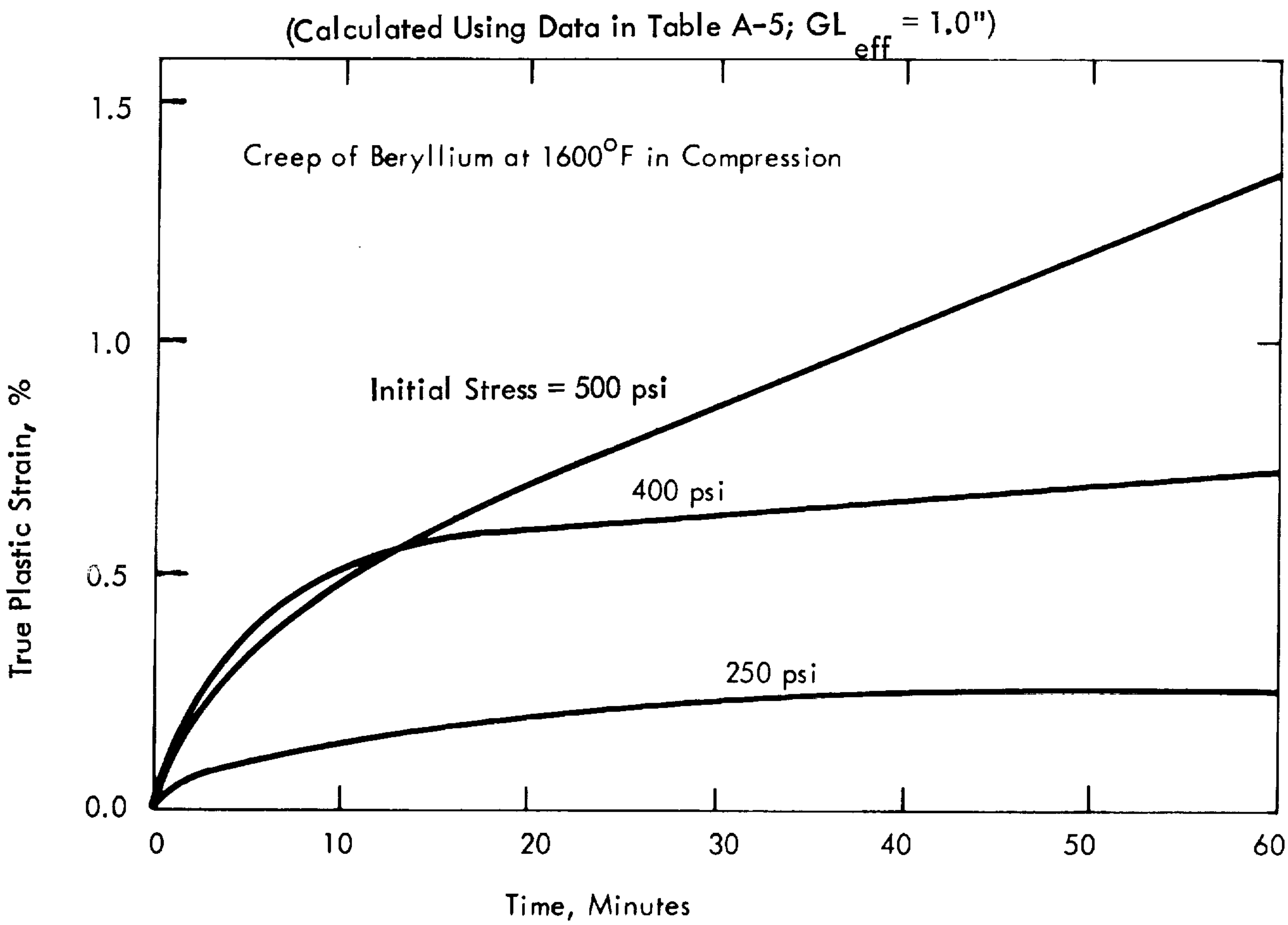

FIGURE 19. Compression Creep Curves for Beryllium at 1600°F

(Calculated Using Data in Table A-6)

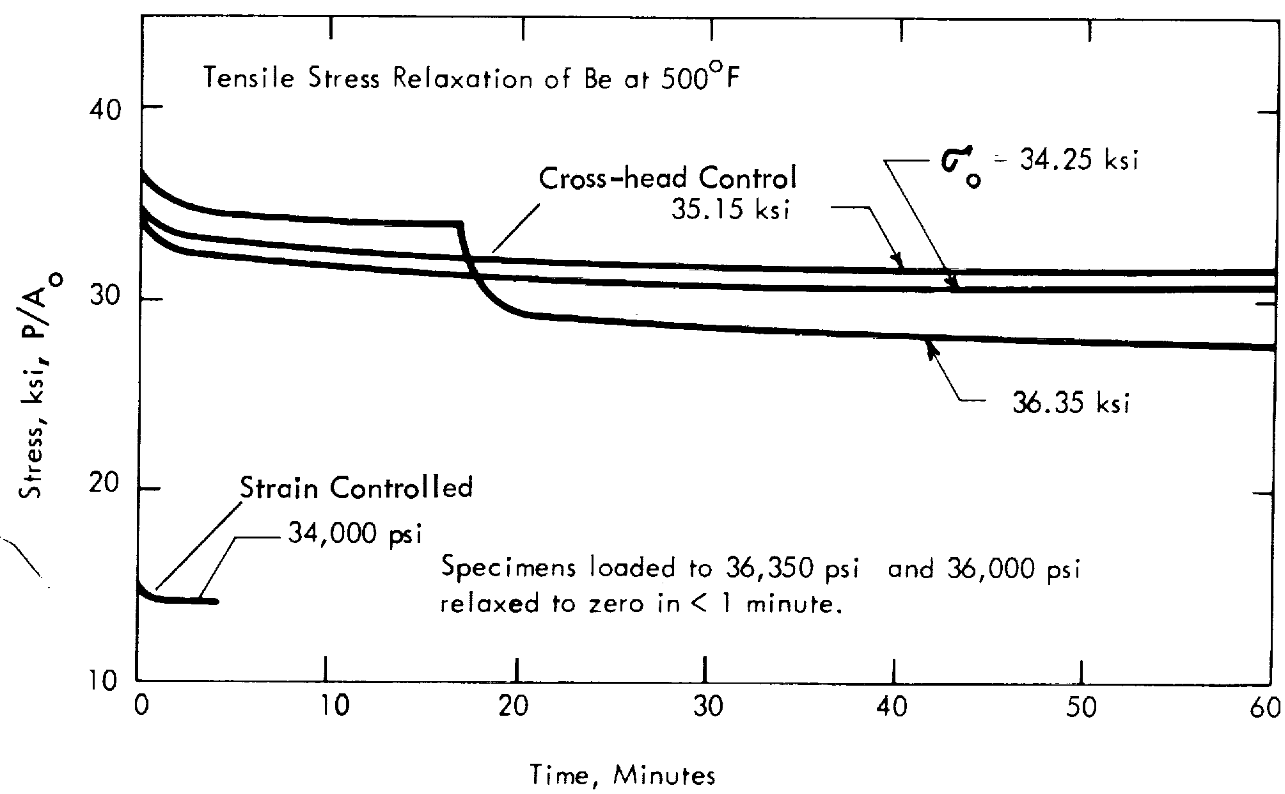

FIGURE 20. Tensile Stress-Relaxation Curves for Beryllium at 500°F (Constant Cross-Head Control Except as Noted)

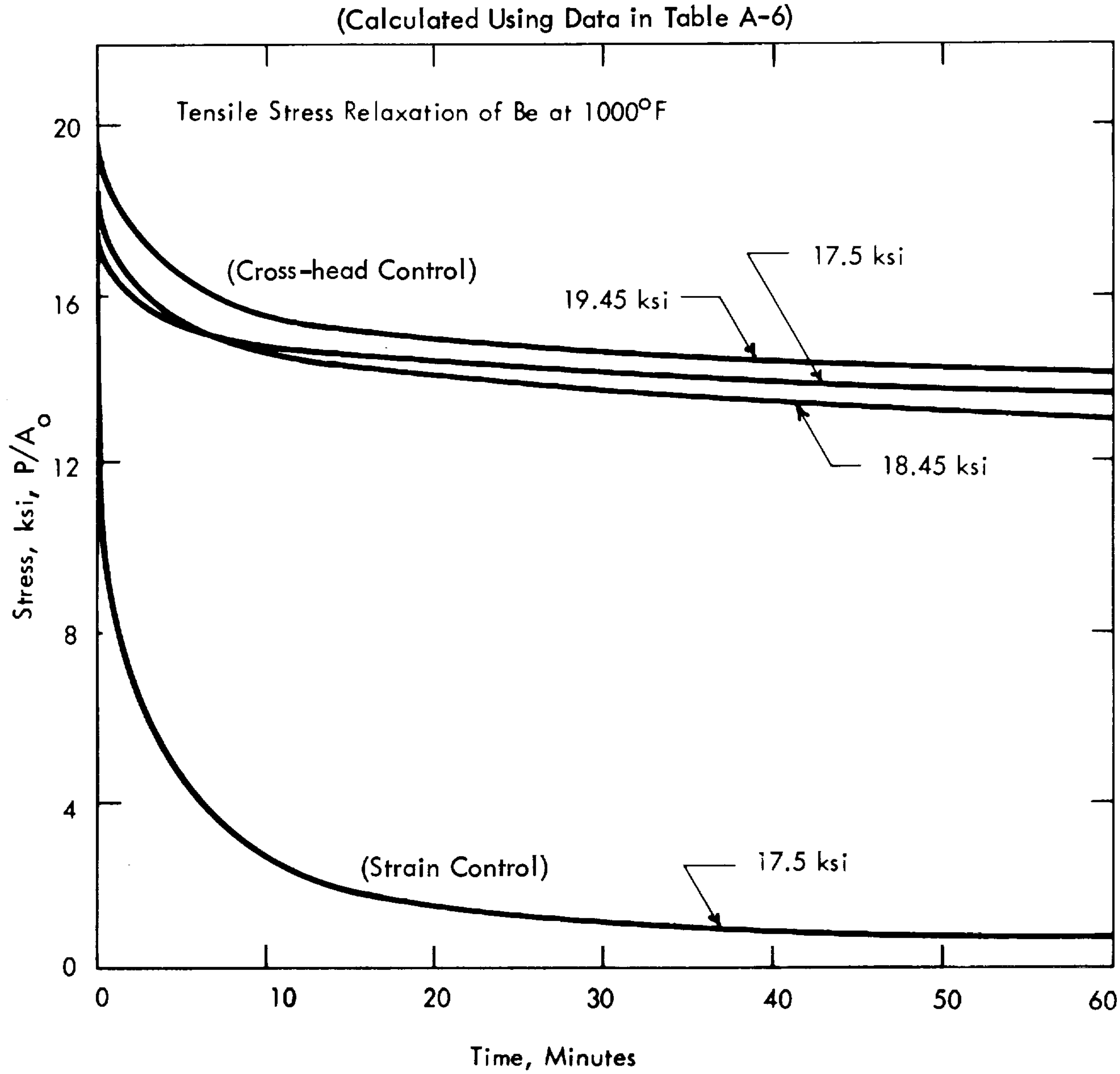

FIGURE 21. Tensile Stress-Relaxation Curves for Beryllium at 1000°F (Constant Cross-Head Control Except as Noted)

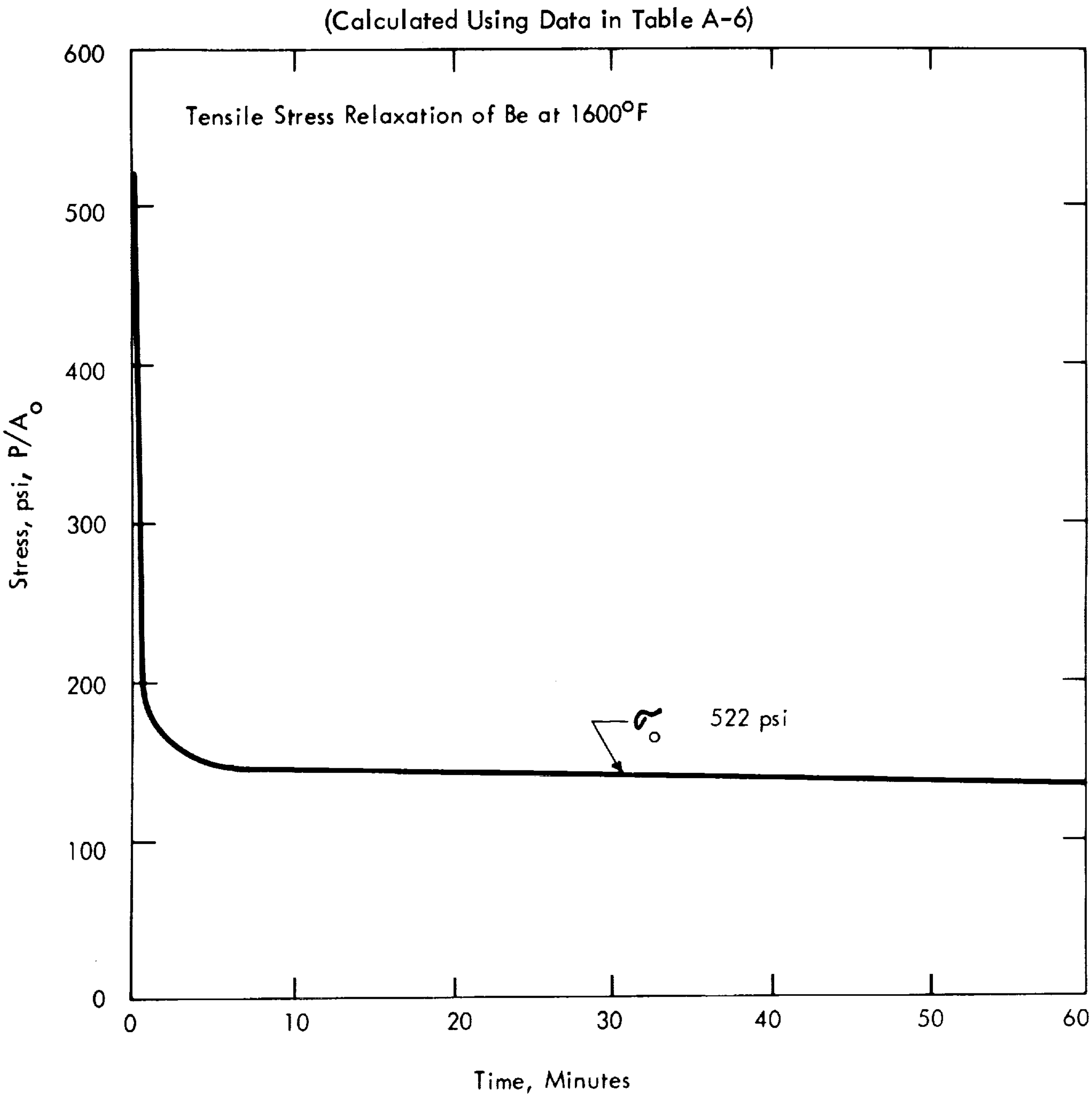

FIGURE 22. Tensile Stress-Relaxation Curves for Beryllium at 1600°F (Constant Cross-Head Control)

(Calculated Using Data in Table A-7)

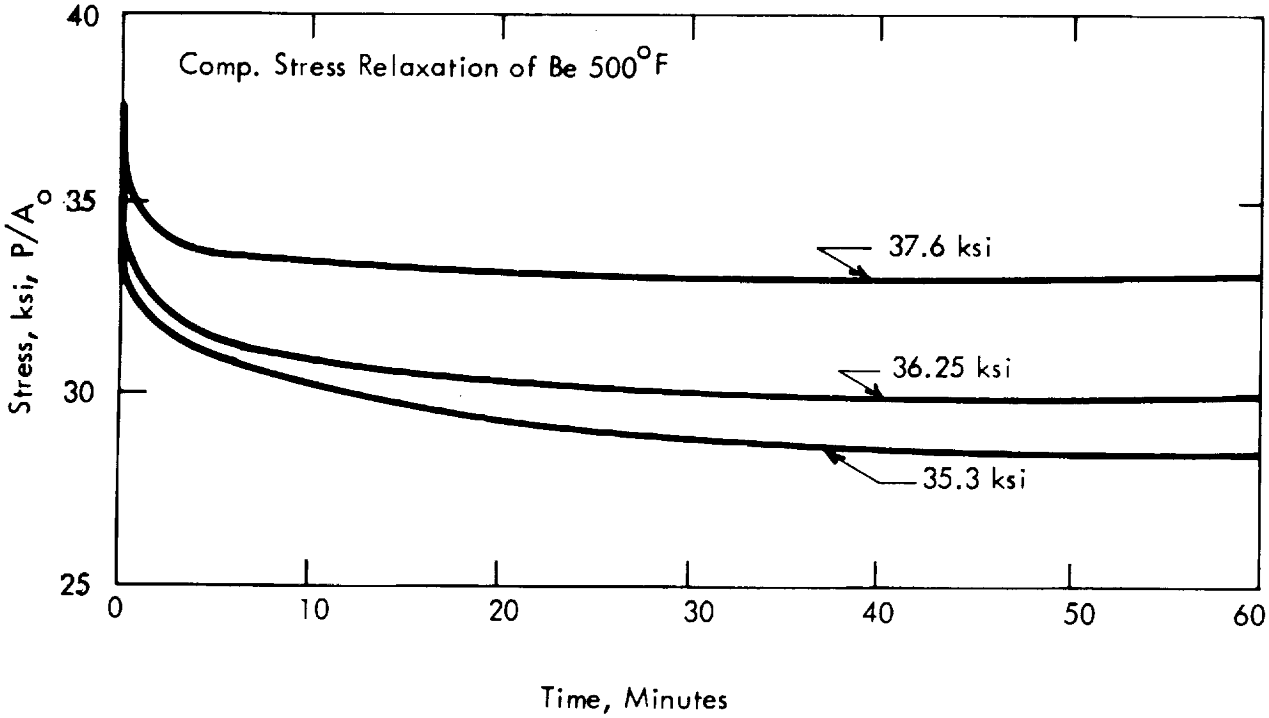

FIGURE 23. Compression Stress-Relaxation Curves for Beryllium at 500°F
(Constant Cross-Head Control)

(Calculated Using Data in Table A-7)

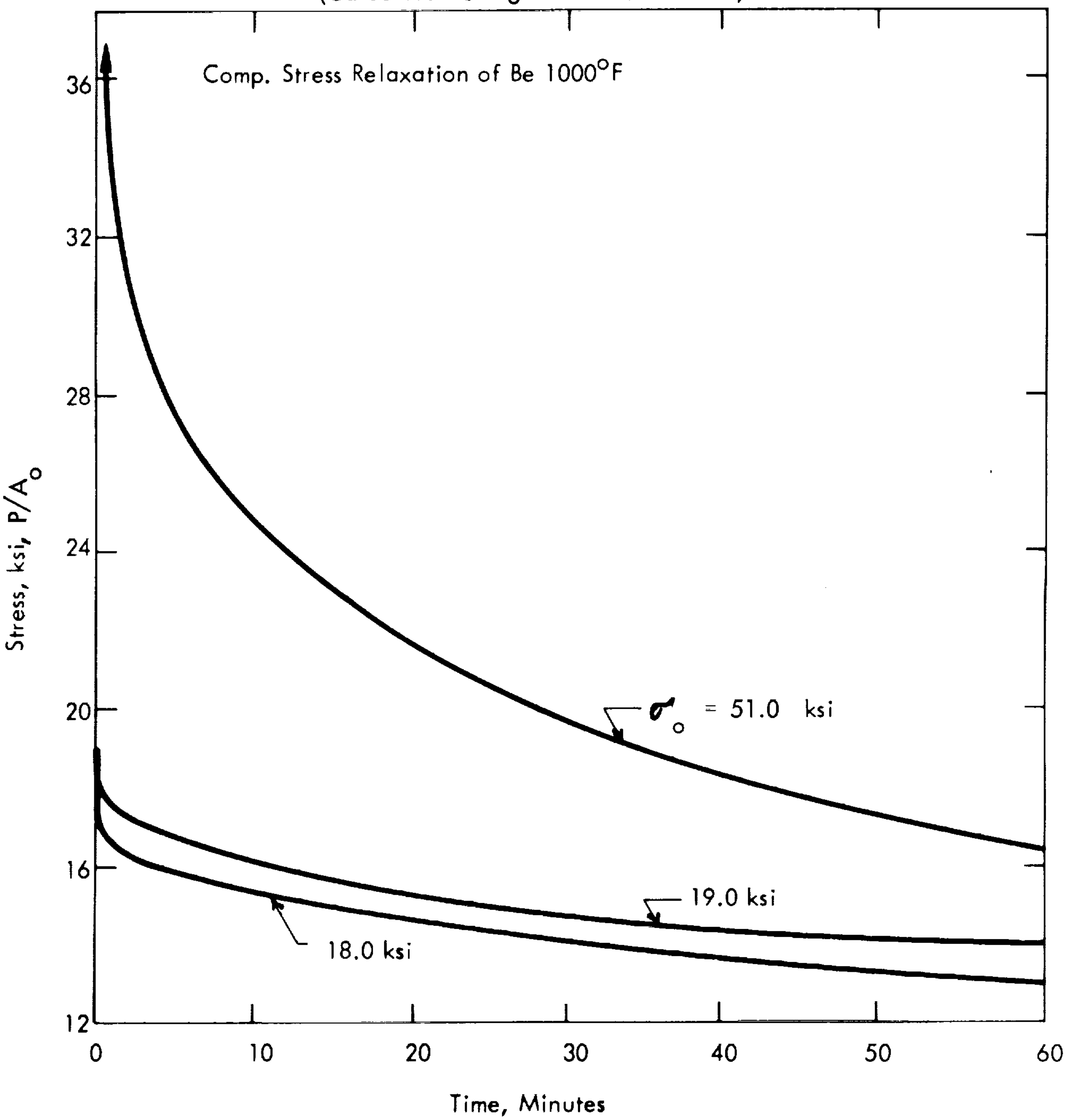

FIGURE 24. Compression Stress-Relaxation Curves for Beryllium at 1000°F (Constant Cross-Head Control

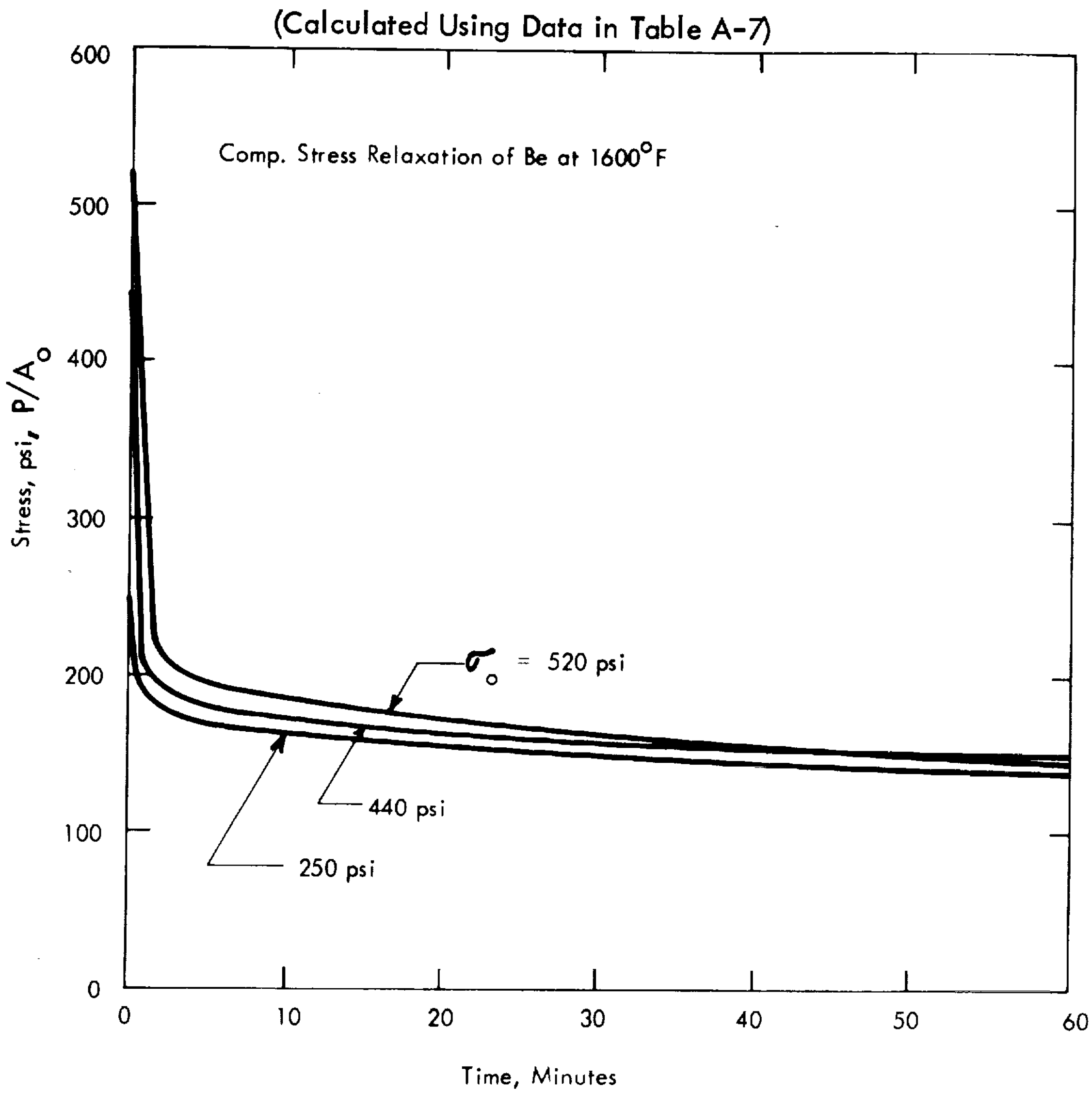

FIGURE 25. Compression Stress-Relaxation Curves for Beryllium at 1600°F (Constant Cross-Head Control)

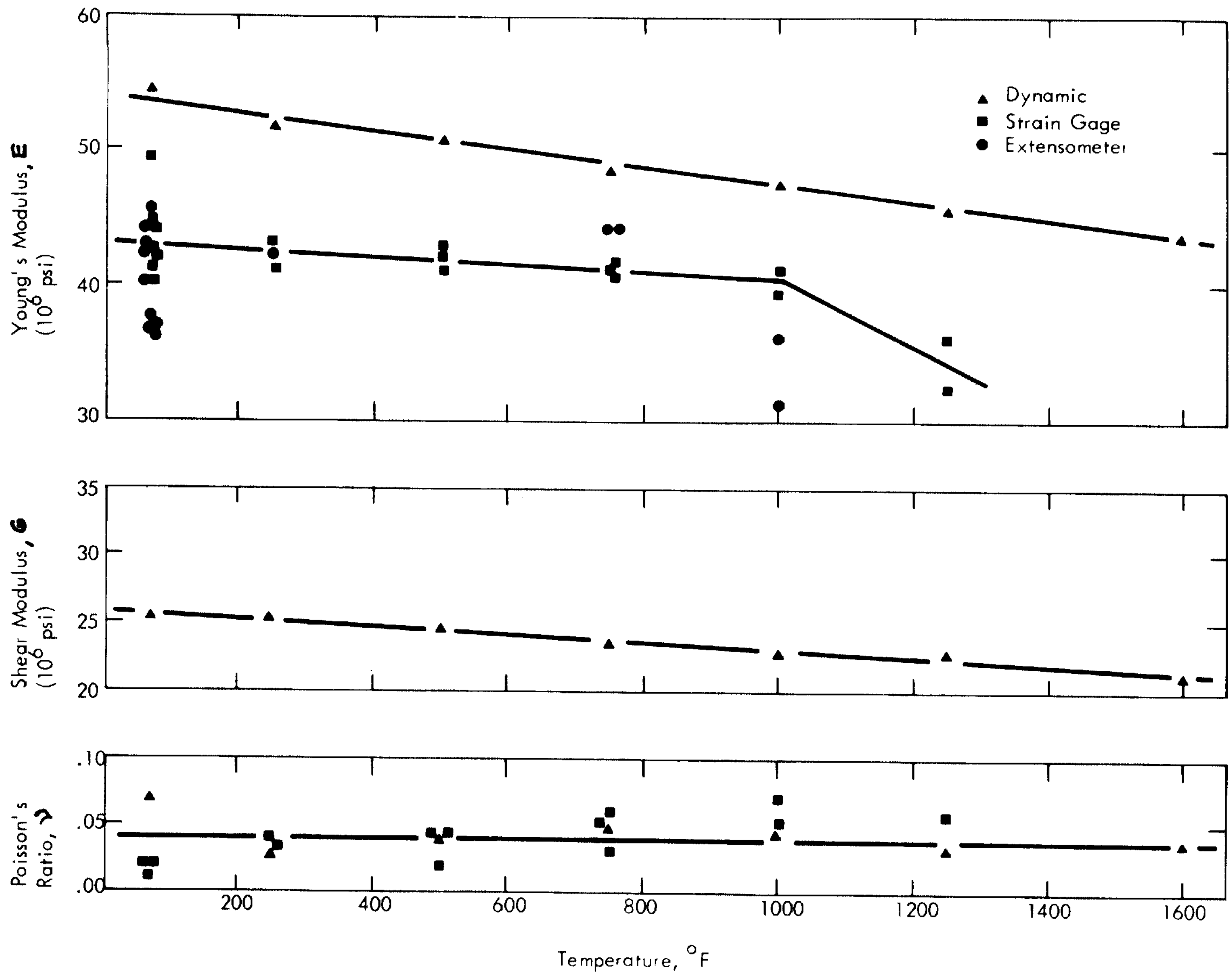

Figure 26. Elastic Properties of Beryllium as a Function of Temperature. (The data are listed in Table A-8)

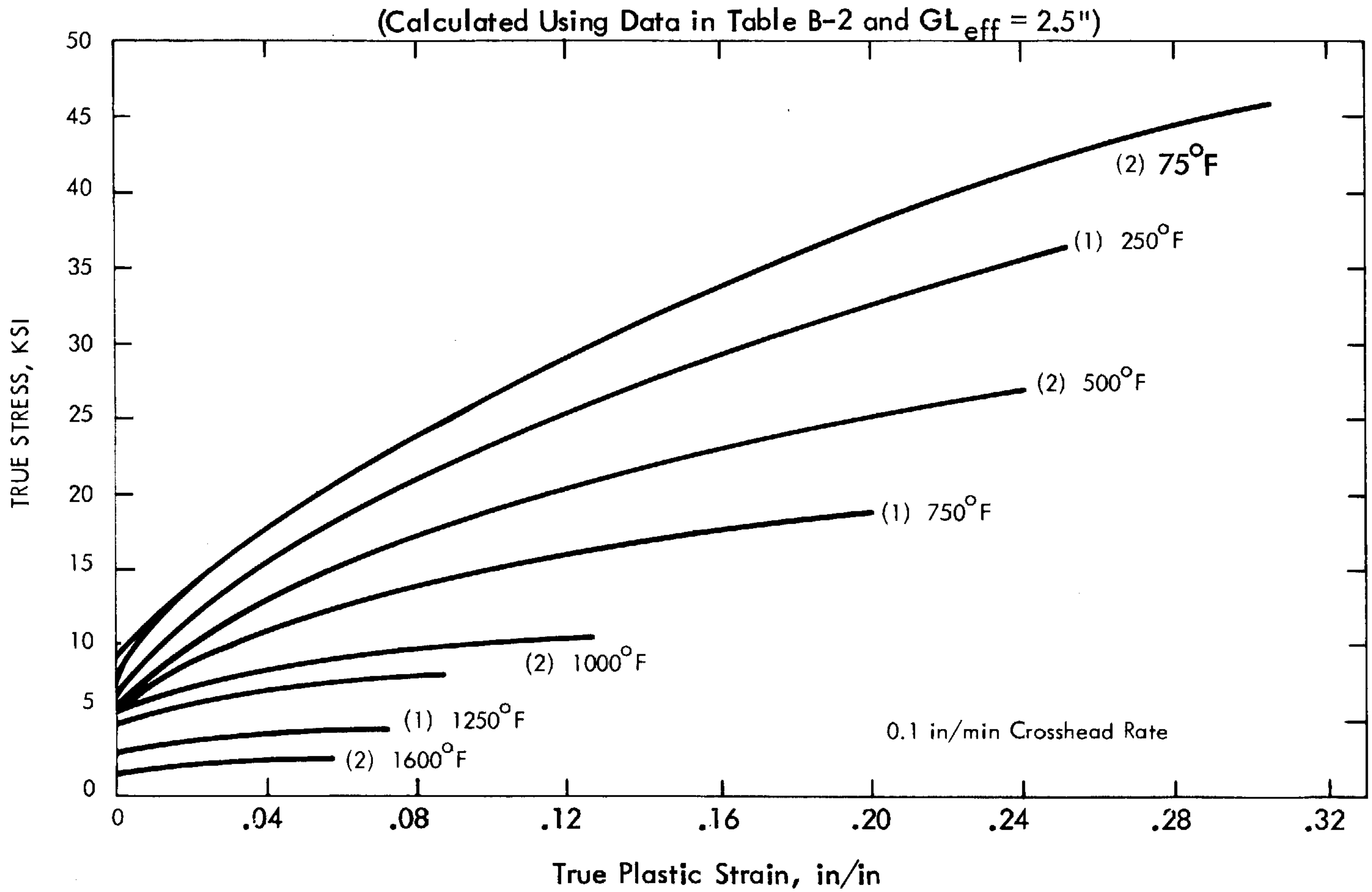

FIGURE 27 - Tensile True Stress-True Strain Curves for OFHC Copper as a Function of Temperature. Numbers in Parenthesis Refer to Number of Tests.

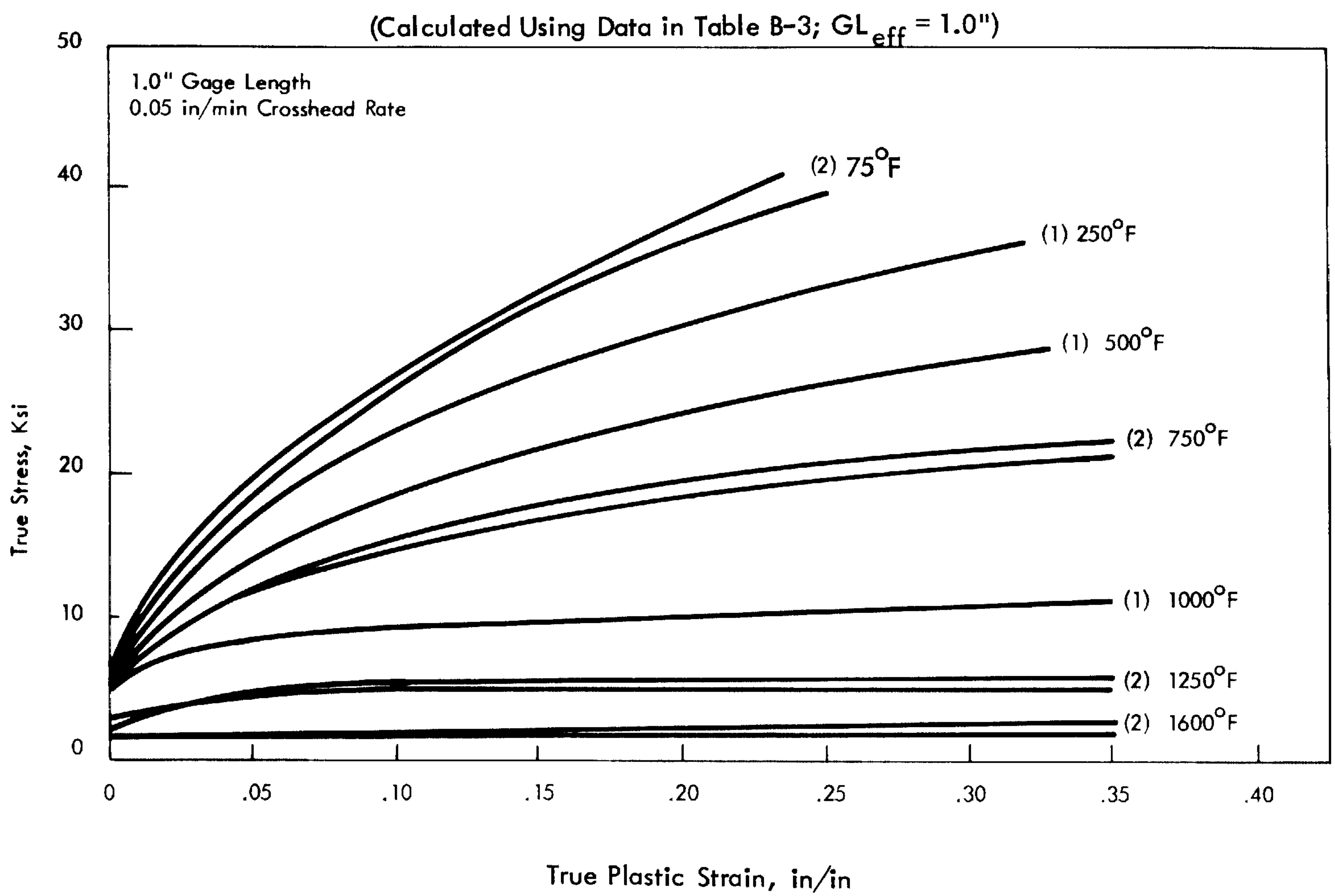

Figure 28. Compression True Stress-True Strain Curves for OFHC Copper as a Function of Temperature. (Numbers in parenthesis refer to number of tests)

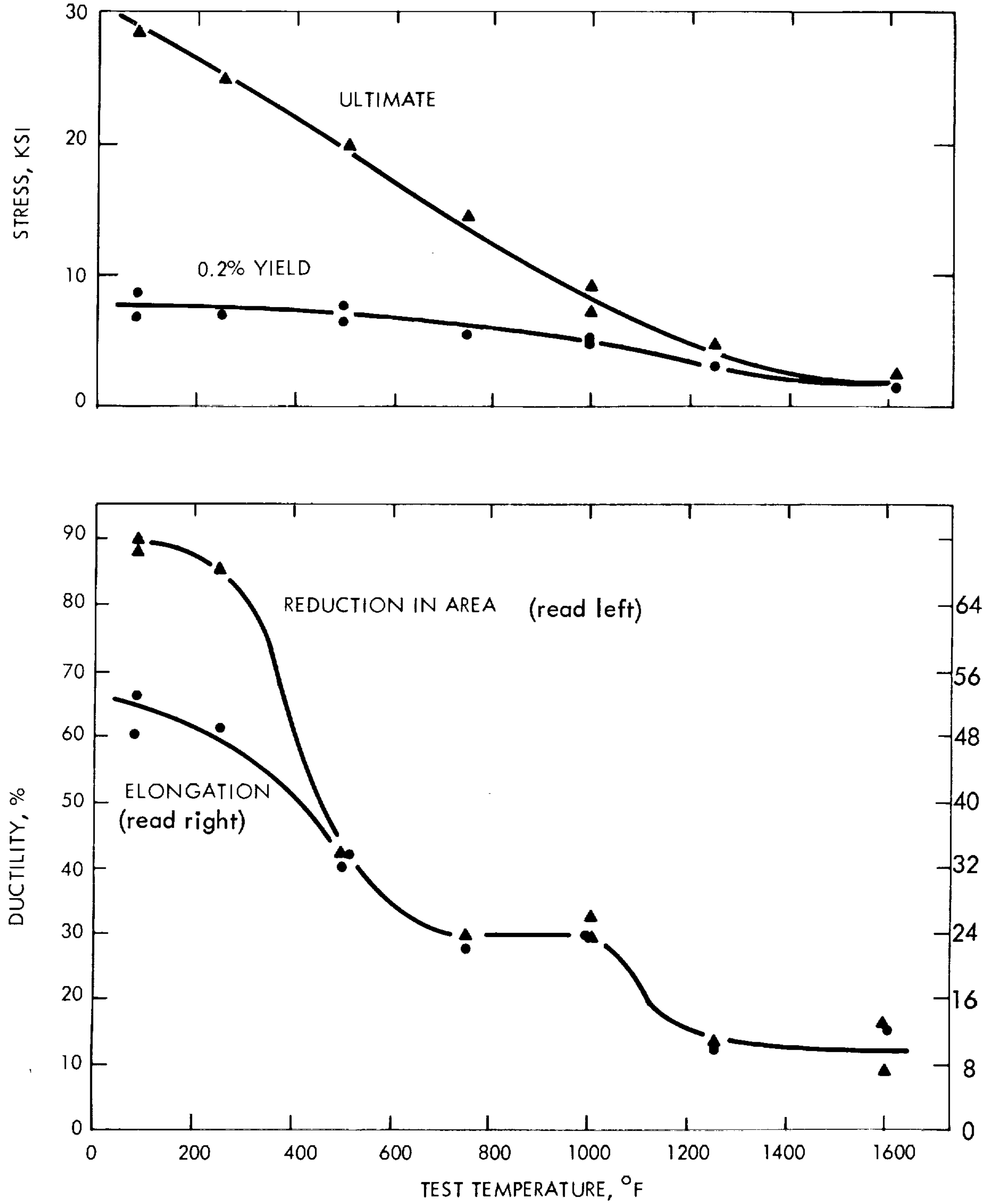

FIGURE 29 - Engineering Tensile Properties of OFHC Copper as a Function of Temperature

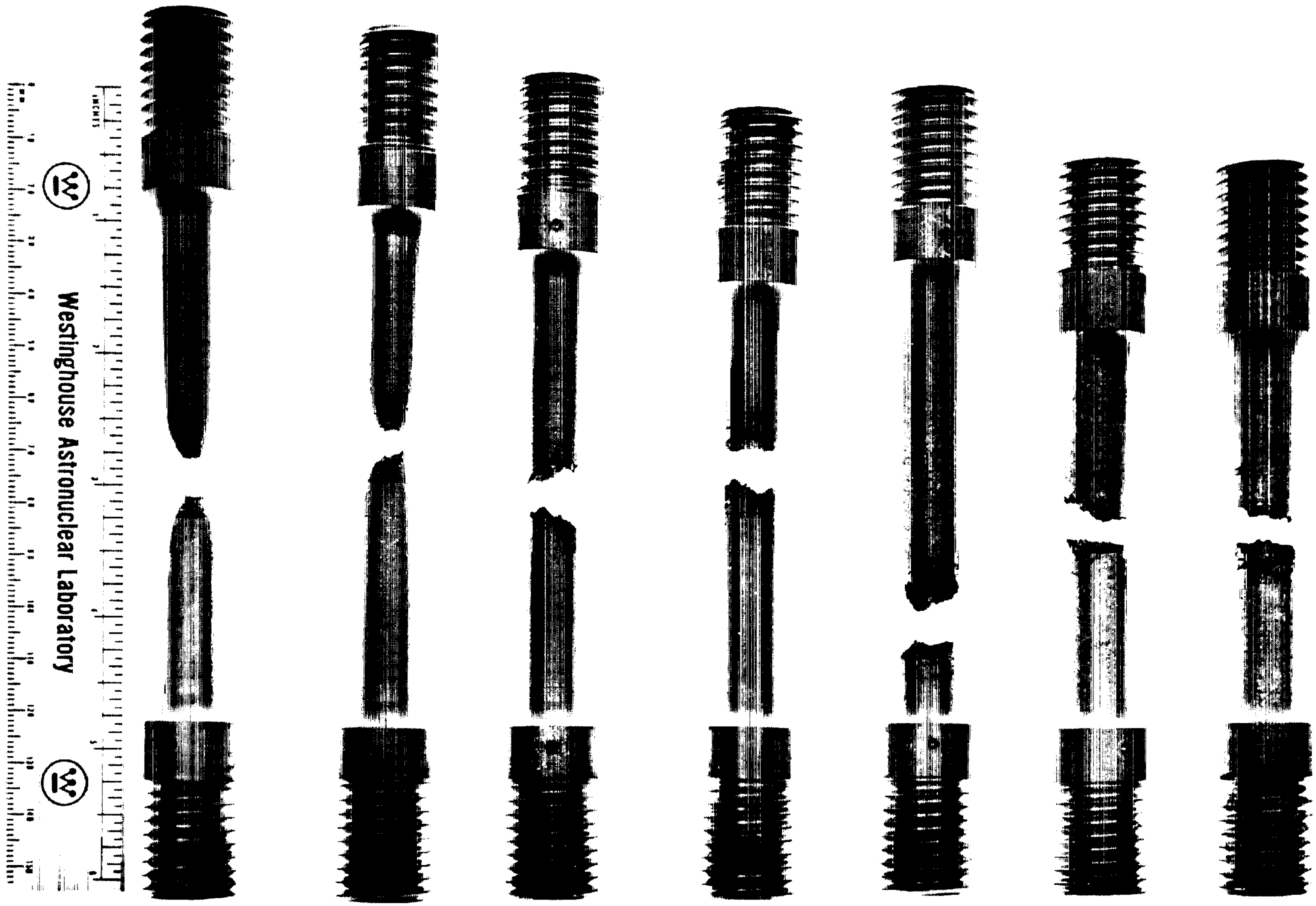

Test. Temp.	80°F	250°F	500°F	750°F	1000°F	1250°F	1600°F
% Elong. in 2"	61.2	61.0	37.9	27.0	36.7	17.3	14.8
% RA	88.1	85.3	42.3	28.9	32.1	12.9	8.7

FIGURE 30. OFHC Copper Tensile Specimens After Testing as a Function of Temperature. Tension Tests Run at 0.1 in/min Crosshead Rate.

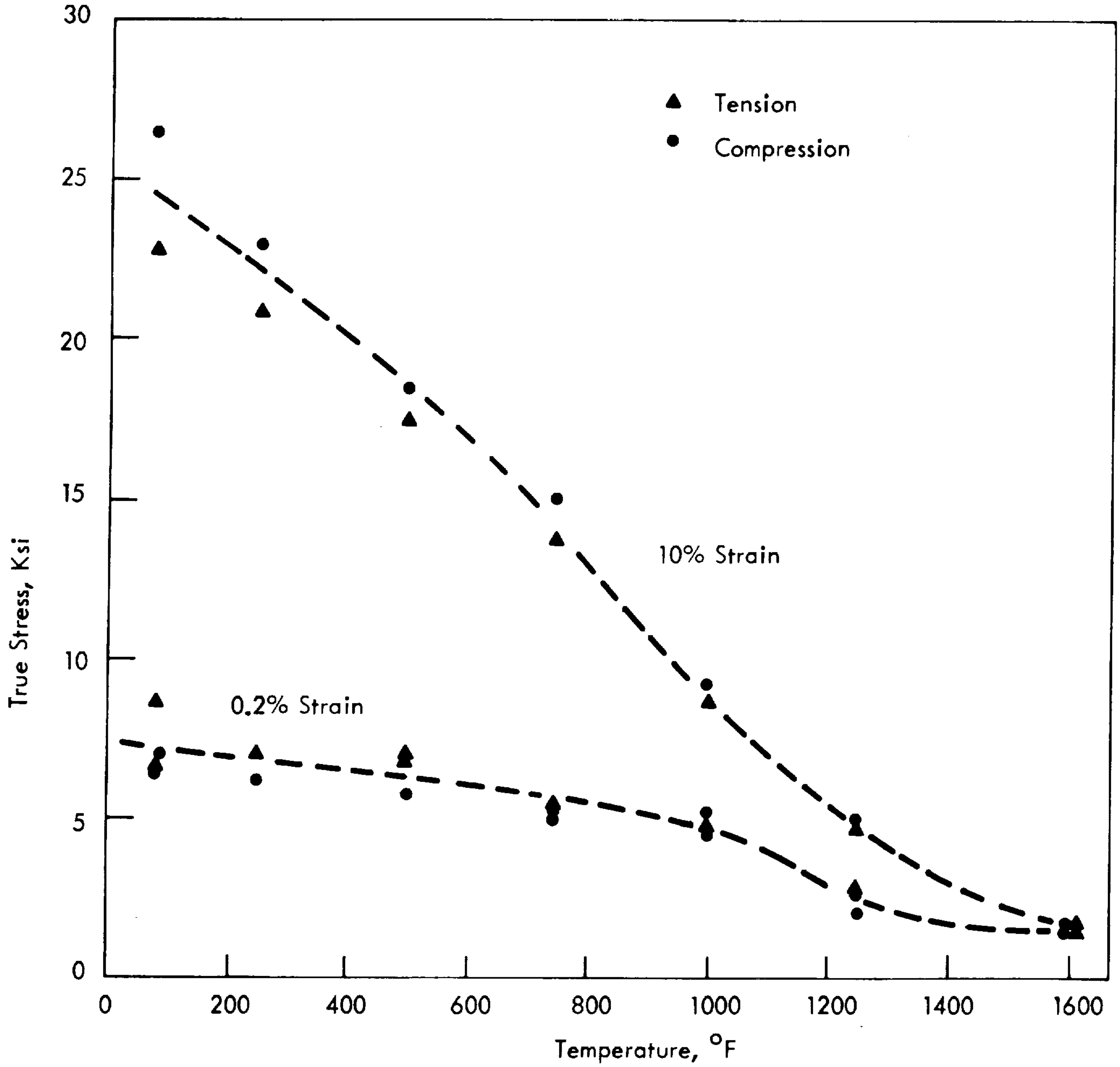

FIGURE 31. Yield Stress (0.2% Strain) and Flow Stress at 10% True Strain of OFHC Copper in Tension and Compression as a Function of Temperature

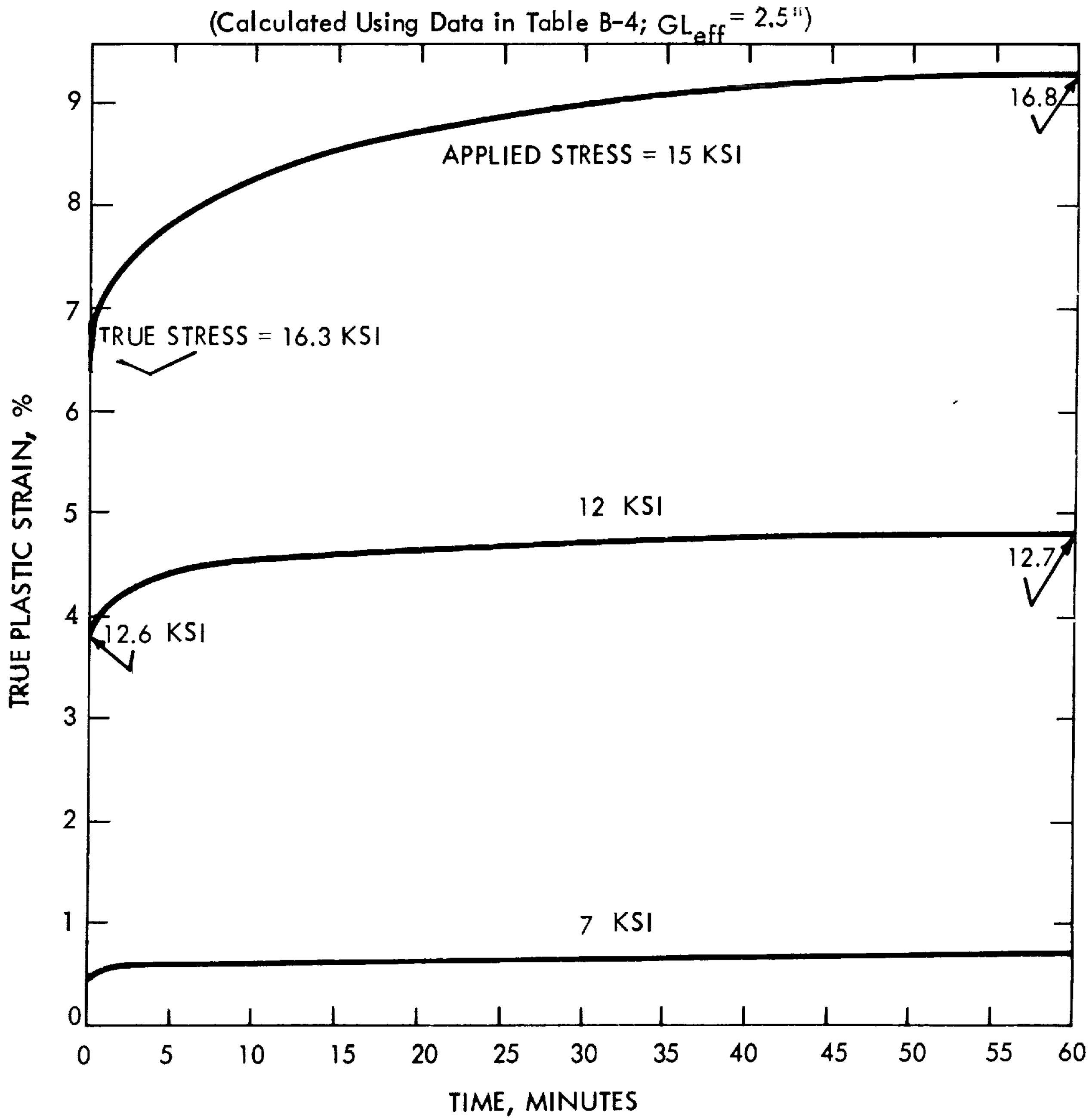

FIGURE 32 - Tensile Creep Curves on OFHC Copper at 500°F

(Calculated Using Data in Table B-4; GL_{eff} = 2.5")

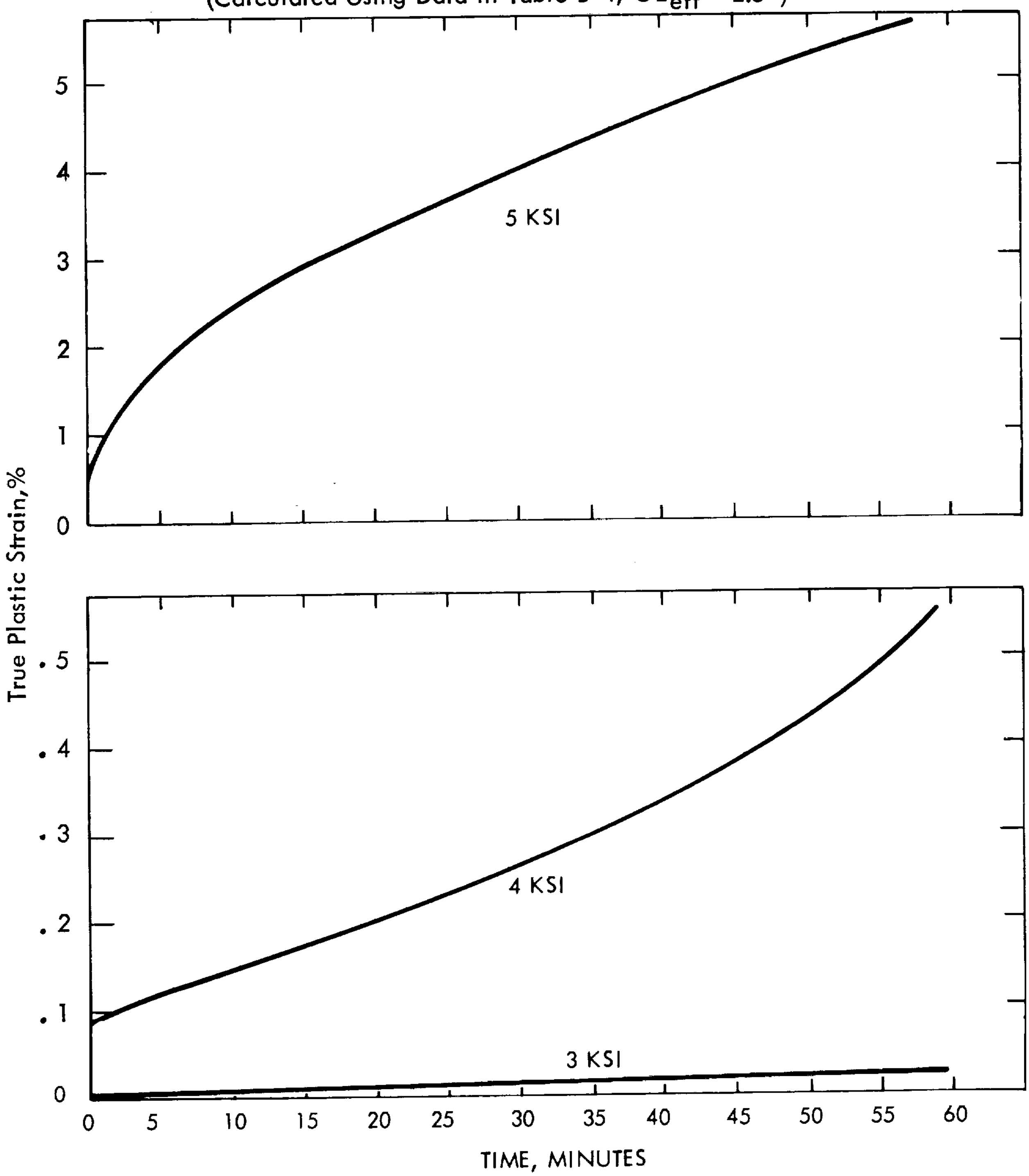

FIGURE 33 - Tensile Creep Curves on OFHC Copper at 1000°F

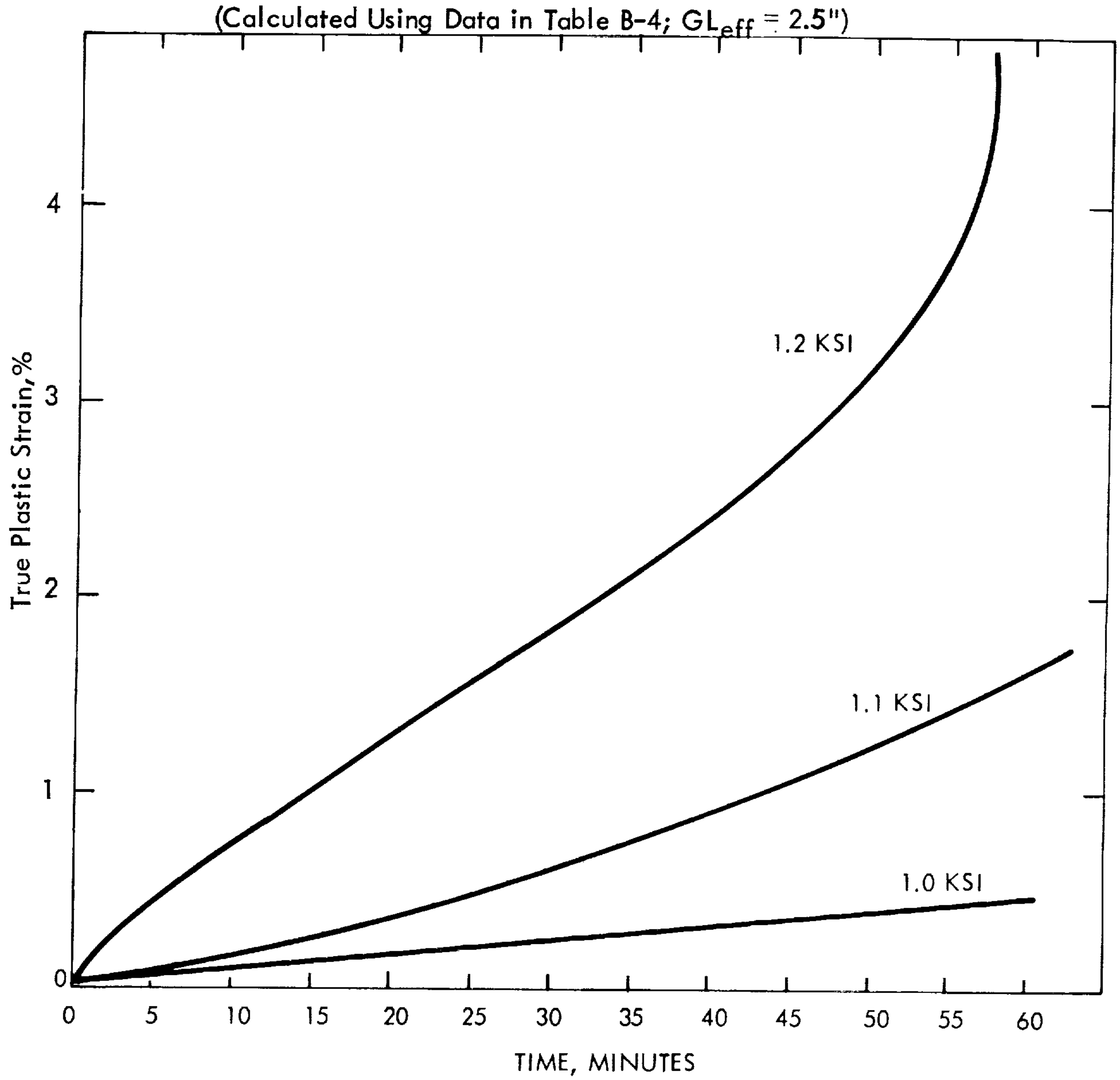

FIGURE 34 - Tensile Creep Curves on OFHC Copper at 1600°F

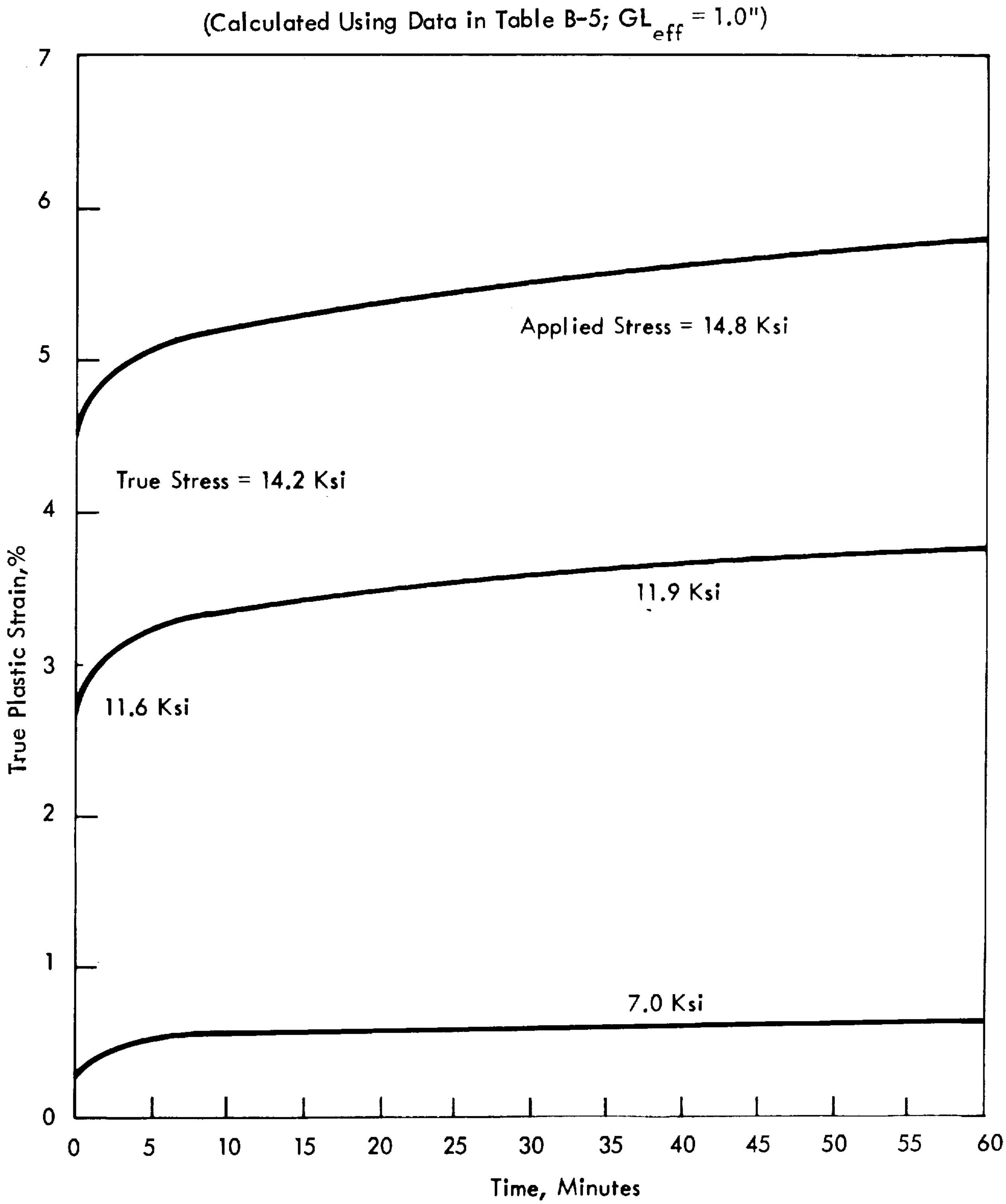

FIGURE 35 - Compression Creep Curves on OFHC Copper at 500°F

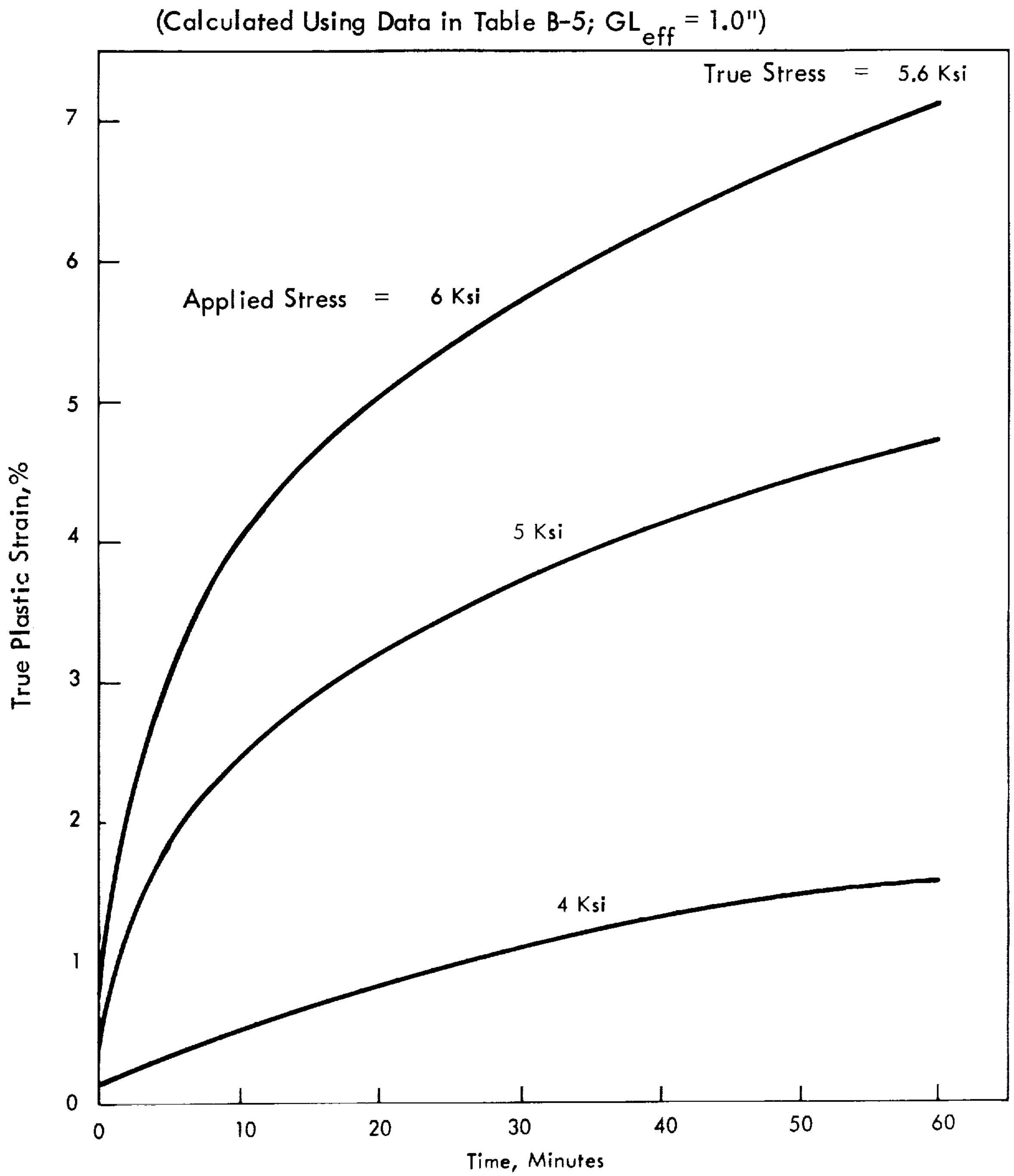

Figure 36. Compression Creep Curves on OFHC Copper at 1000°F

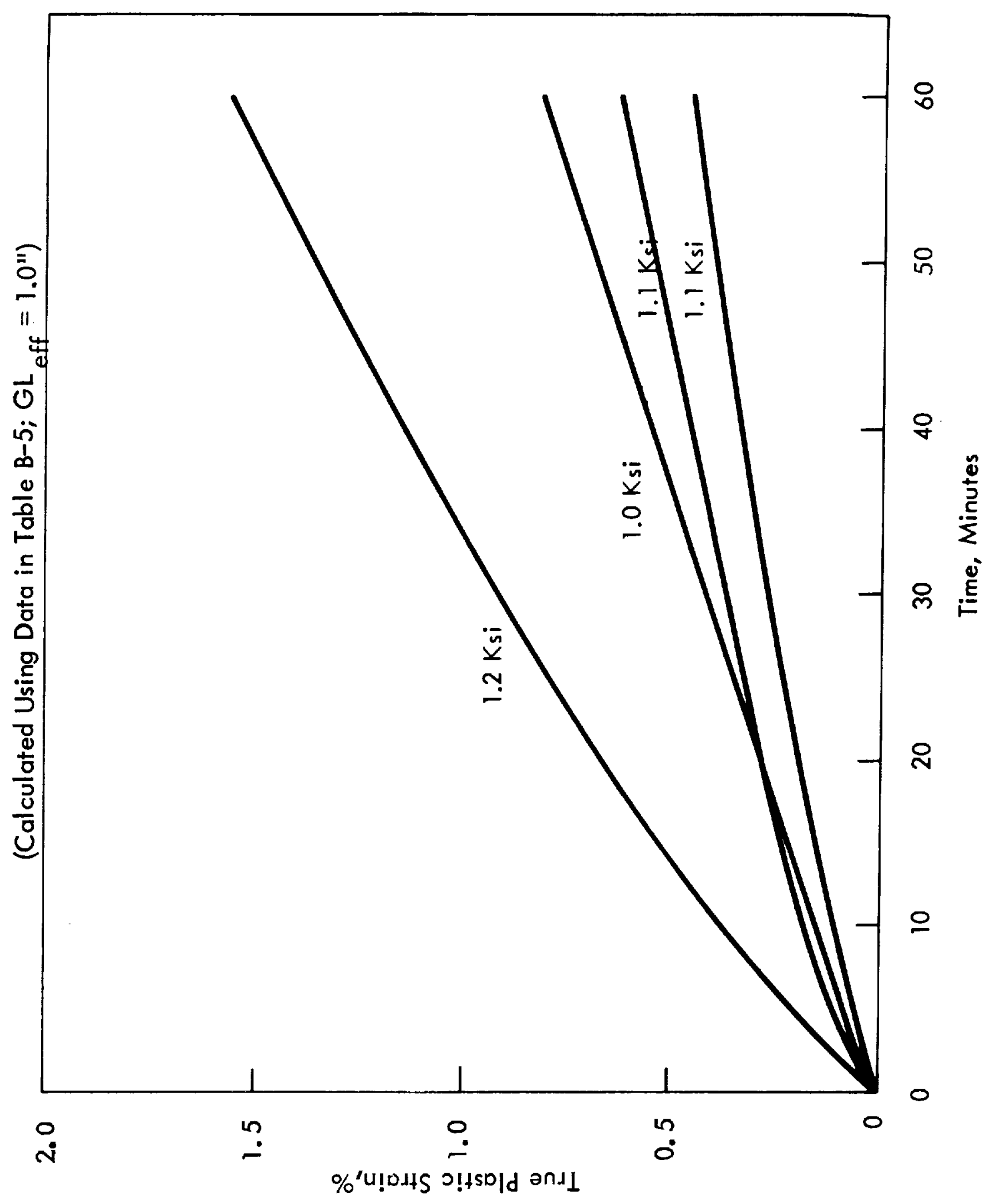

FIGURE 37 - Compression Creep Curves on OFHC Copper at 1600°F.

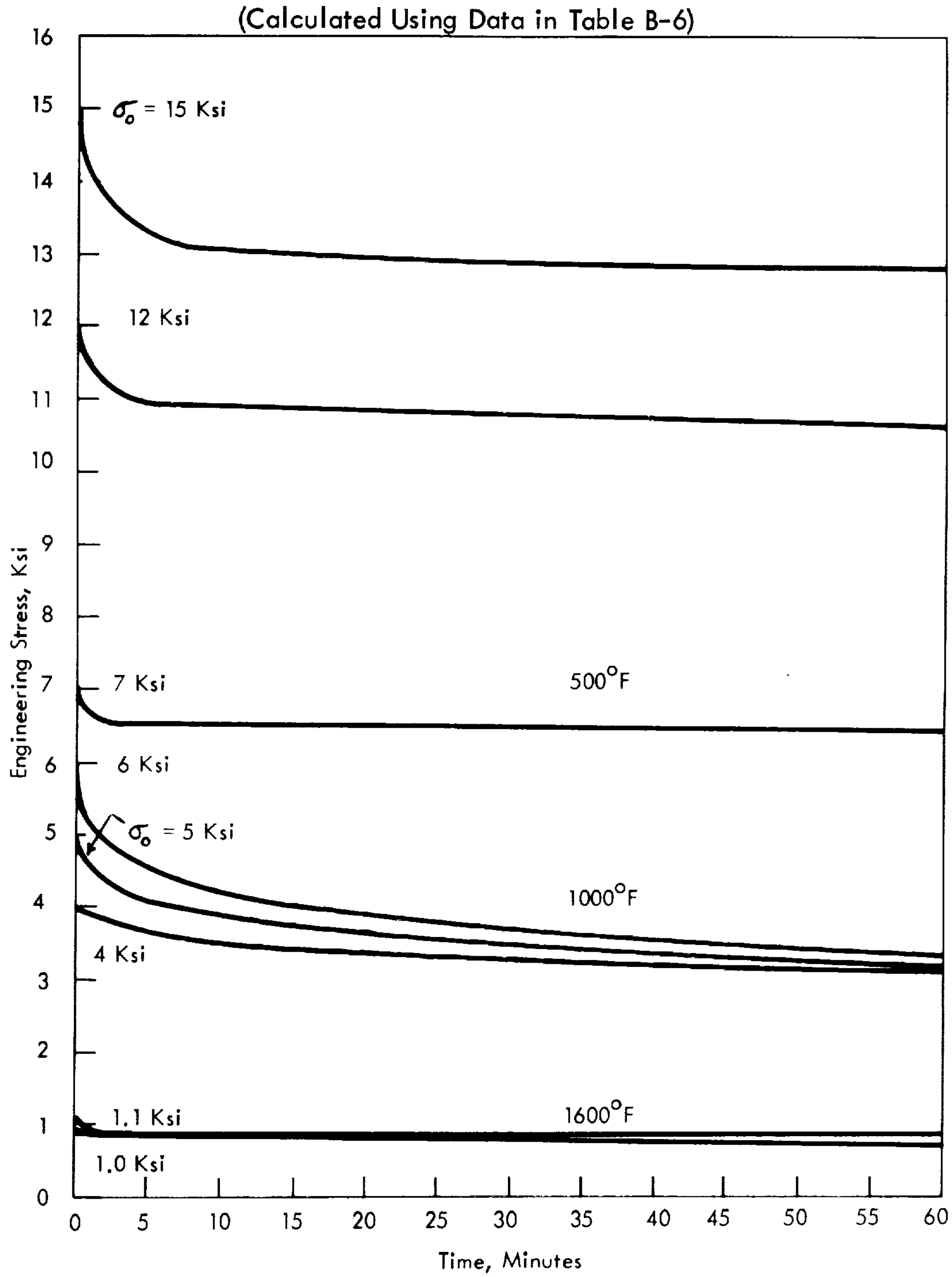

Figure 38. Tension Stress-Relaxation Curves for OFHC Copper (Constant Cross-Head Control)

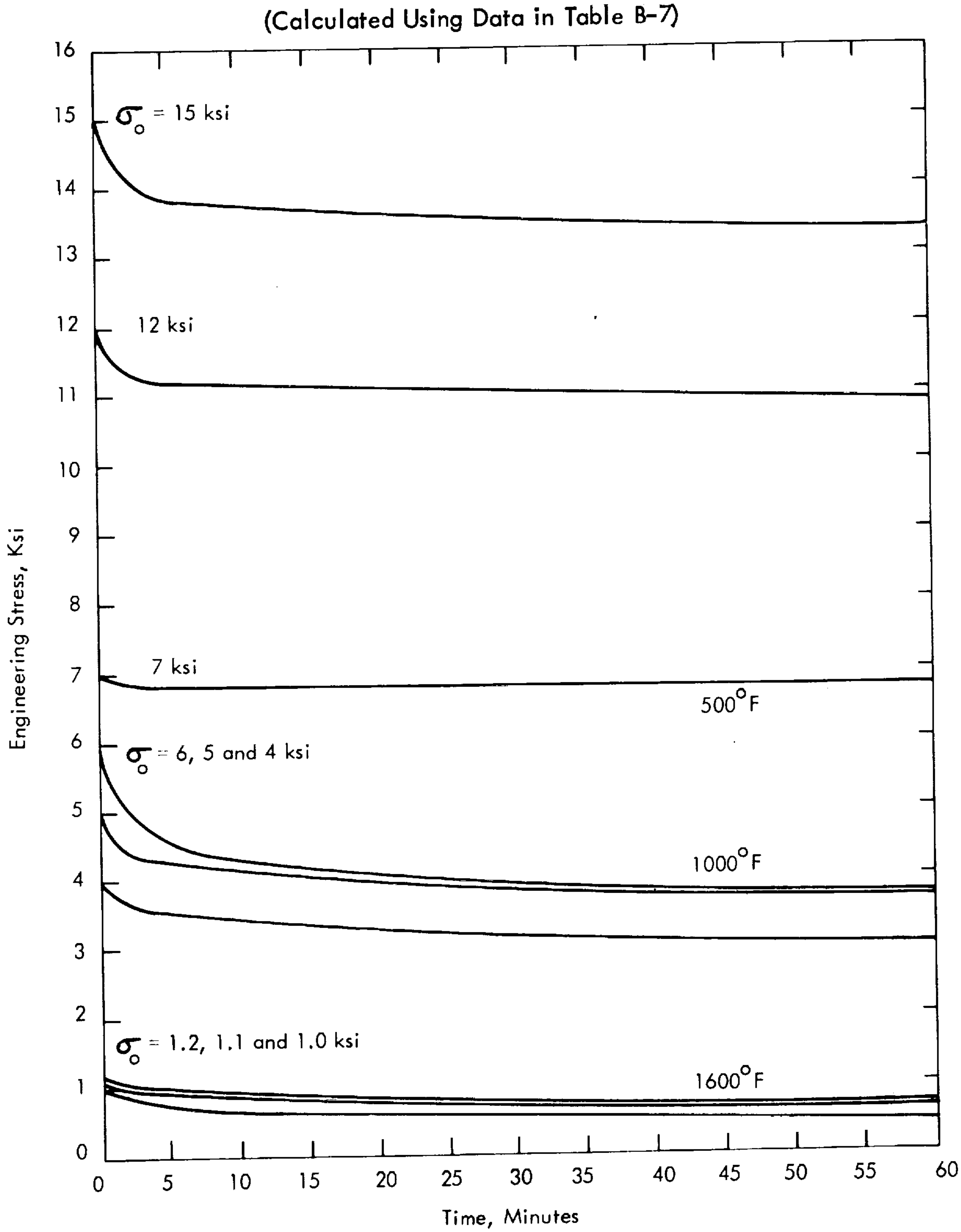

FIGURE 39 - Compression Stress-Relaxtion Curves for OFHC Copper (Constant Cross-Head Control)

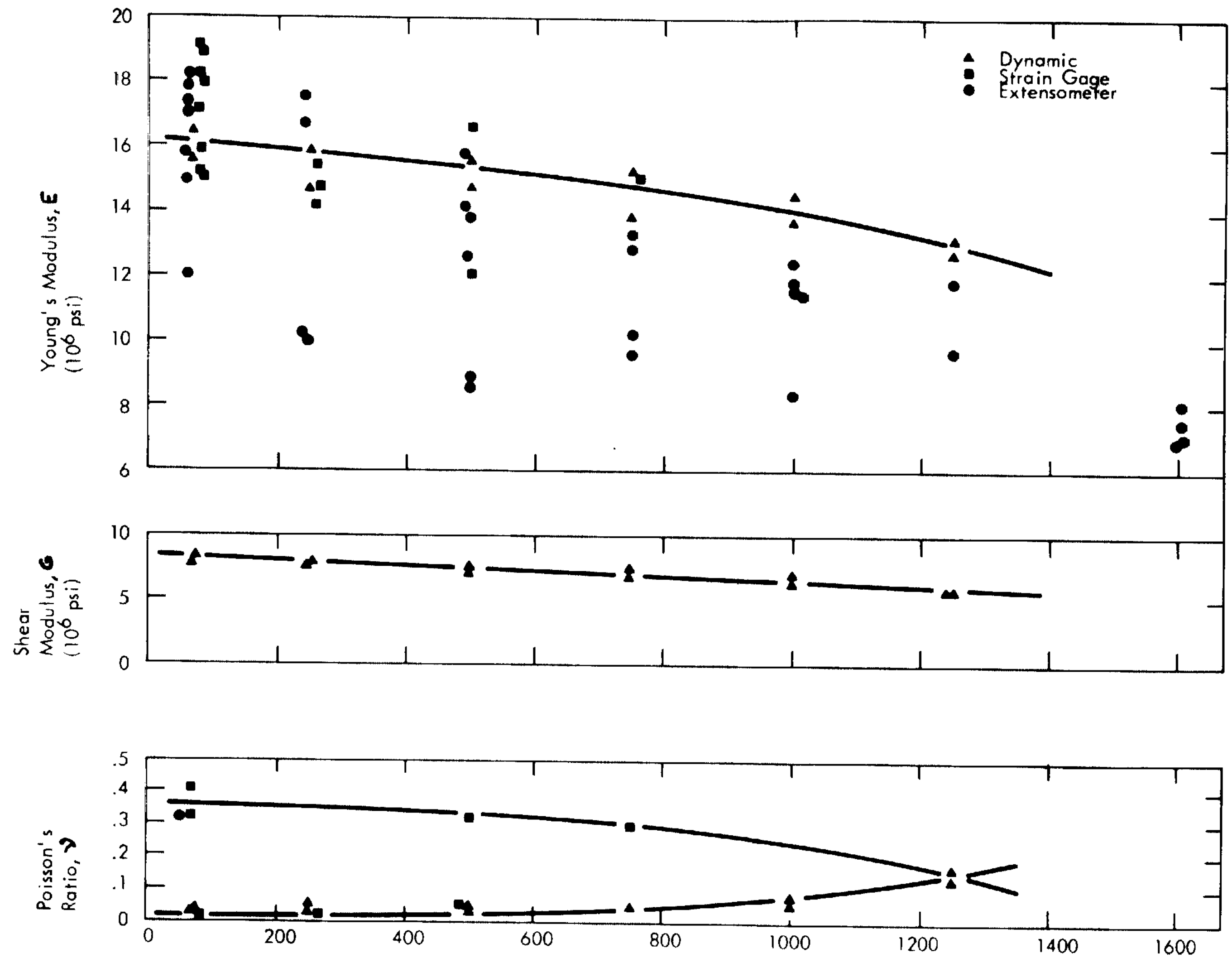

Figure 40. Elastic Properties of OFHC Copper as a Function of Temperature. (The data are listed in Table B-8)

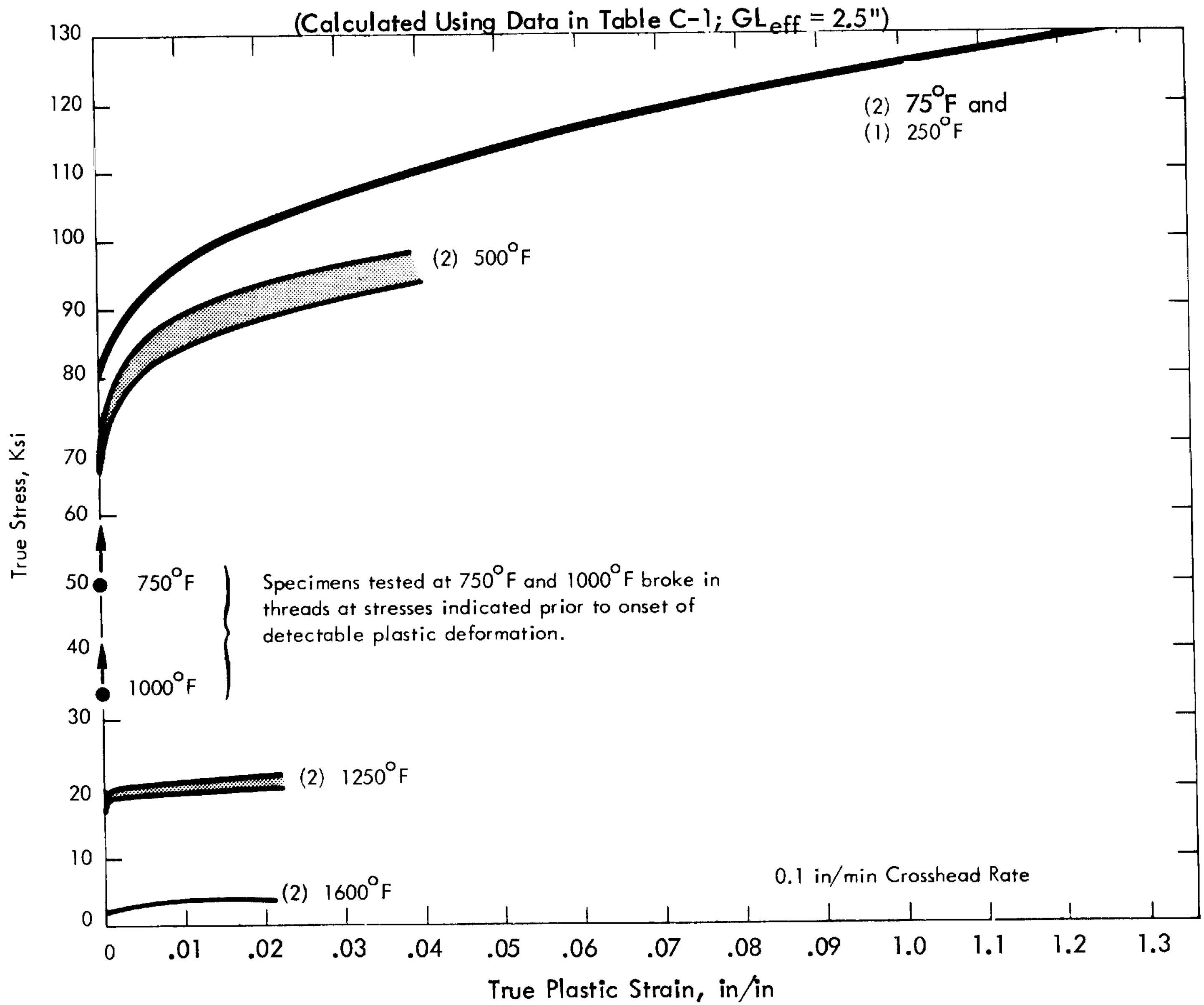

FIGURE 41 - Tensile True Stress - True Strain Curves for Beryllium-Copper Alloy (Alloy No. 10) as a Function of Temperature. Numbers in Parenthesis Refer to Number of Tests.

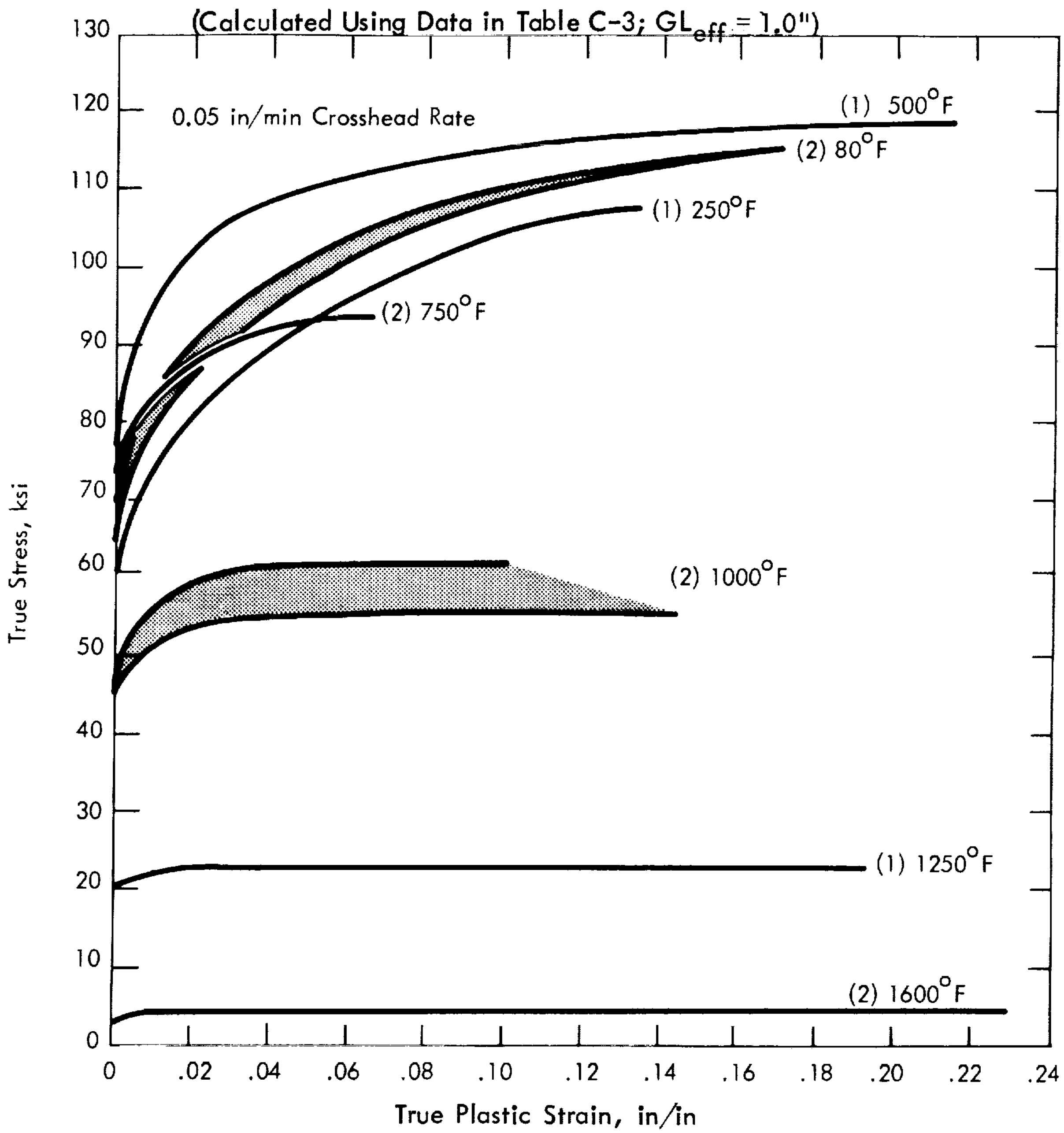

FIGURE 42 - Compression True Stress-True Strain Curves for Beryllium-Copper Alloy (Alloy No. 10) as a Function of Temperature. Numbers in Parenthesis Refer to Number of Tests.

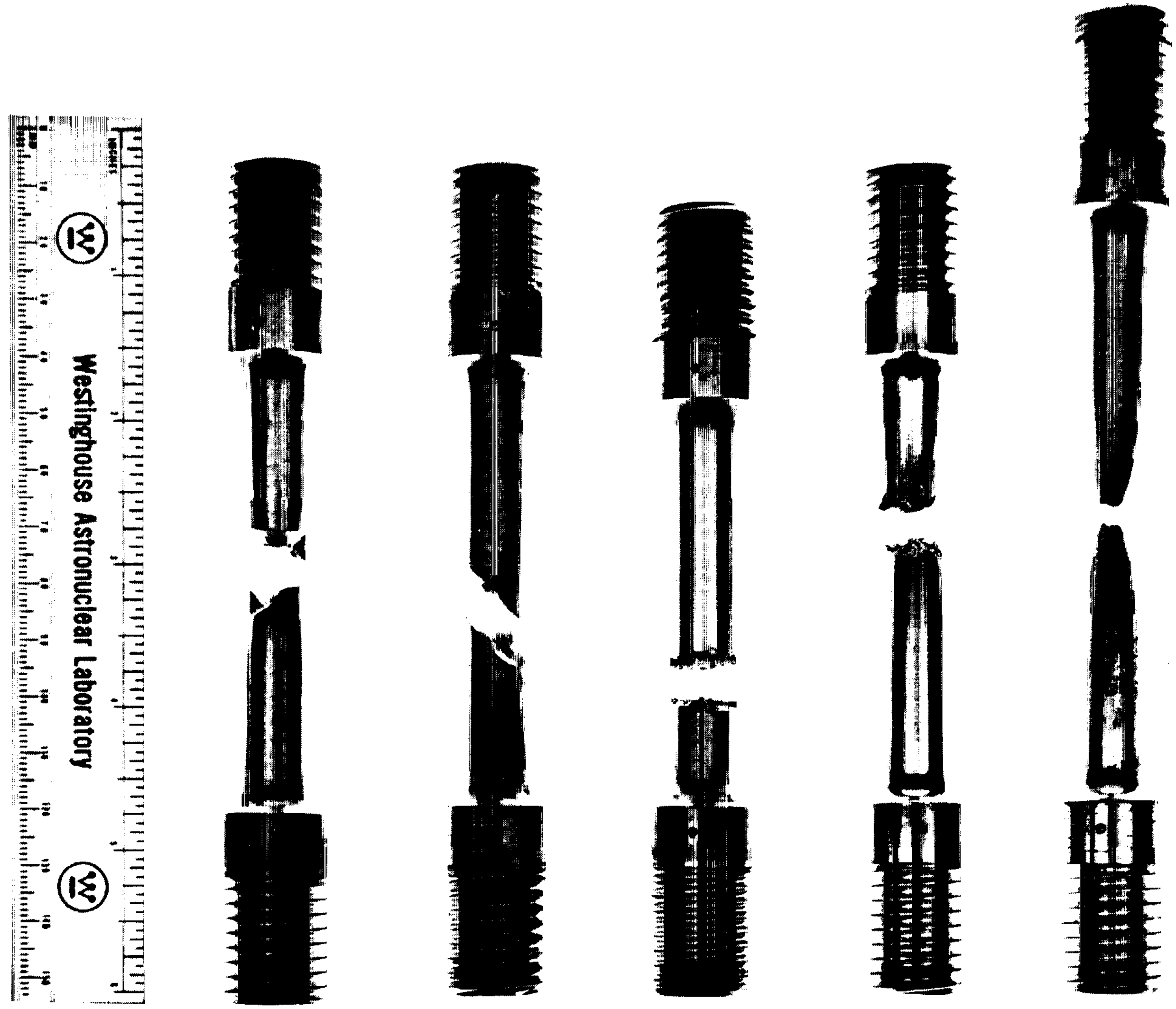

Test Temp.	80°F	250°F	500°F	1250°F	1600°F
% Elong. in 2"	19.3	17.7	5.3	16.7	76.5
% RA	38.9	24.7	8.6	33.9	92.1

FIGURE 43 - Beryllium-Copper Alloy No. 10 Tensile Specimens After Testing as a Function of Temperature. Tension Tests Run at 0.1 in/min Crosshead Rate.

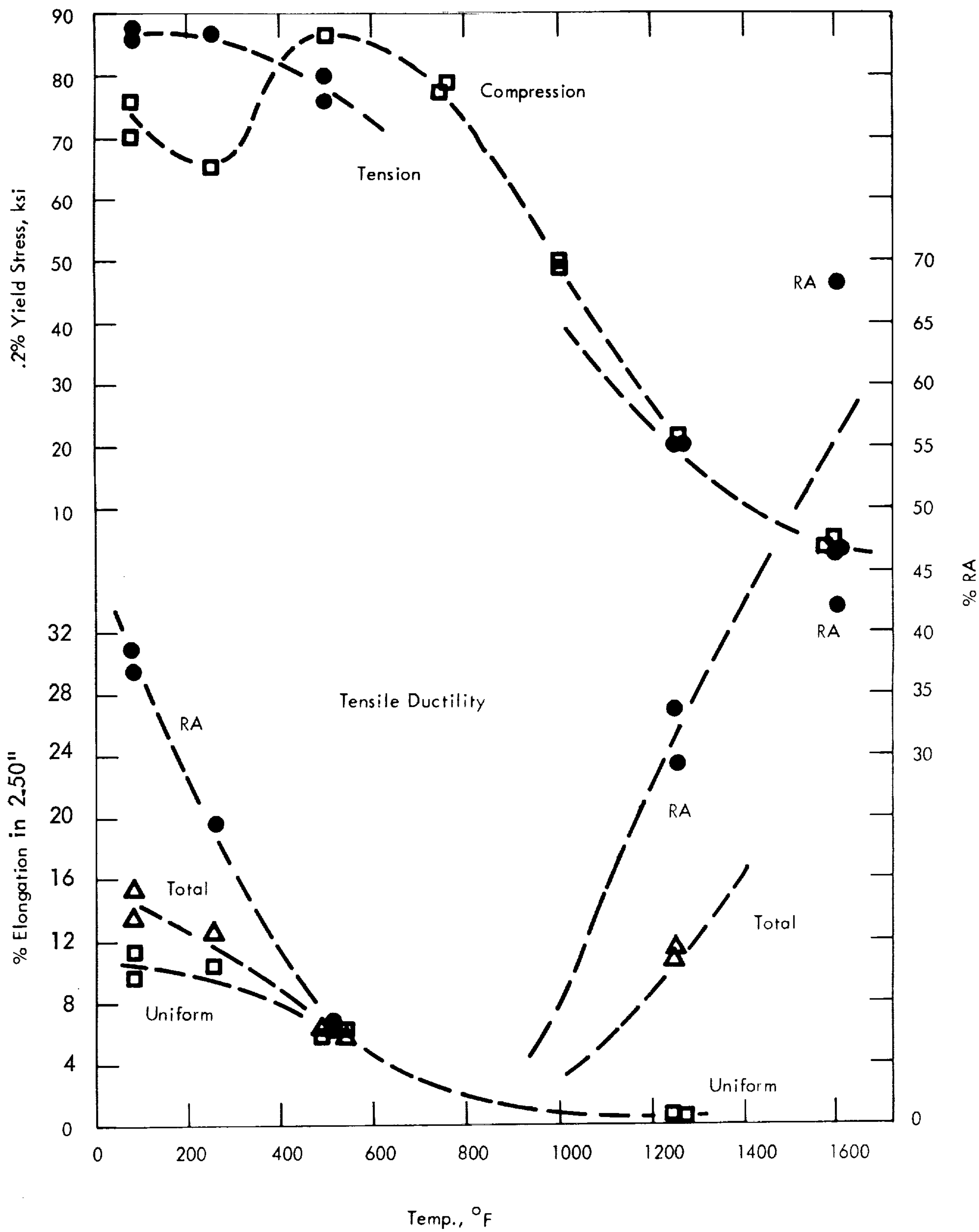

Figure 44 - Tensile Properties of Beryllium-Copper Alloy 10 as a Function of Temperature

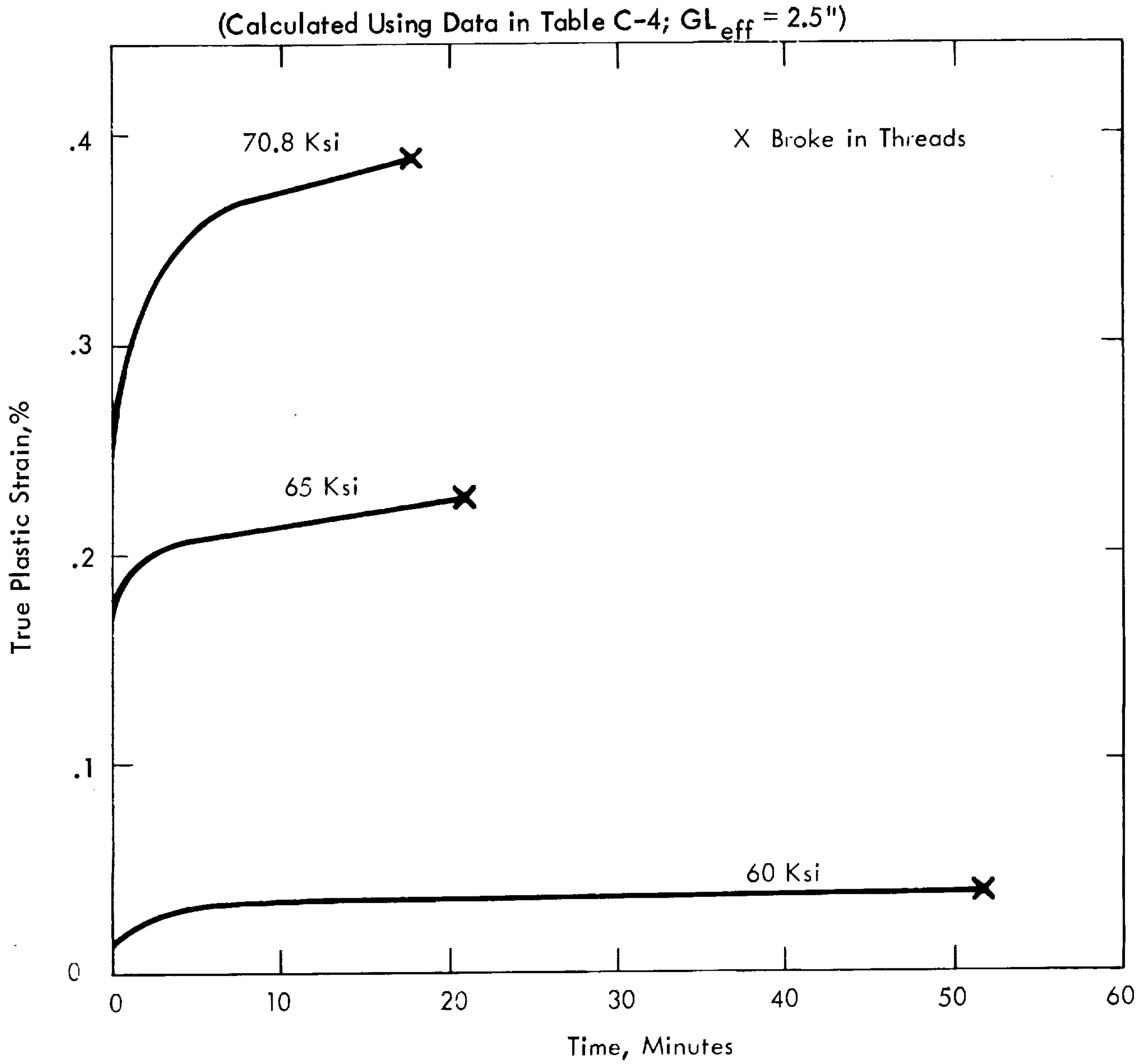

FIGURE 45 - Tension Creep Curves on Beryllium-Copper Alloy No. 10 at 500°F

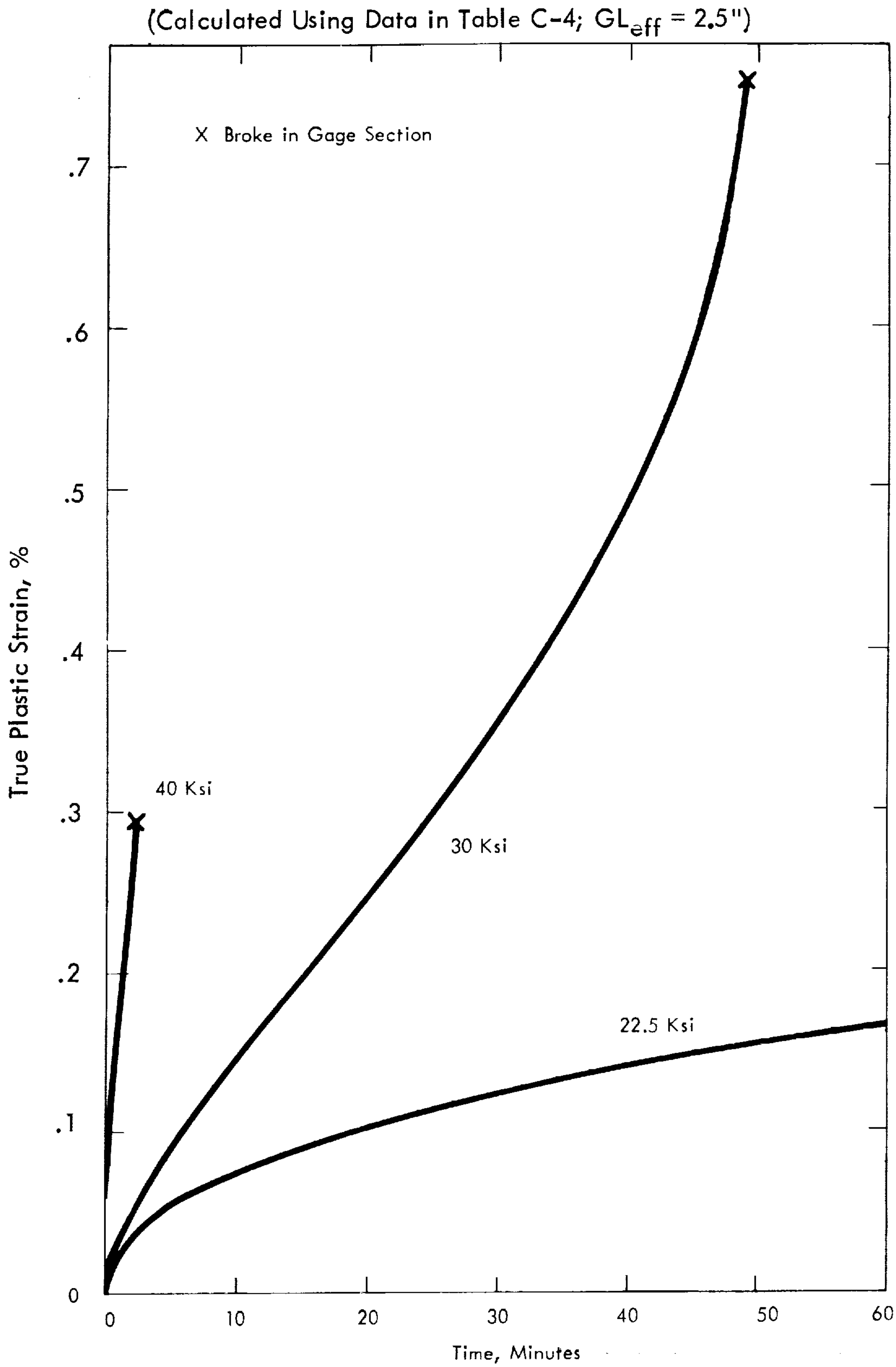

FIGURE 46 - Tension Creep Curves on Beryllium-Copper Alloy No. 10 at 1000°F (0.357" Diameter Gage Section)

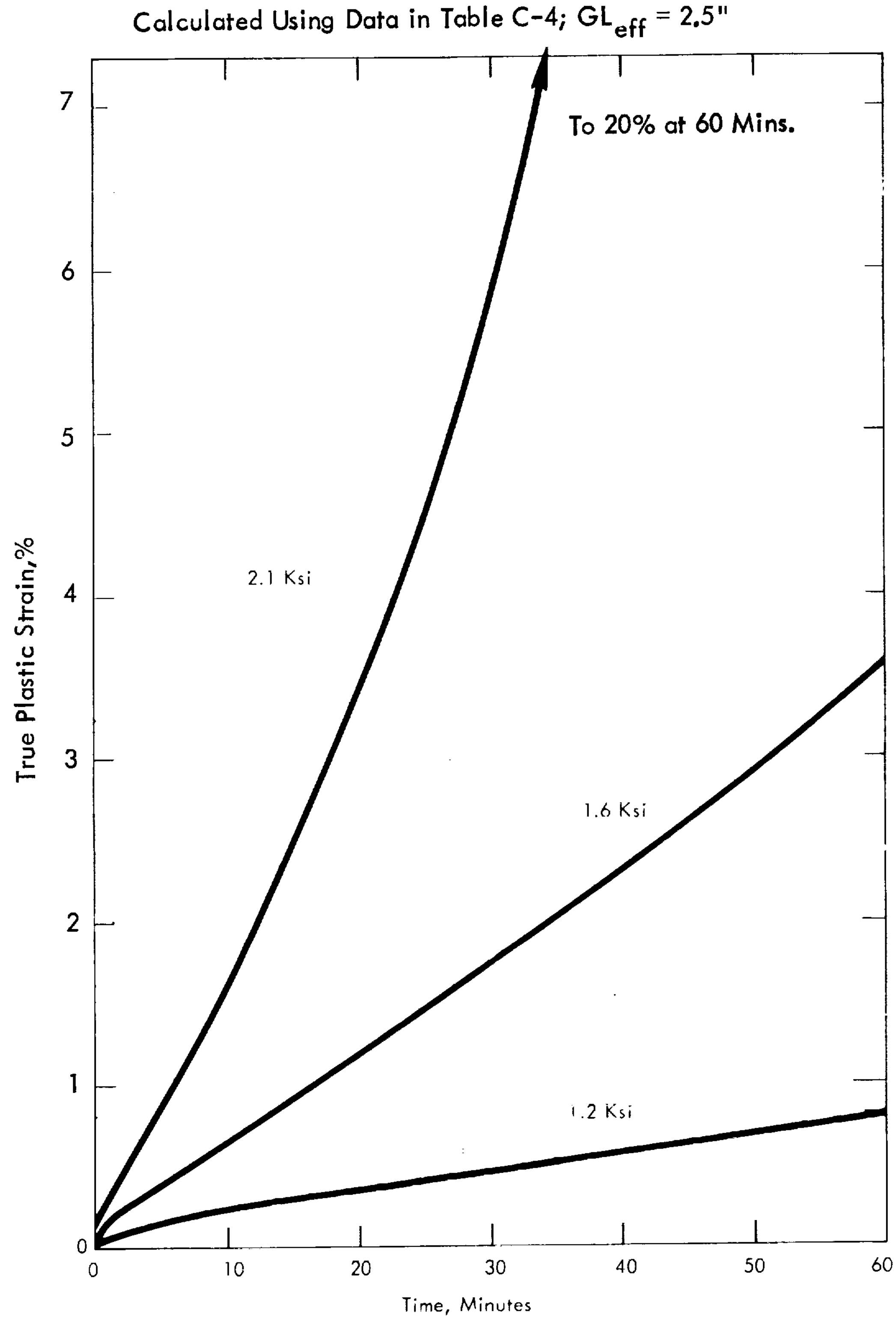

FIGURE 47 - Tension Creep Curves on Beryllium-Copper Alloy No. 10 at 1600°F

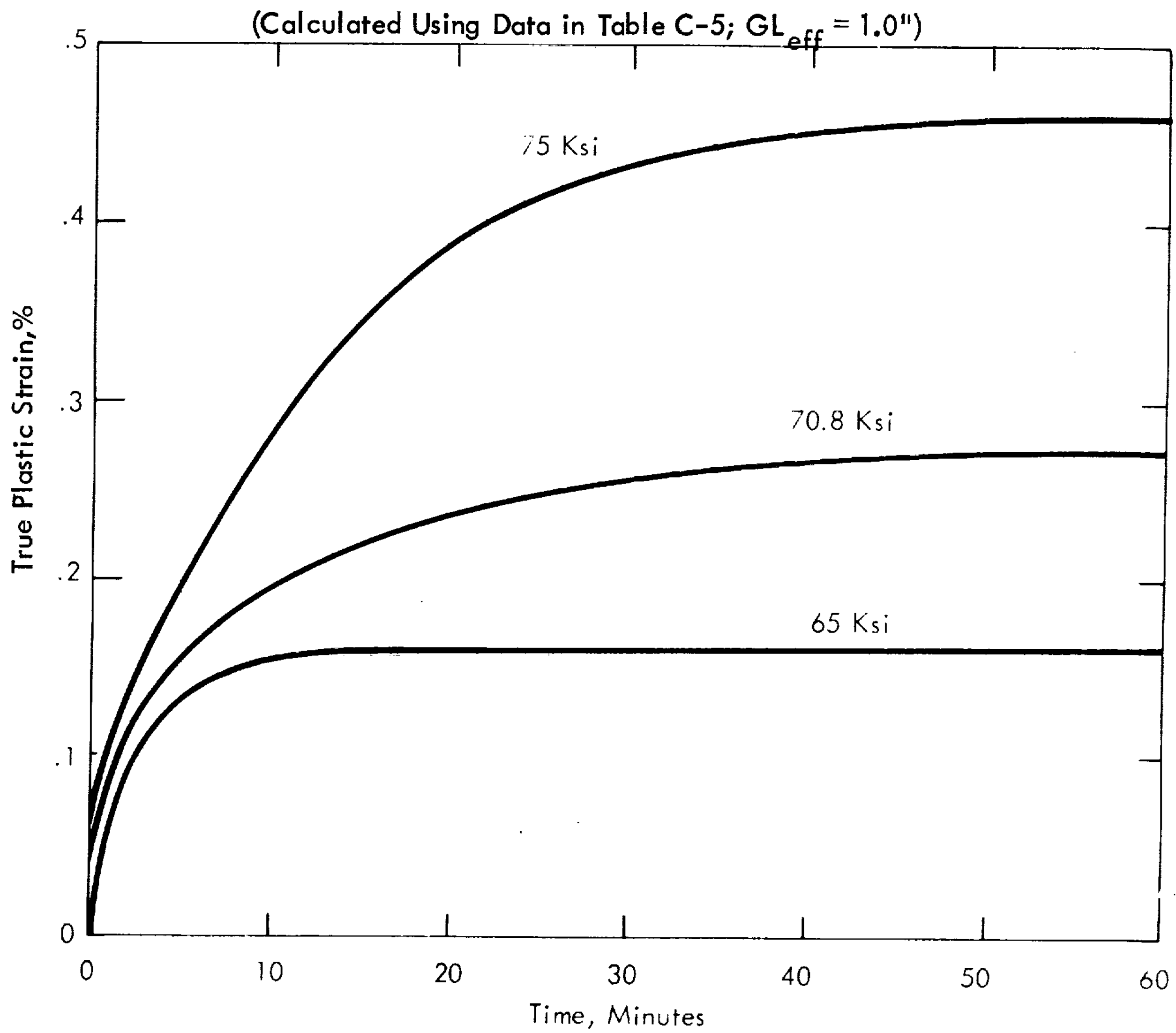

FIGURE 48 – Compression Creep Curves on Beryllium-Copper Alloy No. 10 at 500°F

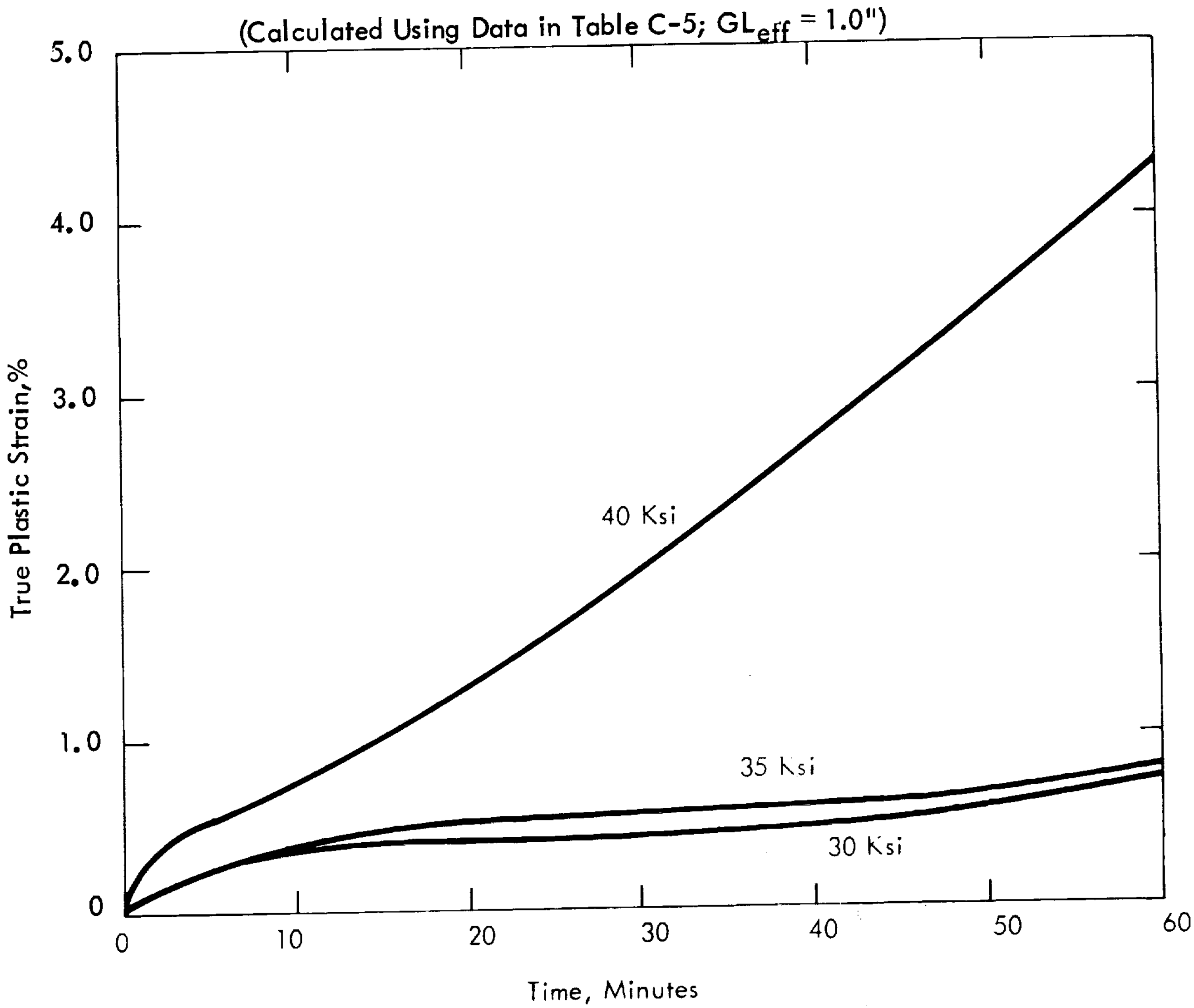

FIGURE 49 - Compression Creep Curves on Beryllium-Copper Alloy No. 10 at 1000°F

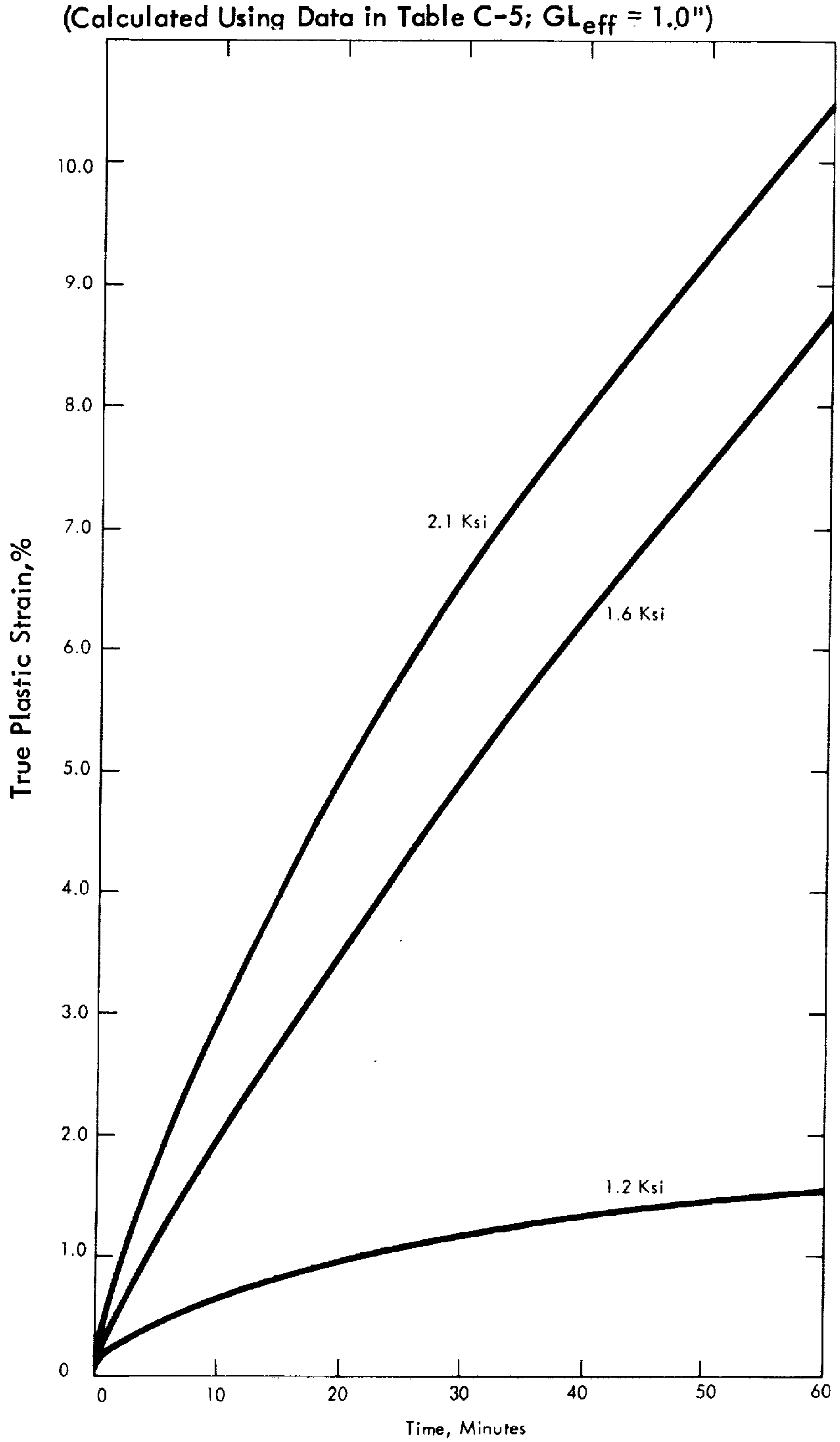

FIGURE 50 - Compression Creep Curves on Beryllium-Copper Alloy No. 10 at 1600°F

(Calculated Using Data in Table C-6)

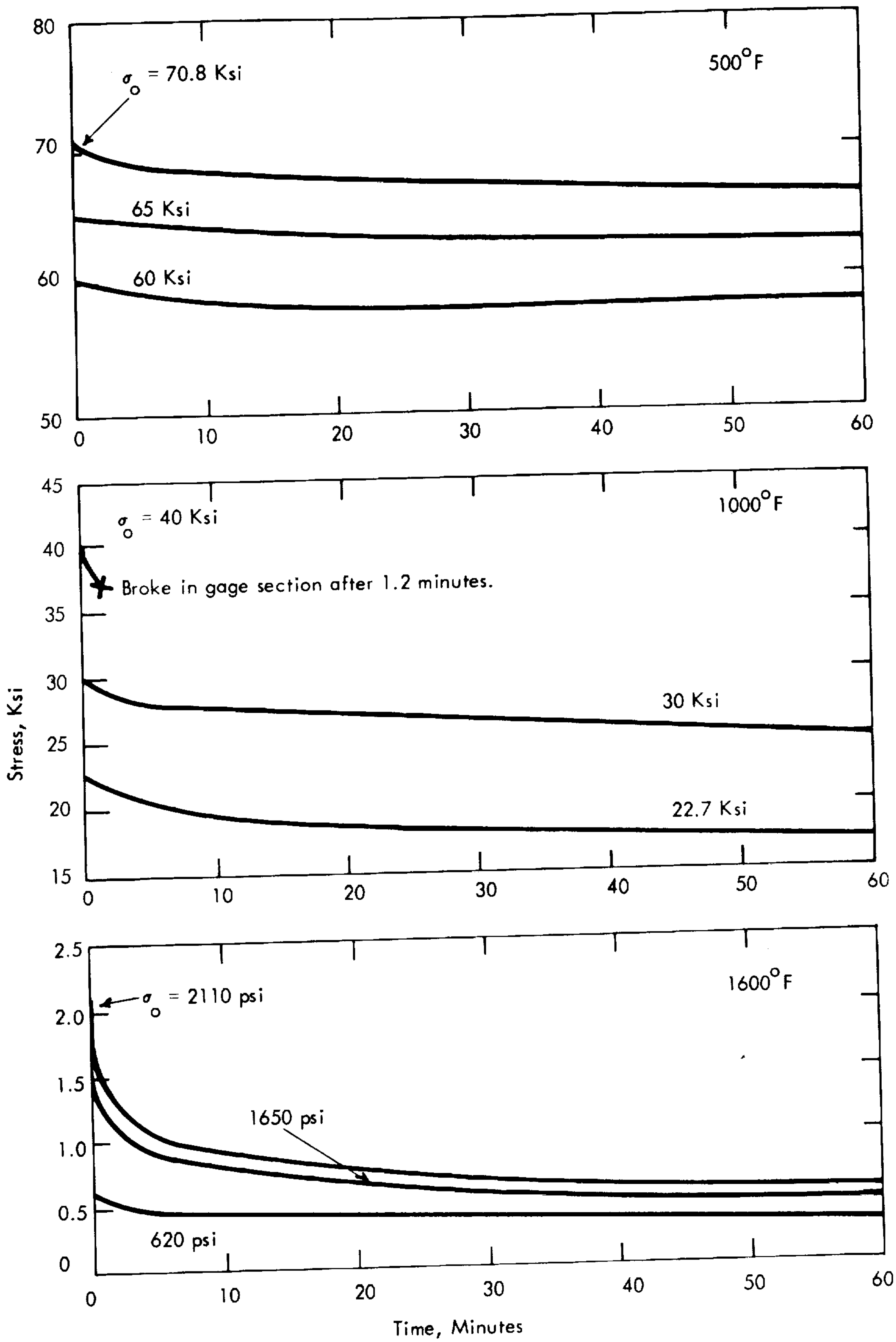

FIGURE 51 - Tension Stress-Relaxation Curves for Beryllium-Copper Alloy No. 10
(Constant Cross-Head Control)

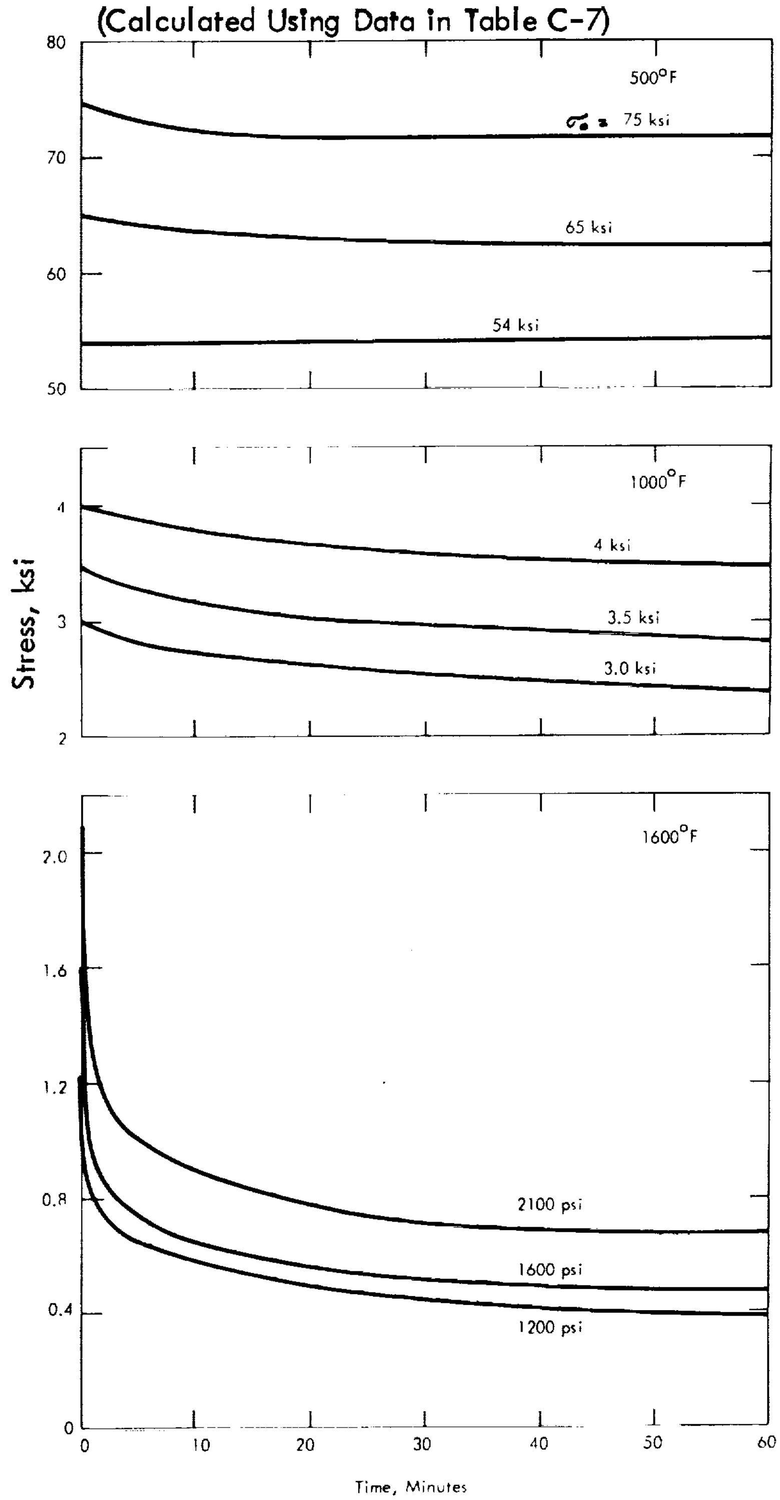

Figure 52 - Compression Stress-Relaxation Curves for Beryllium-Copper Alloy 10
(Constant Cross-Head Control)

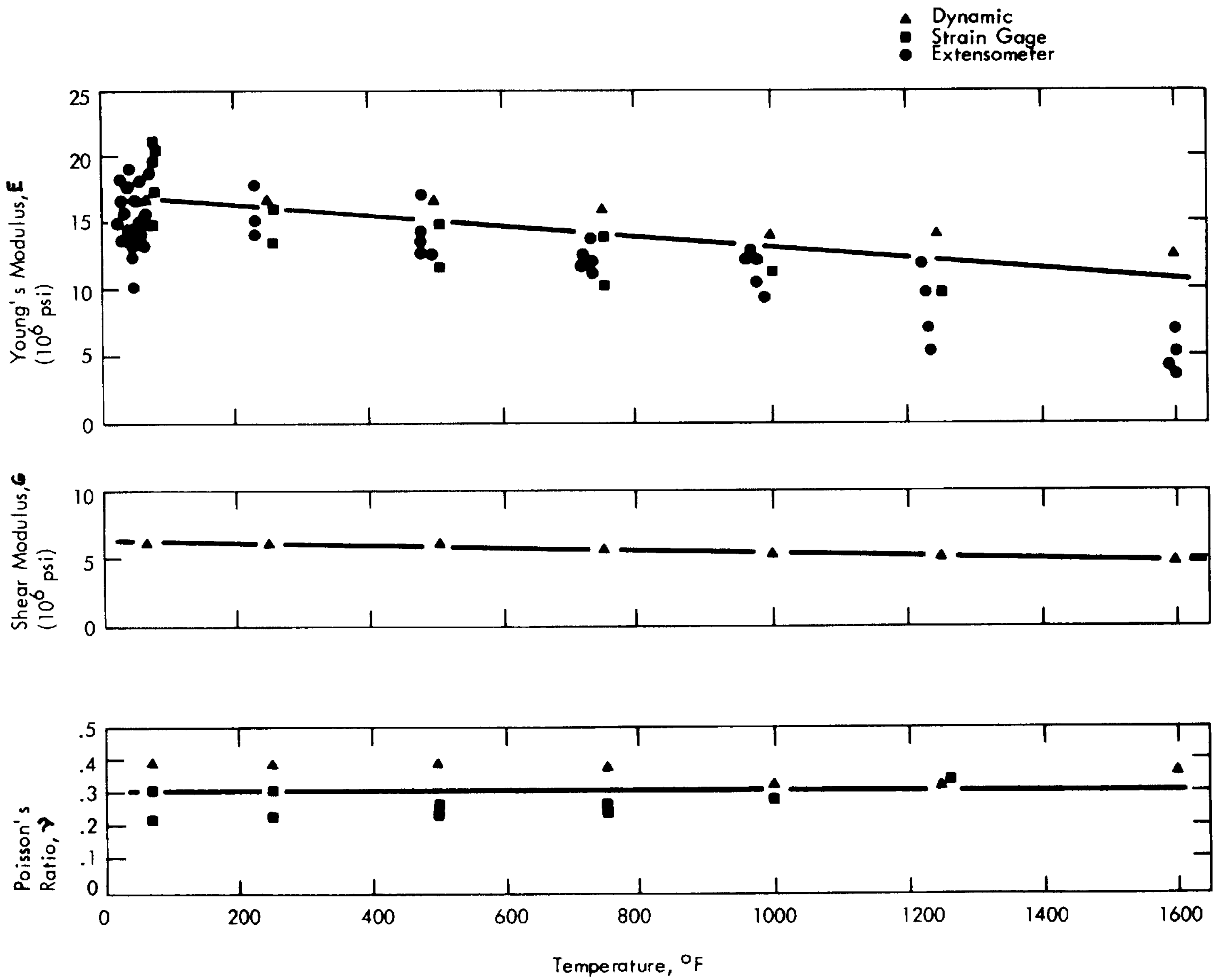

Figure 53. Elastic Properties of Beryllium-Copper Alloy 10 as a Function of Temperature. (The Data are listed in Table C-8)

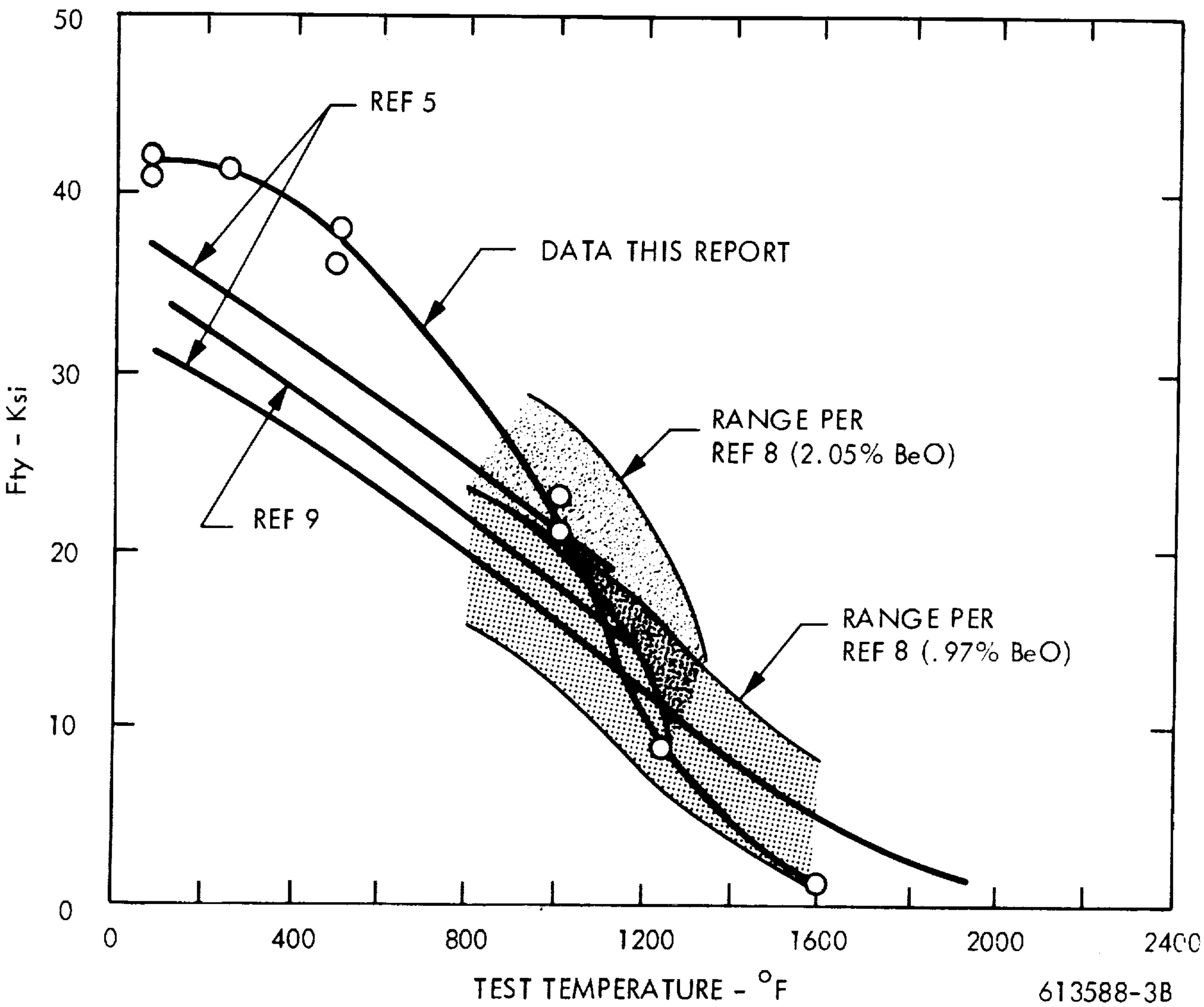

FIGURE 54. Temperature Dependence of .2% Offset Yield Strength of Beryllium

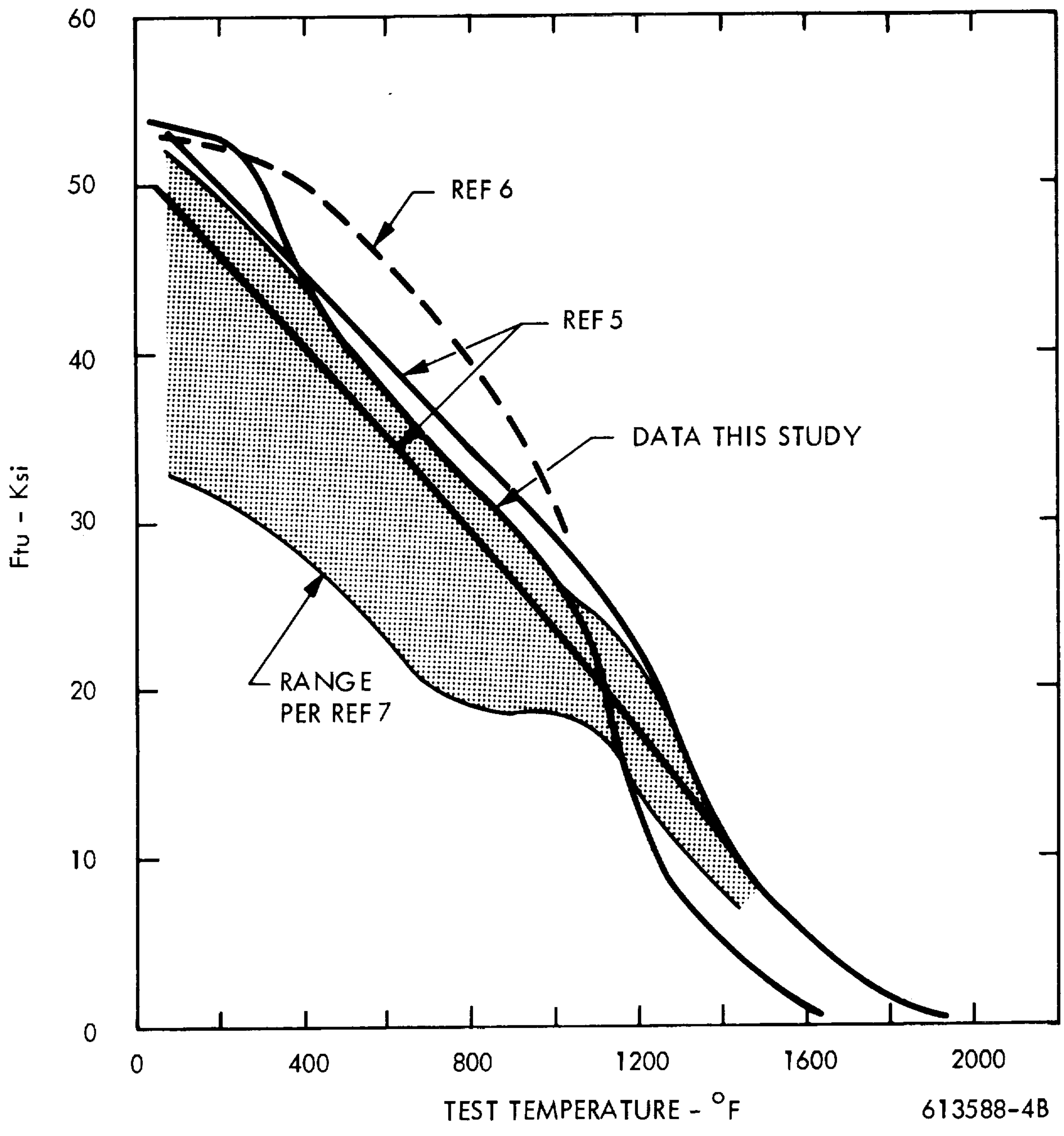

FIGURE 55. Temperature Dependence of Ultimate Tensile Strength of Beryllium

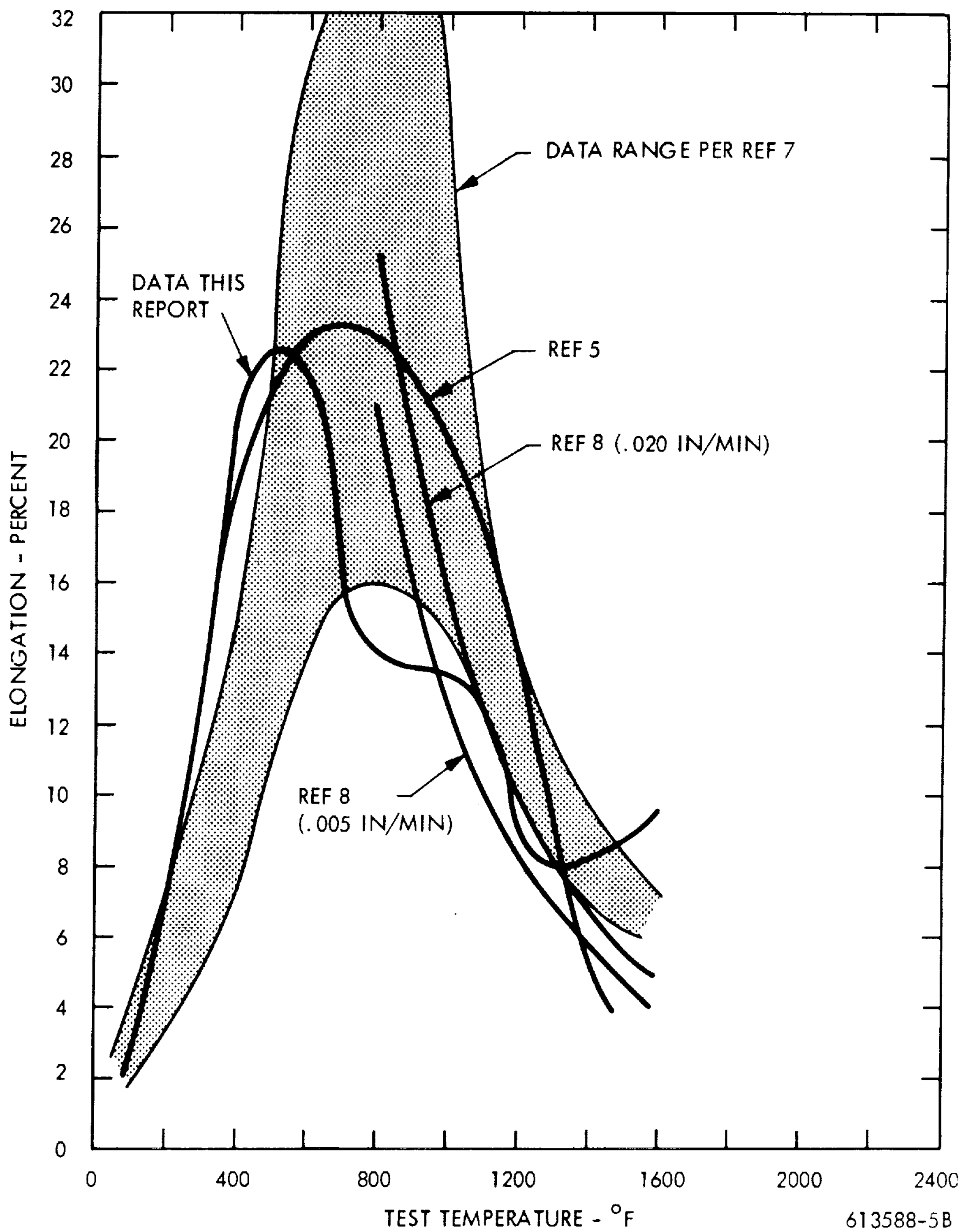

FIGURE 56. Temperature Dependence of Tensile Elongation of Beryllium

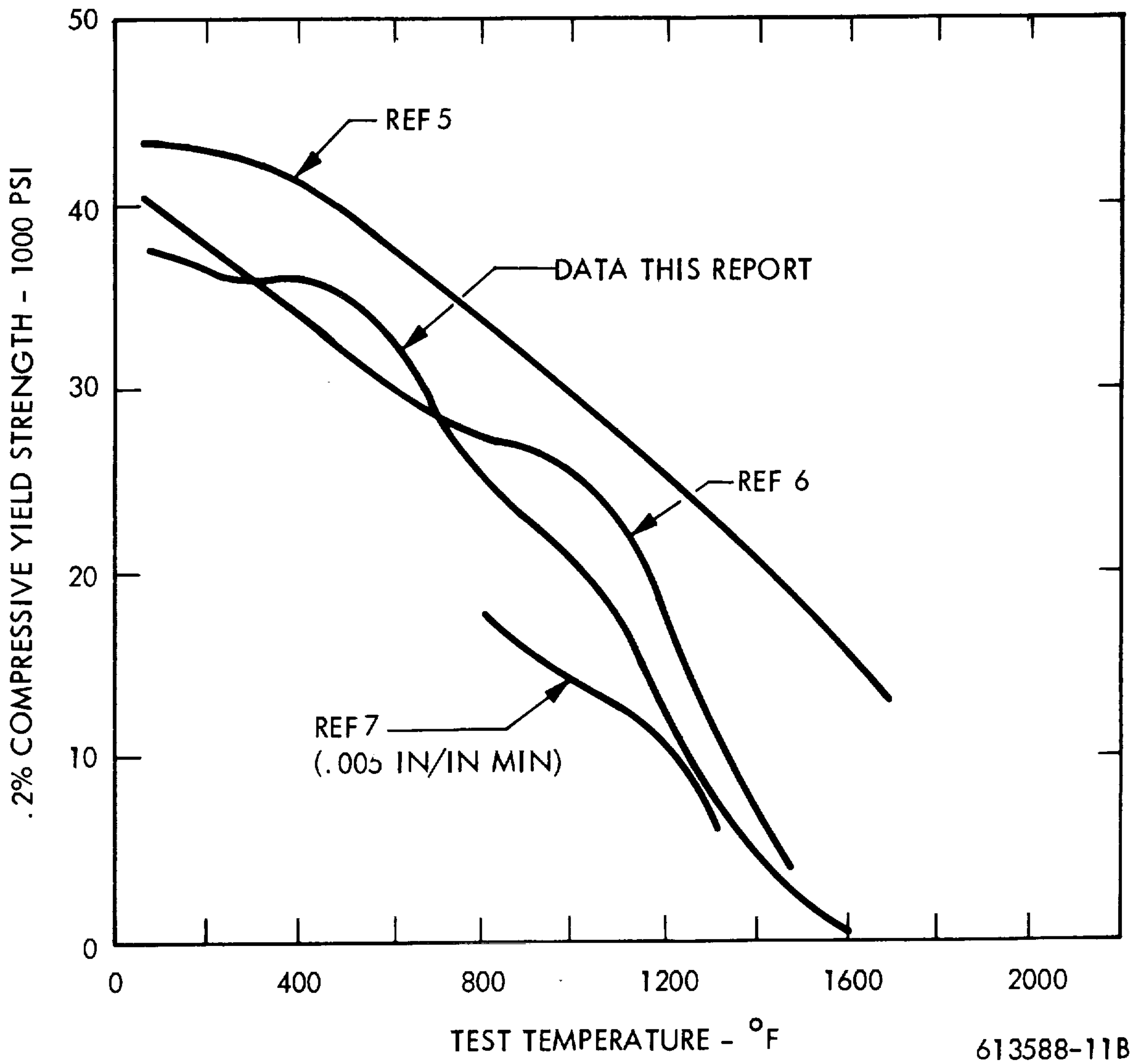

FIGURE 57. Effect of Temperature on the Compressive Yield Strength of Beryllium

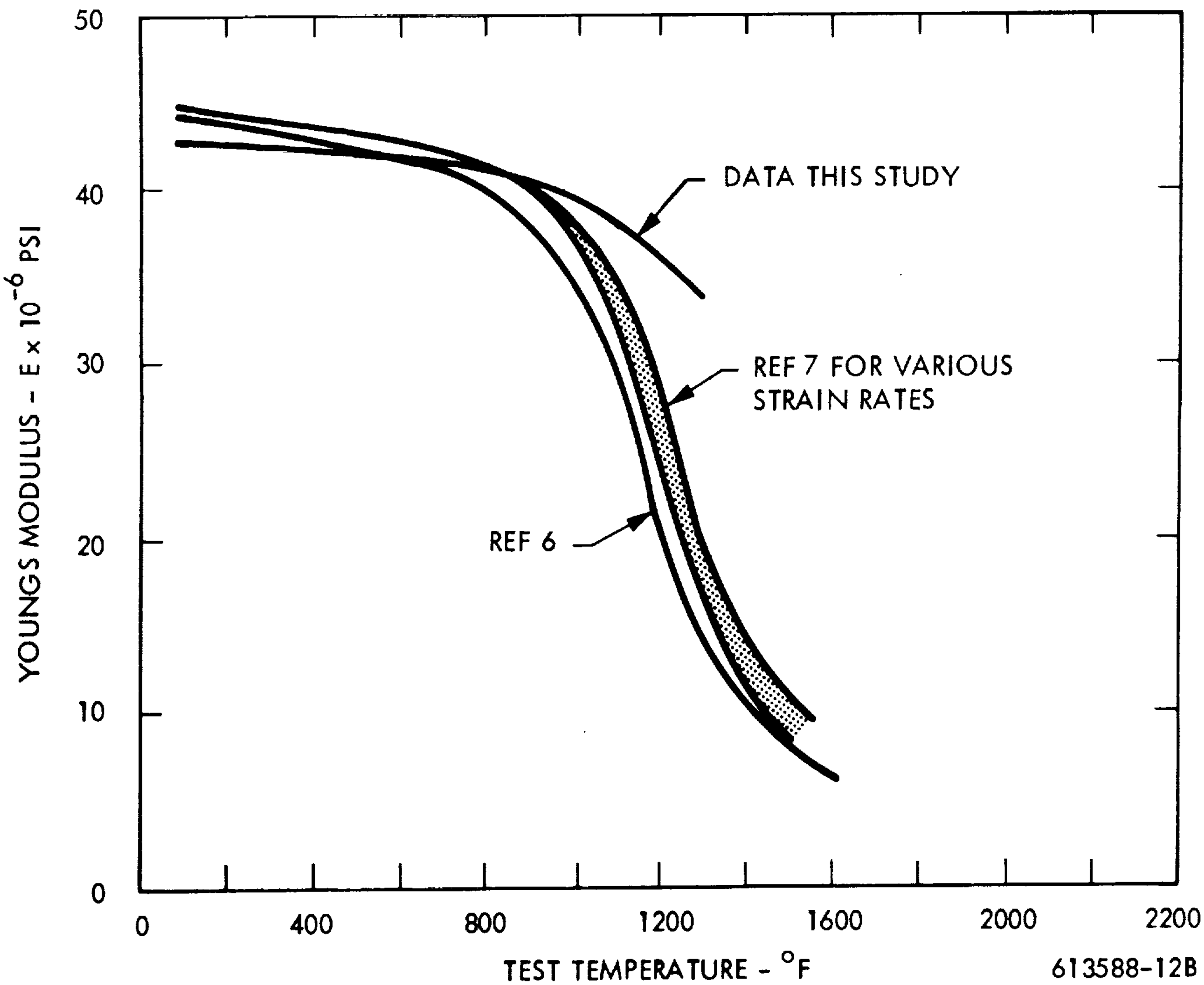

FIGURE 58. Effect of Temperature on Young's Modulus of Beryllium

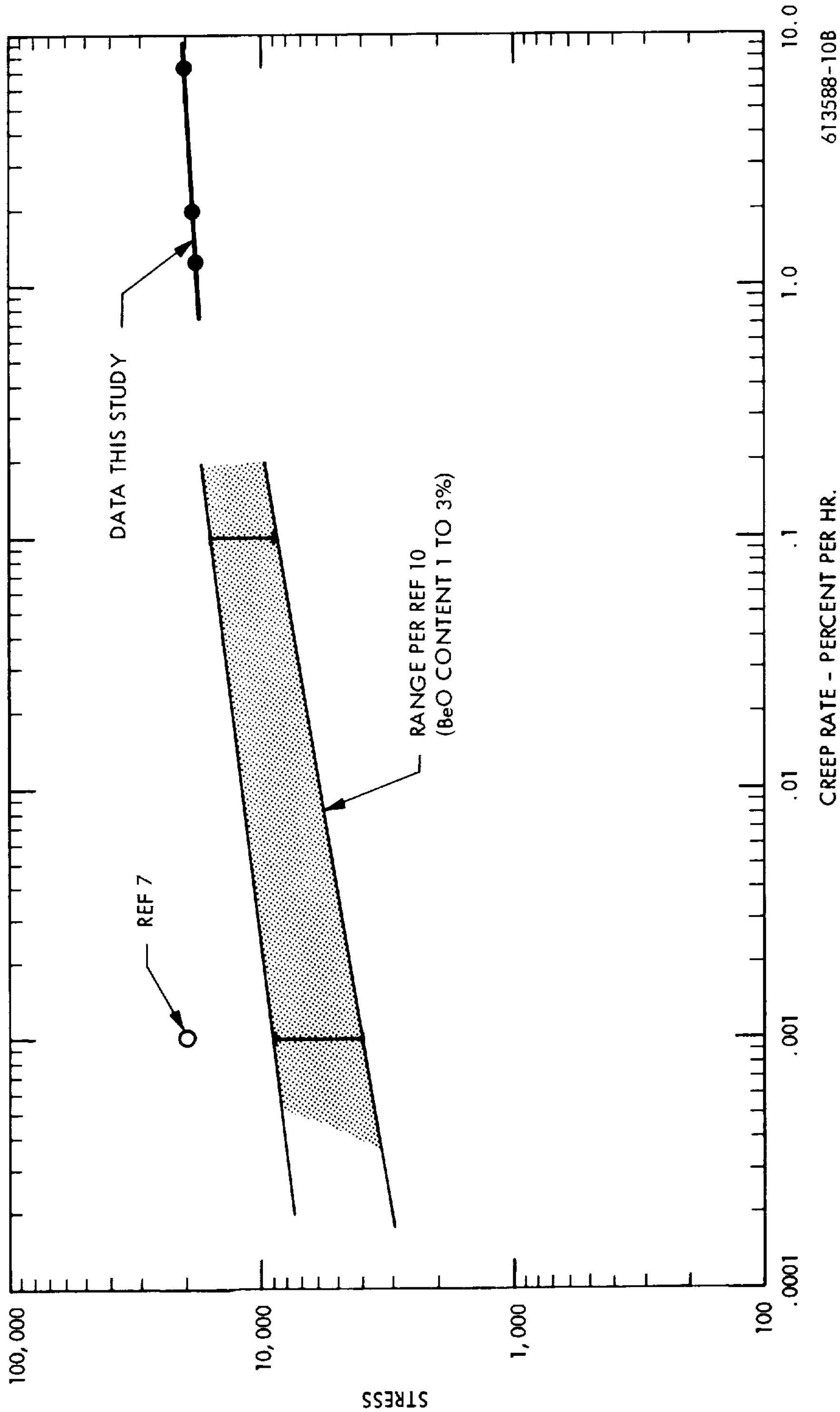

FIGURE 59. Creep Behavior of Beryllium at 1000°F

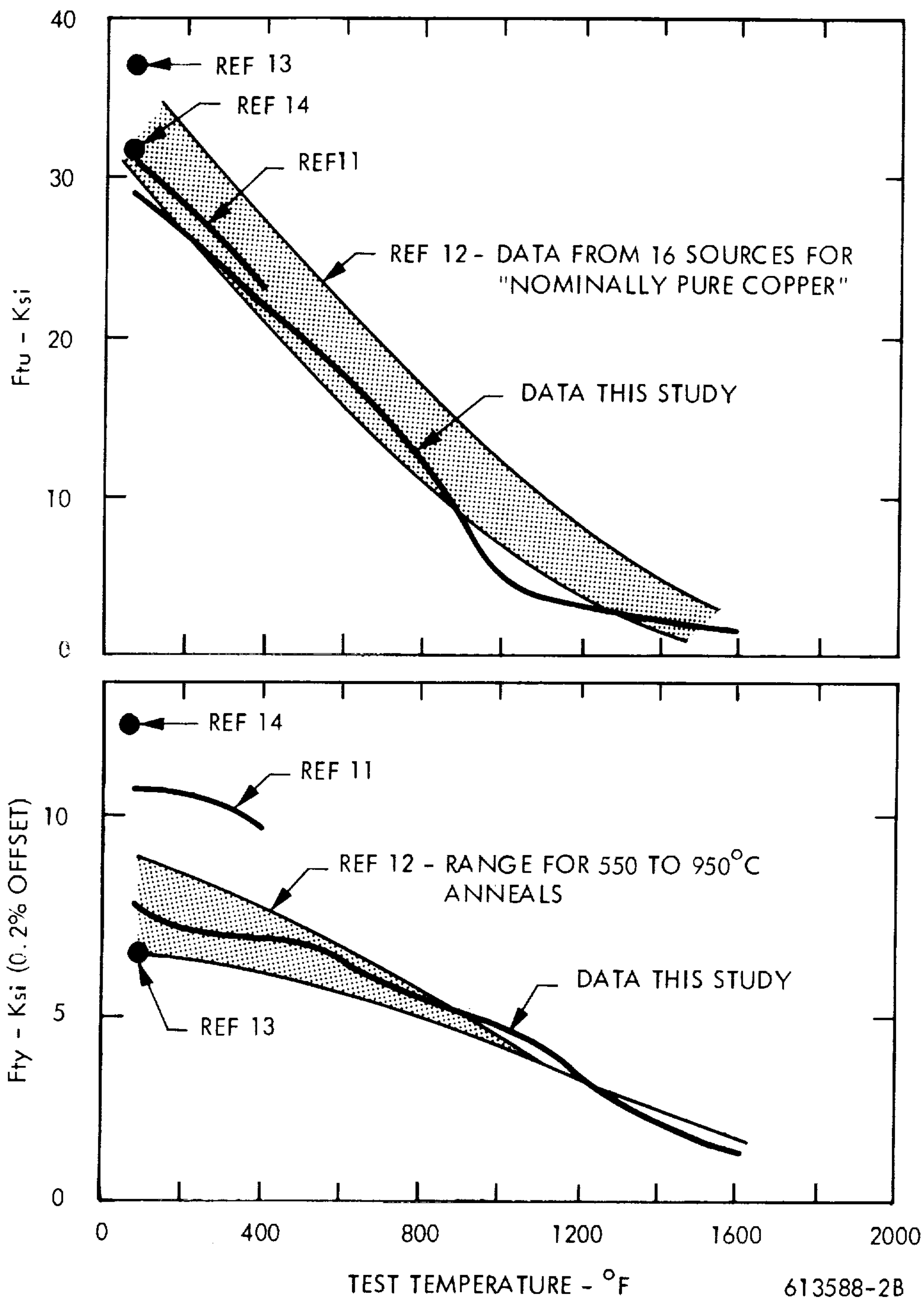

FIGURE 60. Effect of Temperature on the Tensile Properties of O.F.H.C. Copper

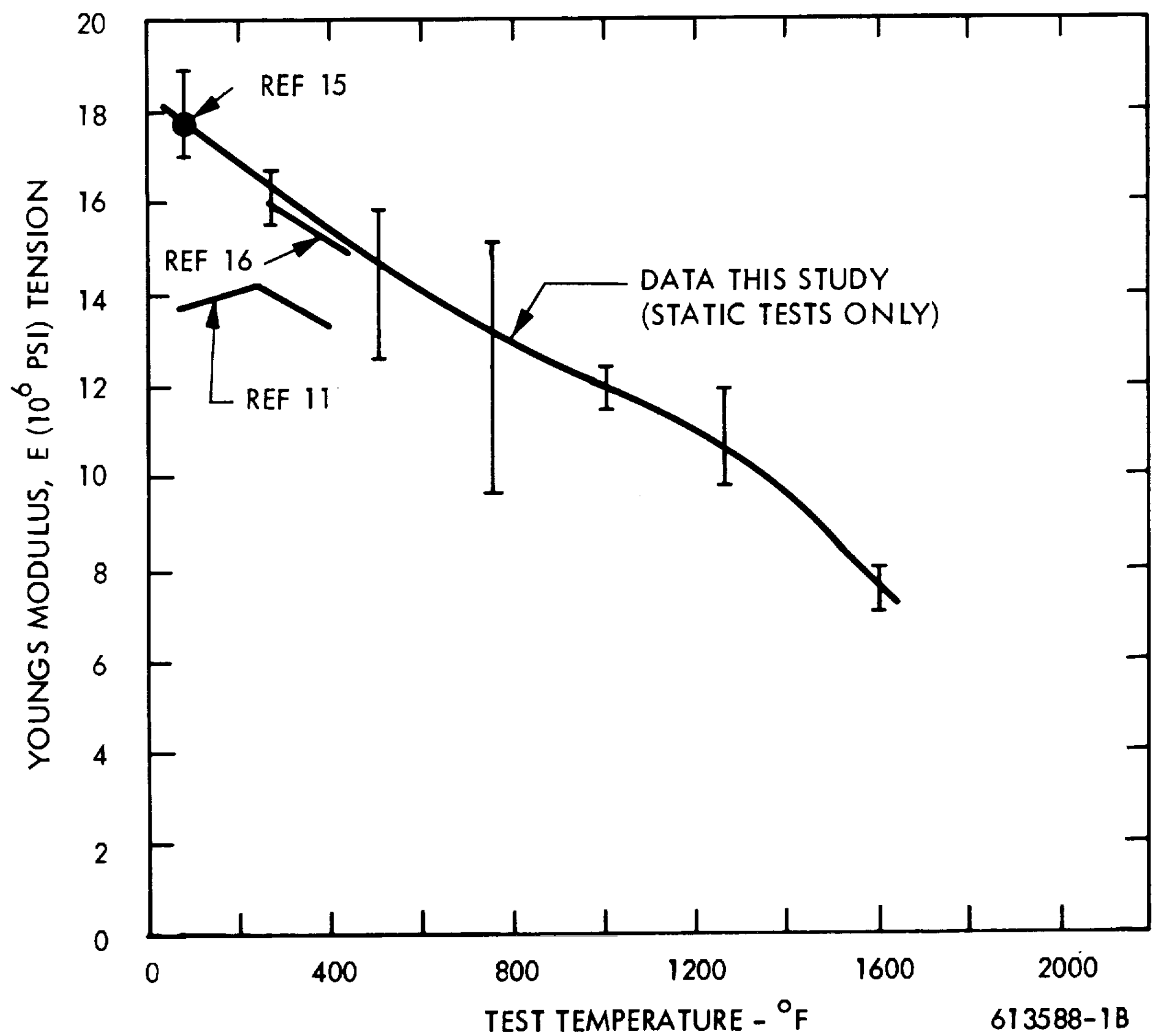

FIGURE 61. Effect of Temperature on Young's Modulus of O.F.H.C. Copper

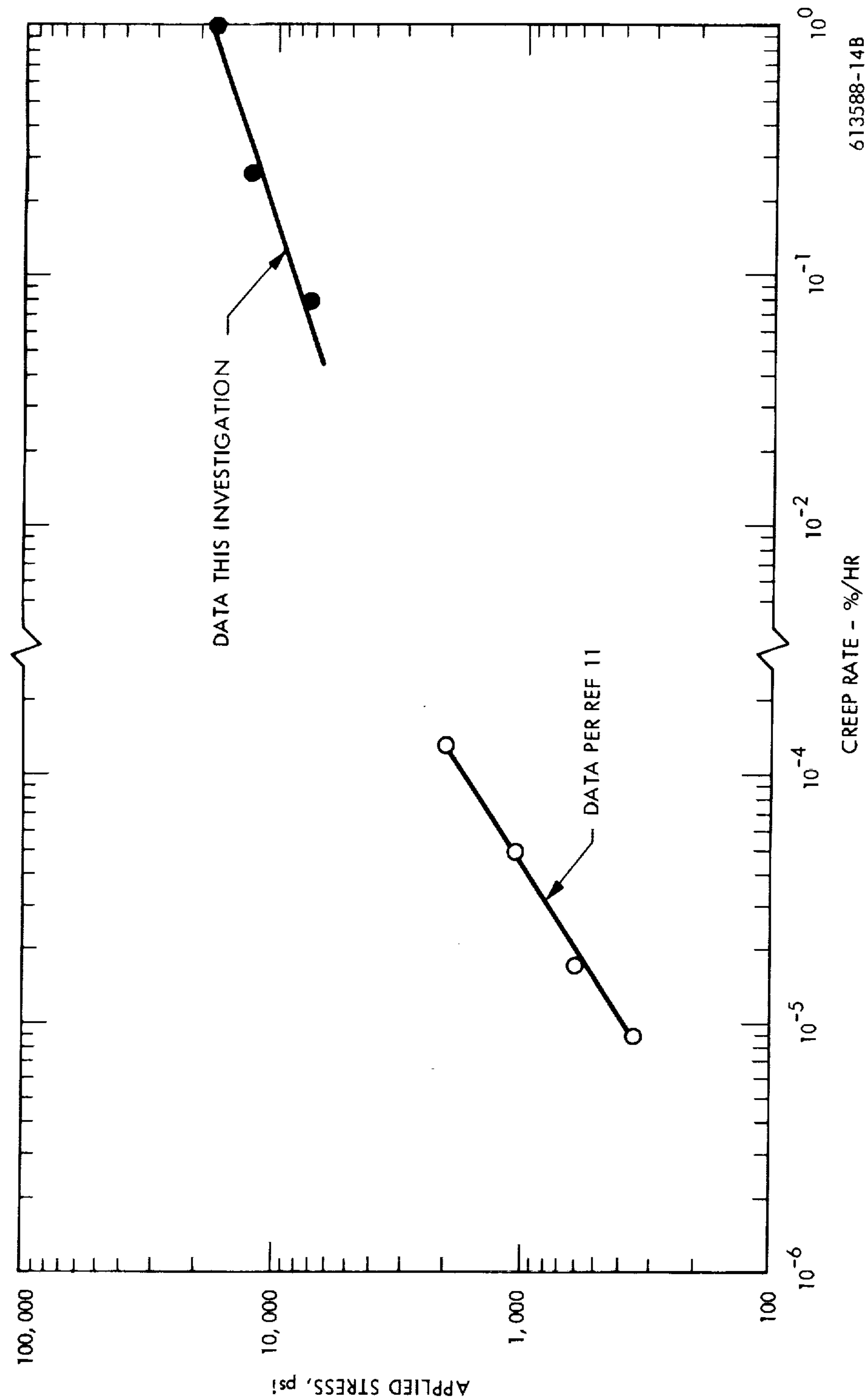

FIGURE 62. Tension Creep Behavior of O.F.H.C. Copper at 500°F

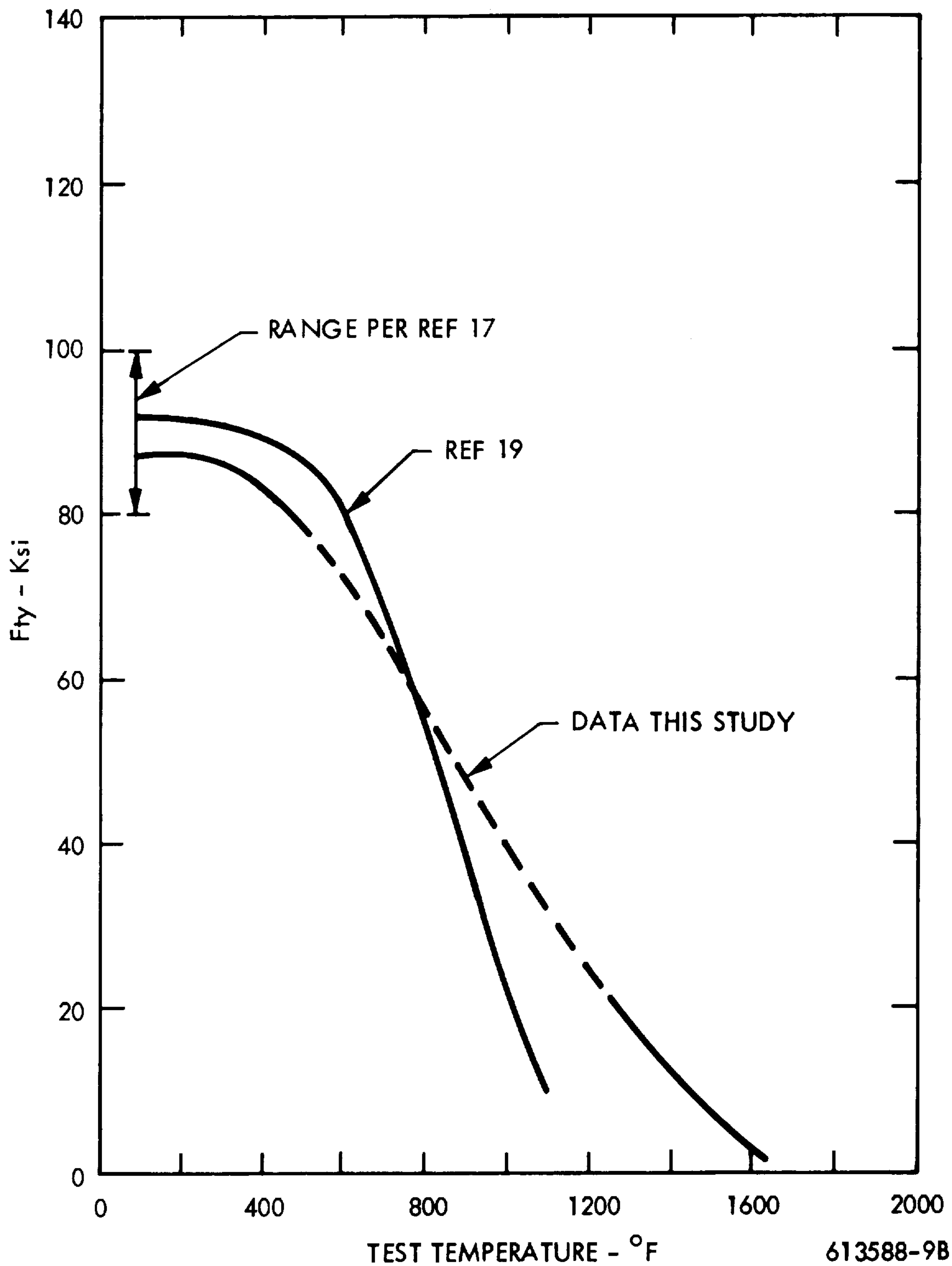

FIGURE 63. Temperature Dependence of Yield Strength of Be-Cu Alloy 10

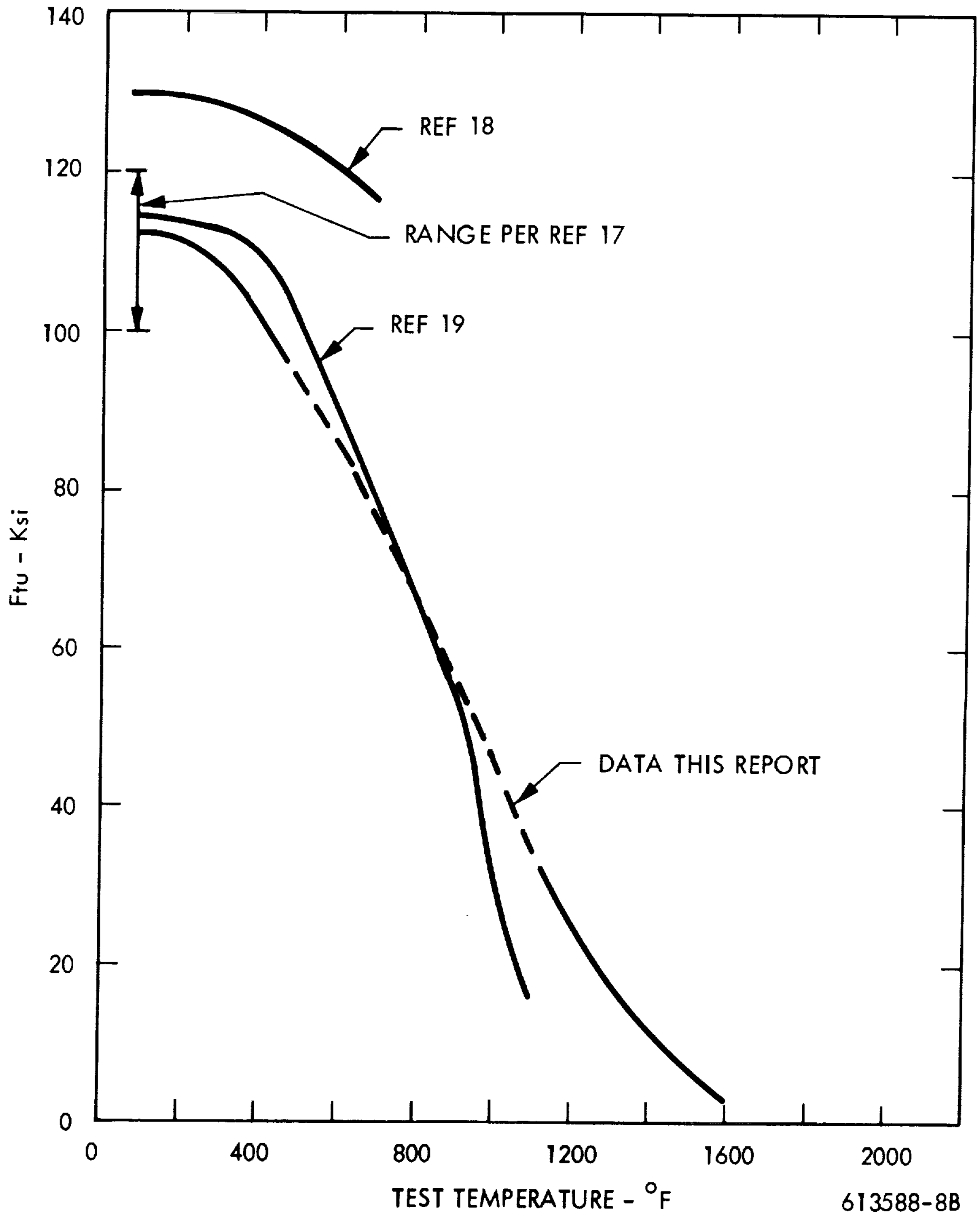

FIGURE 64. Temperature Dependence of Tensile Ultimate Strength of Be-Cu Alloy 10

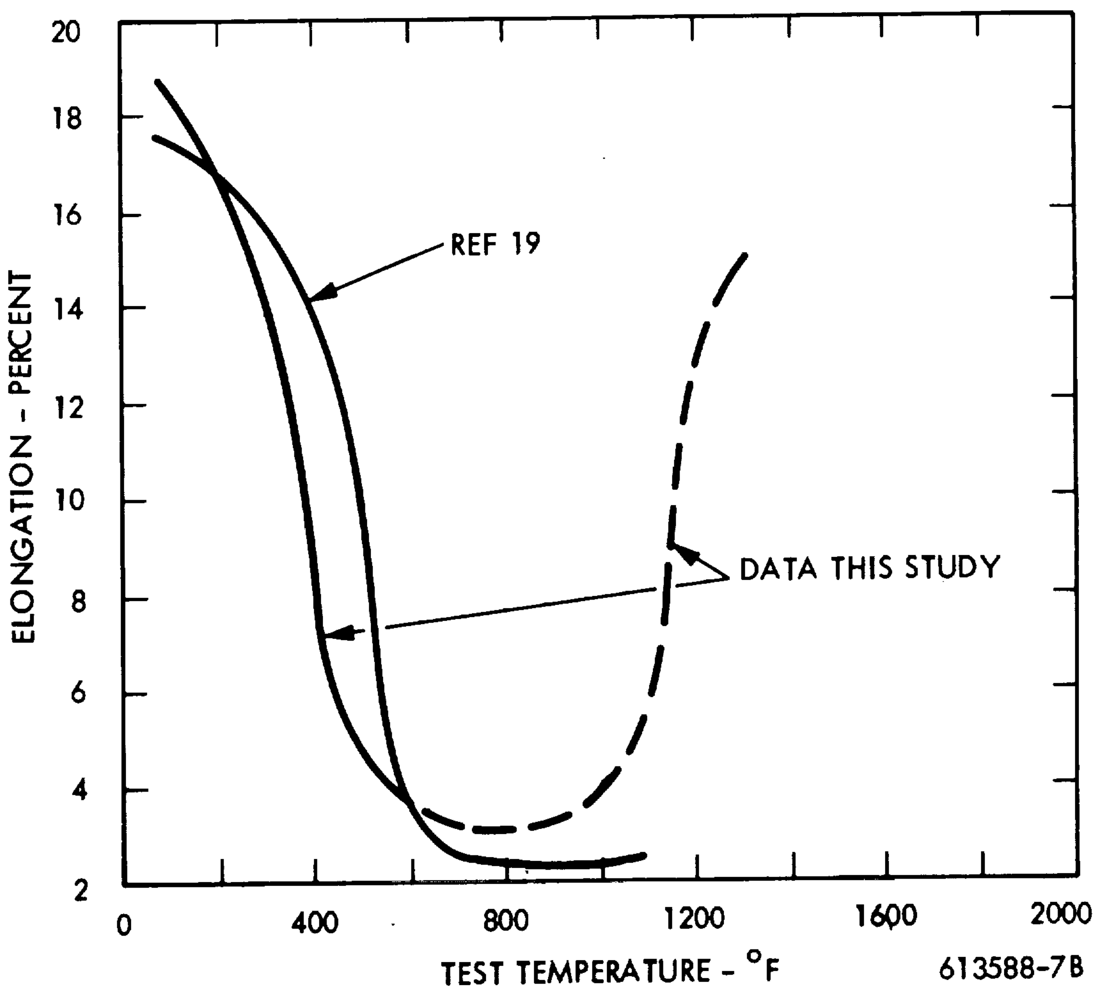

FIGURE 65. Temperature Dependence of Tensile Elongation of Be-Cu Alloy 10

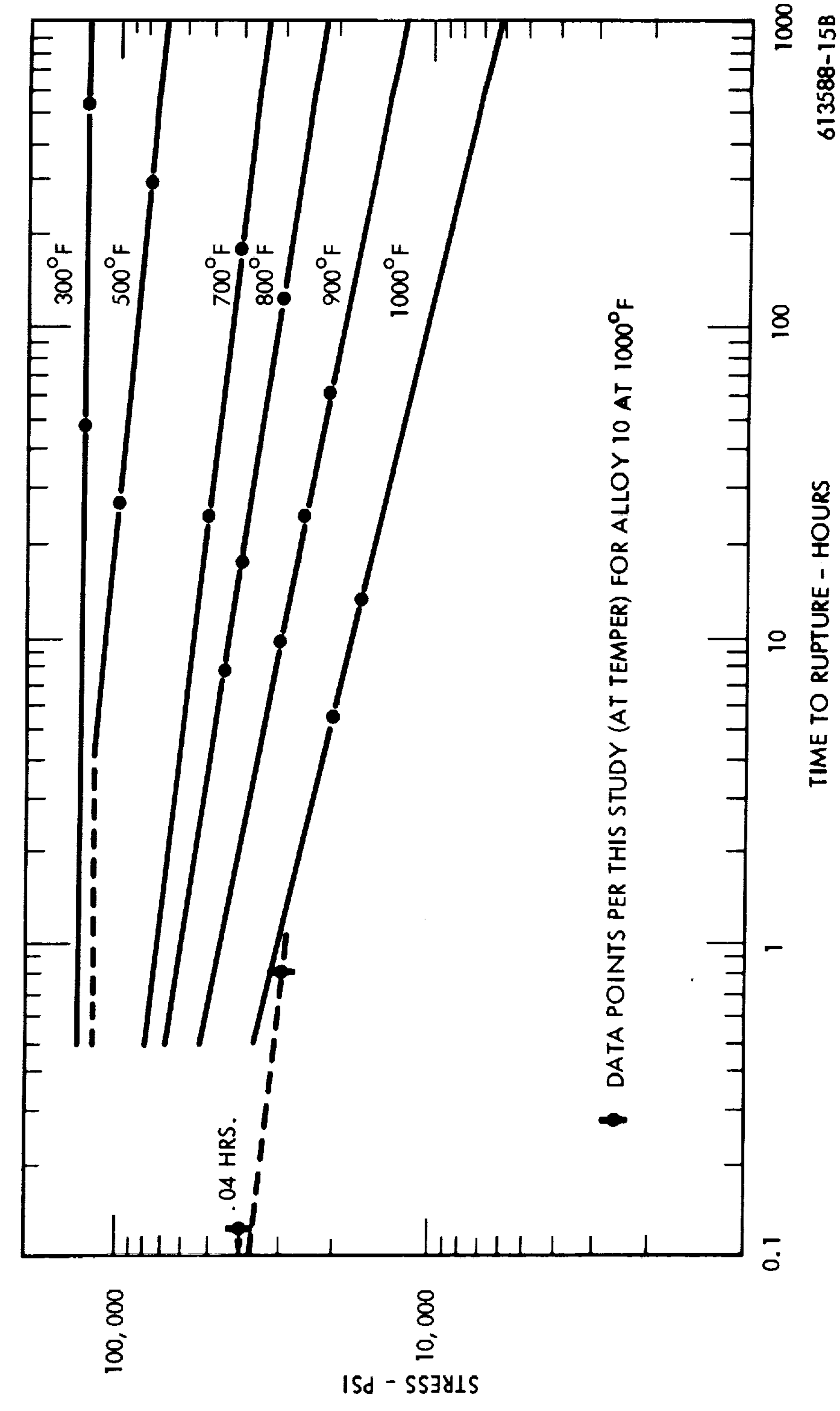

FIGURE 66. Stress-Rupture Properties of Be-Cu Alloy 10 in HT Temper (Ref. 19)

Table I. Properties of Hot Pressed Be Block - Transverse Direction

Material	No. of Tests	Temp.	U.T.S. (ksi)	Y.S. (ksi)	Elong. (%)	Reference
S200E	2	R.T.	53.6	41.6(1)	2.2	This report
S200E	303	R.T.	53.9	37.8	2.6	4
S200	(2)	R.T.	53.38	37.26	2.55	5
S200	Various	Various	Average data is plotted in Figures 54-56			5
S200D	451	R.T.	53.1	38.4	2.7	7

(1) Average of lower yield stress values

(2) Not listed - but app. 500 tests, BeO range from 1.570 to 2.0%
Data probably includes some of tests reported in Ref. 4

APPENDIX I

SUMMARY OF TEST PARAMETERS AND SCHEMATICS OF TEST SETUPS

Table AI-1. Summary of Testing Configuration and Parameters Measured

Type of Test and Test Machine Used	Strain			Load	Cross-Head Displacement Rate	Temperature	Time
	Cross-Head Displacement	Mechanical Extensometer	Strain Gage				
1. Constant Strain Rate Test							
a) Tension (Instron)	X	X	(1)	X	X	X	
b) Compression (Wiedmann)	X	X	(1)	X	X	X	
2. Constant Load Creep Test (SATEC)		X		X		X	X
3. Stress Relaxation (Baldwin)				X		X	X
4. Static Elastic Tests (SATEC[(2)])		X	X	X		X	

(1) One test of each type at room temperature.

(2) Except at room temperature, used Instron.

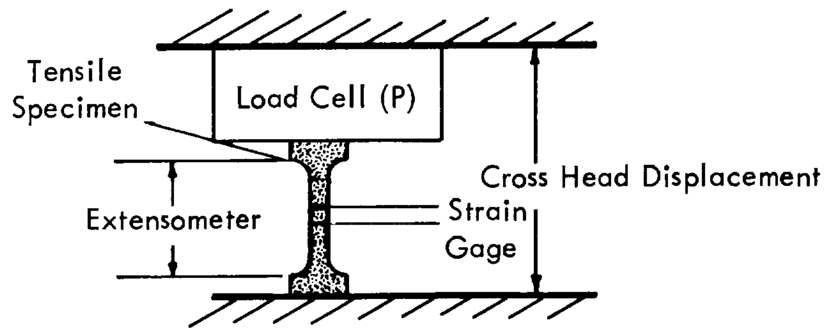

(a) Constant Strain Rate Tension Test

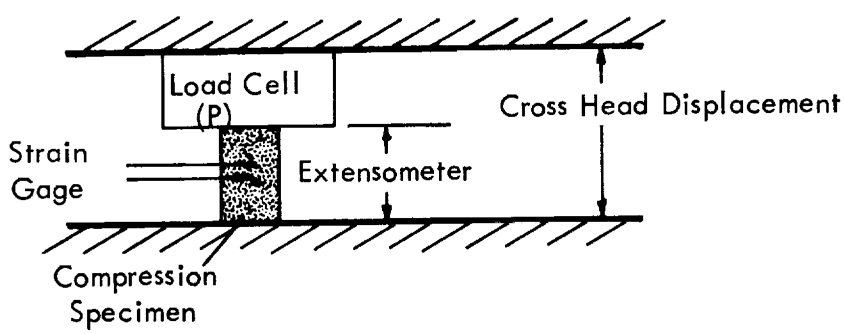

(b) Constant Strain Rate Compression Test

Figure AI-1. Schematic Showing Various Test Setups Used

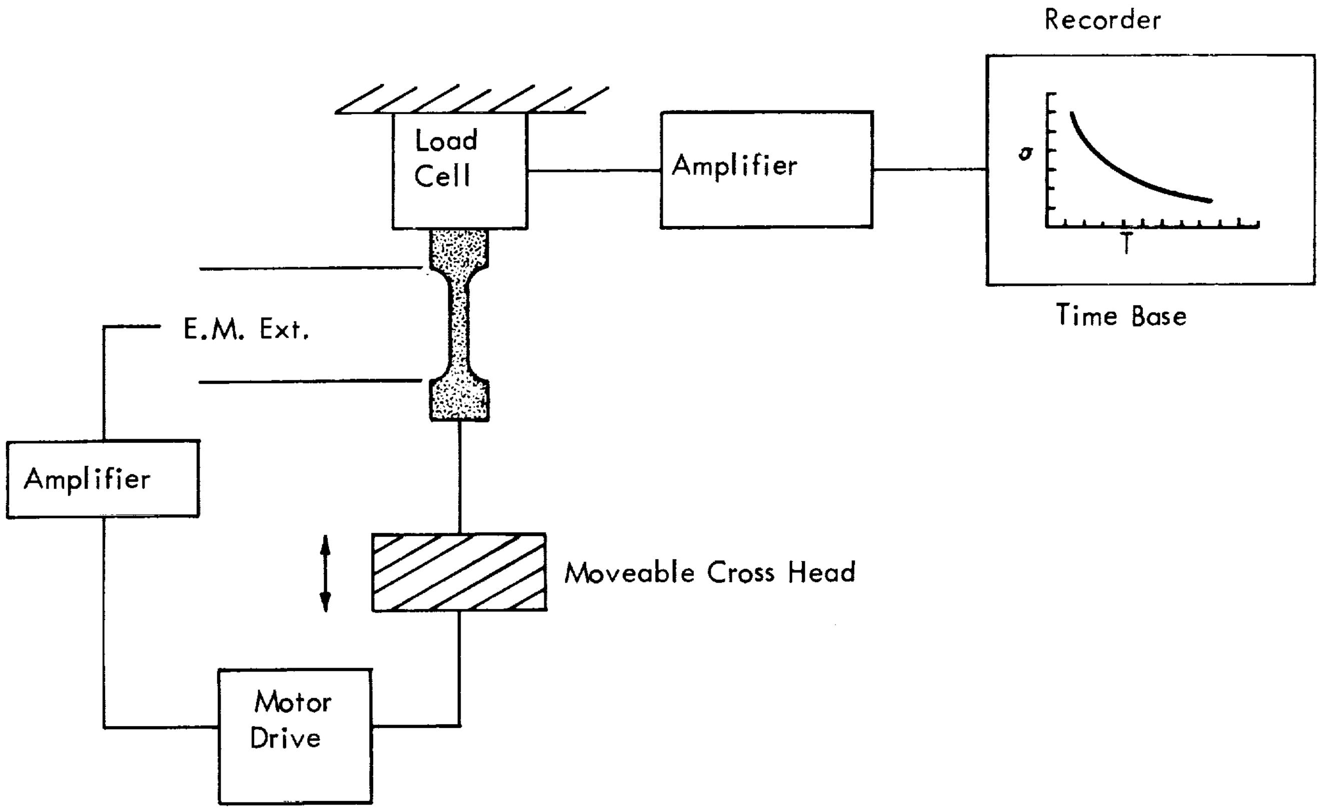

(c) Stress Relaxation

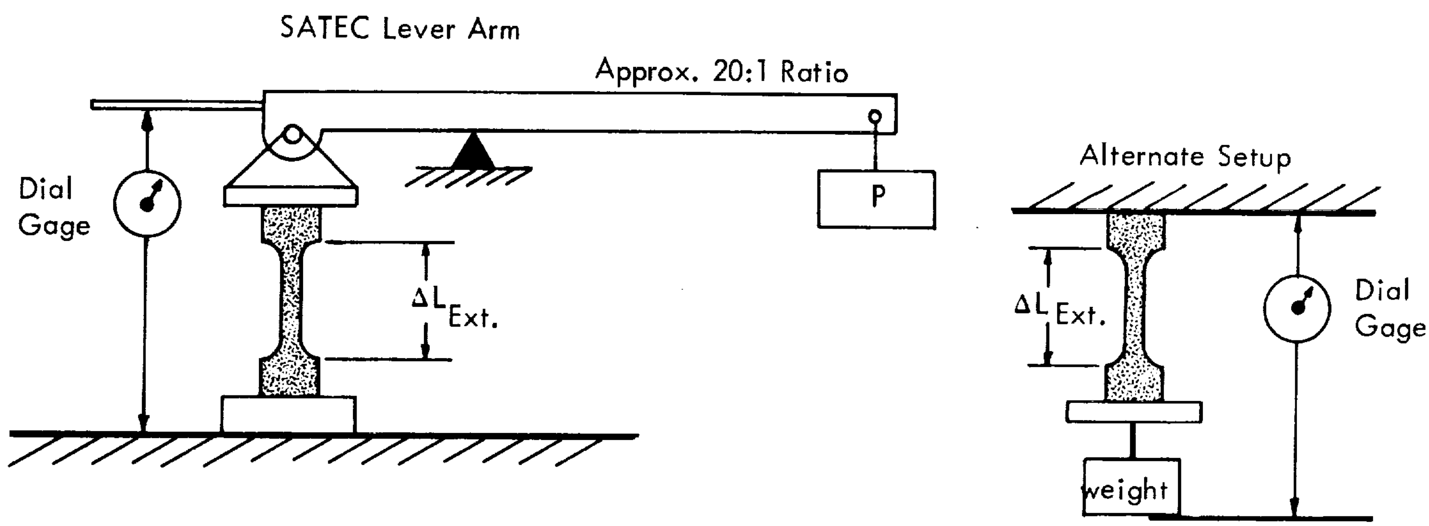

(d) Constant Load Creep Test

Figure AI-1 (Continued)

APPENDIX II

EFFECTIVE GAGE LENGTH

APPENDIX II

EFFECTIVE GAGE LENGTH

The various test specimens were machined to have certain gage lengths as shown in the specimen dimensions in Figures 6-8 of the text. These as-machined gage lengths were as follows:

Material	Specimen As-Machined Gage Length	
	Tension	Compression
Copper	2.0 (2.5)*	1.0
Be-Cu Alloy No. 10	2.0 (2.5)*	1.0
Beryllium	2.12	1.0

Note that the odd gage length of 2.12 in. for tension specimens of beryllium was due to an error in machining; it was intended to be nominally 2.0 in. This error, however, was of no consequence since each specimen was measured prior to testing.

Now the electro-mechanical extensometer used to measure displacements was mounted on the shoulders of the tension specimens (see Figures 6-7 of text) and on the loading platens in the compression tests. This means that the displacement measured by the extensometer included not only the displacement in the as-machined gage length but also that in the fillets and shoulders in the case of tension and in the platens in the case of compression back to where the extensometer was mounted. Since it was the strain in the uniform gage section (as-machined) that was desired, the question arose as to what effective gage length the displacement (change in length) measured by the extensometer should be divided by to give the correct strain. To answer this, specimens were tested which had strain gages mounted on the gage section in addition to the extensometer on the shoulders or platens. Assuming that the strain gage gave the correct strain in the gage section, it follows that:

* Effective gage length - balance $GL_{eff} = GL_{machined}$

$$\text{correct strain} = \text{strain } \epsilon \text{ of strain gage} = \frac{\Delta L \text{ (as-machined gage section)}}{L_o \text{ (as-machined gage section)}}$$

$$= \frac{\Delta L \text{ (extensometer)}}{L \text{ (effective gage length)}}$$

The effective gage length was of particular importance in connection with the elastic property measurements. For the compression tests on all three materials it was found that very little deformation occurred in the platens, i.e., the change in length measured by the extensometer was about the same as that of the specimen, hence the effective gage length was the same as the as-machined gage length. The same was true for the tension tests on beryllium, i.e., the effective gage length was the same as the as-machined gage length of 2.12 inches. However, for the copper and Be-Cu Alloy No. 10, there was considerable elastic deformation in the shoulders of the tension specimens, and the effective gage length was found to be 2.5 inches. This is the gage length listed in Tables B-8 and C-8 for the constant strain rate tests, except for specimen No. 9 which was of different specimen design.

It should be noted that the effective gage length for the elastic property measurements was determined at room temperature and assumed to be the same at elevated temperatures. The effective gage length in the plastic range would not necessarily be the same as in the elastic range and could be different in constant strain rate tests, creep tests, and stress relaxation tests. In this program, the appropriate effective gage length in the plastic range was not determined.

APPENDIX III

STRESS RELAXATION AND CORRELATION OF STRESS RELAXATION AND CREEP

APPENDIX III

STRESS RELAXATION AND CORRELATION OF STRESS RELAXATION AND CREEP

Stress relaxation refers to the decrease in stress in a specimen held at constant length (strain) due to the gradual conversion of the initial elastic strains (which gives rise to the initial stress) into plastic strains as a result of creep or time dependent plastic deformation. It is virtually impossible to experimentally measure stress relaxation in specimens held at absolutely constant length since there would be no way to measure the change in load. Experimentally, two approaches are commonly used.

In one method, referred to as "stress relaxation at constant cross head displacement", the specimen is loaded in series with a load cell to an initial length and then the cross head is held in a fixed position. The specimen then creeps continuously under continuously decreasing stress. The analysis of the stress relaxation must include not only the deflections in the specimen but also those in the loading system, load cell, load bars, etc.

In the other method, referred to as "stress relaxation at constant specimen length", true "strain controlled stress relaxation" is approximated by allowing the specimen to creep a small amount at constant cross head displacement and then the cross head is moved, thereby relaxing the load even further, to bring the specimen back to its original strained length. This process is repeated incrementally.

Since stress relaxation occurs as a result of creep, it follows that there should be a relationship between the two.

In this Appendix, stress relaxation and its correlation with creep are discussed.

Parts A and B describe stress relaxation in such a way as to clarify the experimental details. Part C rederives succinctly, the main results of Parts A and B, but with the details omitted. Part D discusses the relationship between the two methods of measuring stress relaxation, and Part E discusses the relationship between stress relaxation and creep.

A. Stress Relaxation at Constant Cross Head Displacement

As the specimen is loaded, there is deflection not only in the specimen but also in the load cell, loading bars, and frame of the test machine. For simplicity, all the deflection other than that in the specimen is considered to be in the load cell. Thus, the specimen is in series with the load cell as shown in Figure AIII-1a. After loading to some initial load, P_i, the cross head displacement is held fixed, Figure AIII-1b. Thereafter, the specimen elongates due to creep. The load cell relaxes and the load drops from P_i to some lower load P' while the total deflection remains constant at L + l, Figure AIII-1c and d.

The initial loading to P_i might produce plastic as well as elastic deformation of the specimen, Figure AIII-1e. The load is the same on the load cell and specimen and is related to the elastic deflection in each as shown in Figure AIII-1f, where k is the spring constant of the load cell and K is the spring constant of the specimen.

At P_i and L_i, i.e., at $t_i \equiv 0$, the specimen extends to L' and at t' the load has dropped to P'. Thus,

$$L' = L_i + \Delta L'$$

where $\Delta L'$ = the difference between the "plastic" extension $\Delta L'_p$ and the "elastic" contraction $\Delta L'_e$ due to the load drop.

$$= L_i + (\Delta L'_p - \Delta L'_e)$$

$$= L_i + \Delta L'_p - \frac{(P_i - P')}{K}$$

or,

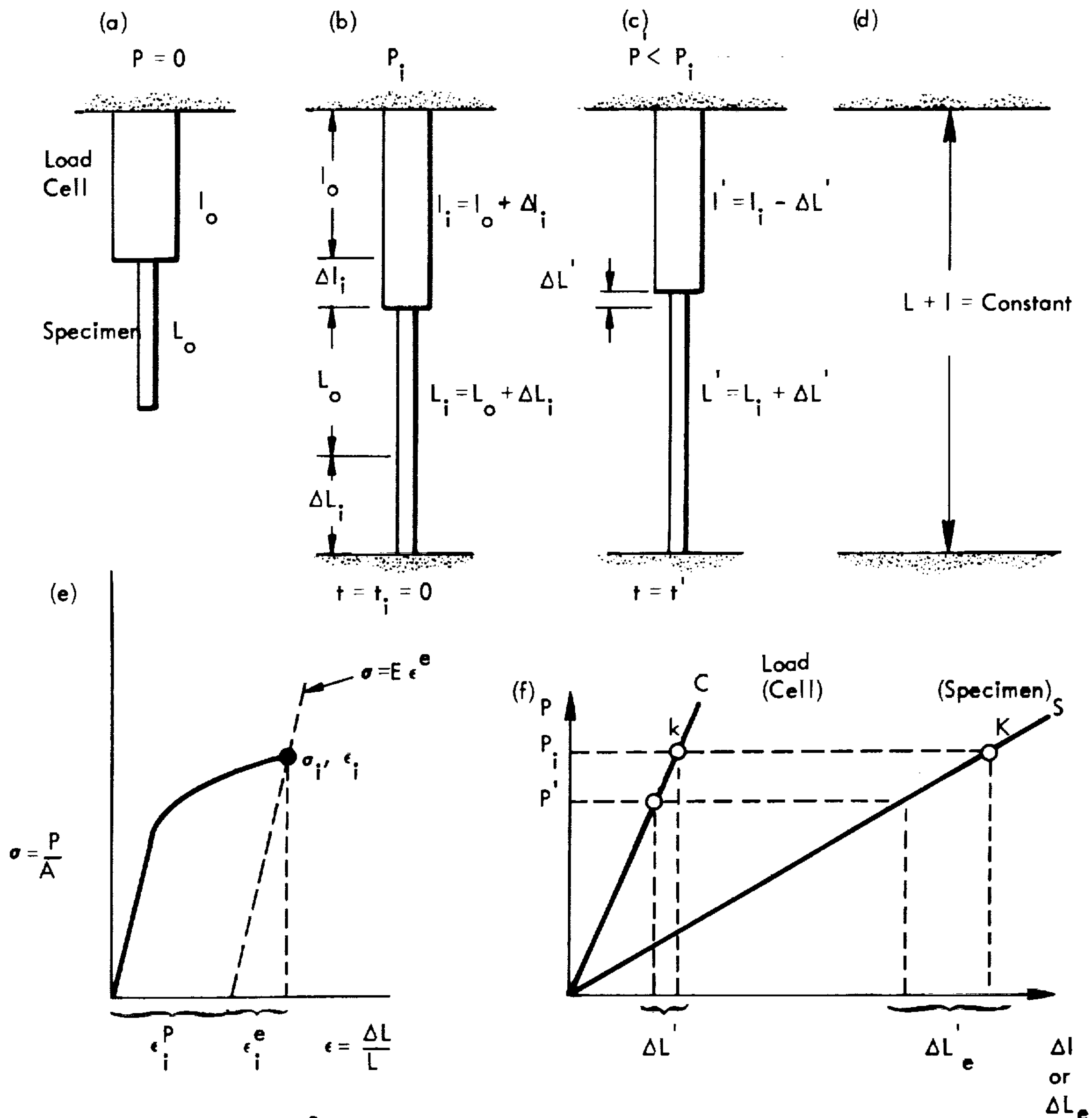

$$\sigma_i = \frac{P_i}{A_o} = E\,\epsilon_i^e = E\,\frac{\Delta L_i^e}{L_o}$$

$$P = k\,\Delta l$$

$$P = K\,\Delta L_e$$

$$K = \frac{P_i}{\Delta L_i^e} = \frac{A_o}{L_o}\,E$$

FIGURE AIII-1. Stress Relaxation for Constant Crosshead Displacement

$$L' - L_i + \frac{(P_i - P')}{K} = \Delta L'_p$$

$$\frac{(P_i - P')}{k} + \frac{(P_i - P')}{K} = \Delta L'_p$$

$$(\sigma_i - \sigma') \frac{A_o}{L_o} \left(\frac{1}{k} + \frac{1}{K} \right) = \epsilon'_p$$

We now define $\sigma_i \equiv \sigma_o$, the initial stress on loading, and drop the superscripts; thus

$$(\sigma_o - \sigma) \frac{A_o}{L_o} \left(\frac{k + K}{kK}\right) = \epsilon_p$$

where

σ_o = initial applied stress

σ = stress after some time t

ϵ_p = plastic (creep) strain of specimen after time t

In terms of rates, by differentiating with respect to time t,

$$- \dot{\sigma} \frac{A_o}{L_o} \left(\frac{k + K}{kK} \right) = \dot{\epsilon}_p$$

Note the following:

i) The maximum range of specimen extension during relaxation is limited by Δl_i, i.e., the initial extension of the load cell, which is all elastic.

ii) The maximum range of specimen plastic (creep) extension during relaxation is limited by $(\Delta l_i + \Delta L_i^e)$

iii) There is also a correction needed for "machine relaxation" (here considered to be entirely in the load cell) which occurs independently of any extension in the specimen. The machine relaxation data is given in Tables D1 and D2 of Appendix IV.

iv) For the experimental setup employed in the stress relaxation tests at constant crosshead displacement, the value of k was $k = 6 \times 10^4$ pounds/inch, where k is the spring constant of the machine (including grips, load bars, and load cell).

B. Stress Relaxation at Constant Specimen Length

After loading the specimen to an initial load P_i, the specimen creeps and relaxes the load to P' as shown in Figure AIII-2a (which is the same at this point in time as Figure AIII-1c). Now in order to keep the specimen length constant, the cross head is moved to bring the specimen length back to L_i, the initial length after loading. The load further relaxes from P' to P'' as shown in Figure AIII-2b and c. Thus,

$$P'' = P_i - (P_i - P') - (P' - P'')$$

and $$P_i - P'' = (P_i - P') + (P' - P'')$$

$$= k\,\Delta L' + k\,\Delta l'' \quad \ldots \quad \Delta L'' = \Delta l' = \Delta L'$$

$$= k\,\Delta L' + K\,\Delta L' \quad \ldots \quad P' - P'' = k\,\Delta l'' = K\Delta L''$$

$$\therefore \quad \Delta l'' = \frac{K}{k}\,\Delta L''$$

$$= k\Delta L' + K\,(\Delta L'_p - \Delta L'_e)$$

$$= k\Delta L' + K\Delta L'_p - K\,\frac{k}{K}\,\Delta L' \quad \ldots \quad P_i - P' = k\Delta L' = K\Delta L'_e$$

$$\therefore \quad \Delta L'_e = \frac{k}{K}\,\Delta L'$$

and

$$P_i - P'' = K\Delta L'_p$$

or $$\sigma_i - \sigma'' = \frac{L_o}{A_o}\,K\,\epsilon''_p = E\,\epsilon''_p$$

Again, defining $\sigma_i \equiv \sigma_o$, the initial stress on loading, and dropping superscripts,

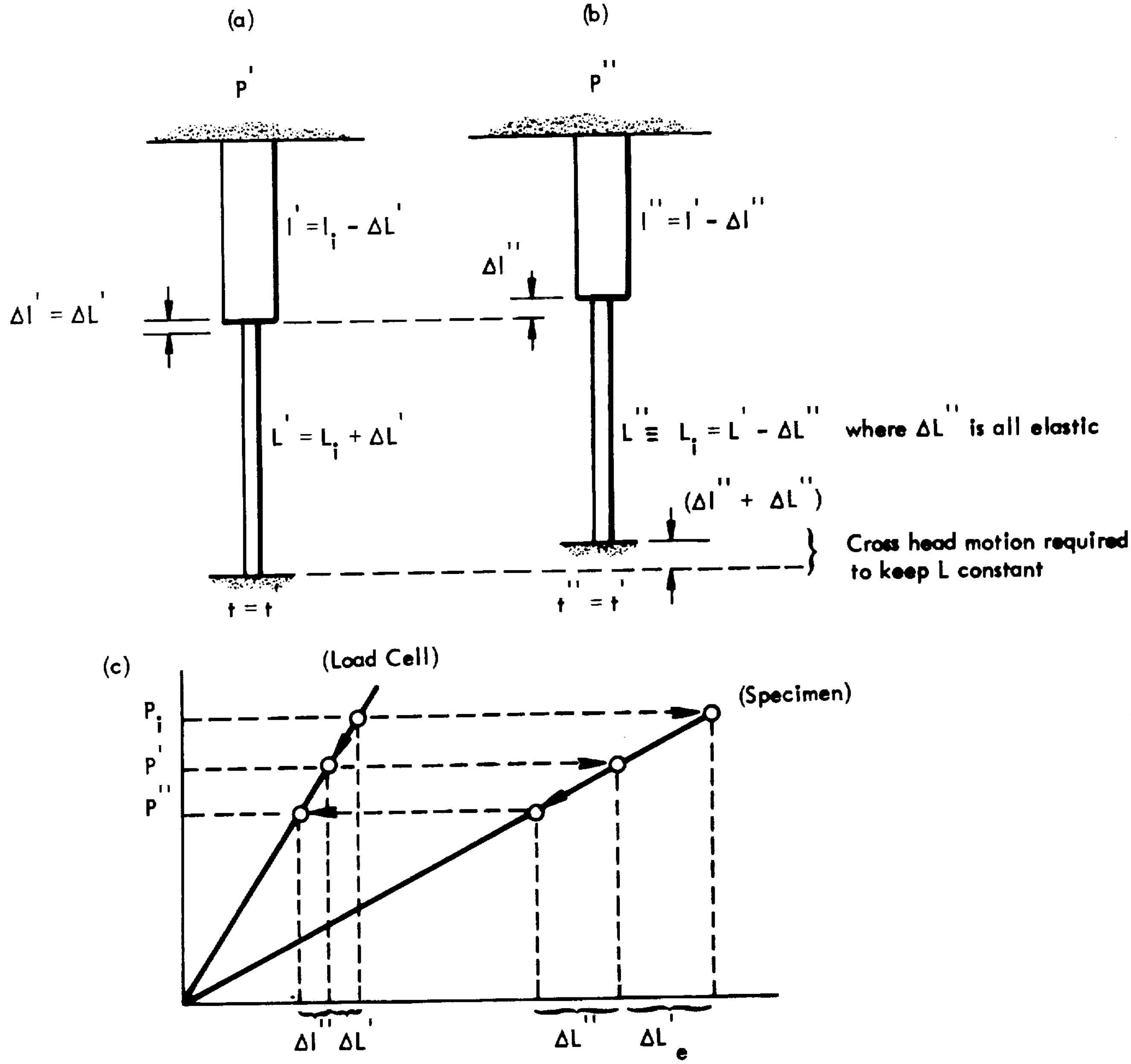

FIGURE AIII-2. Stress Relaxation for Constant Specimen Length

$$\sigma_o - \sigma = \frac{L_o}{A_o} \quad K \epsilon_p = E \epsilon_p$$

where σ = stress after time t

E = specimen modulus

ϵ_p = specimen plastic (creep) strain after time t

In terms of rates,

$$- \dot{\sigma} = \frac{L_o}{A_o} K \dot{\epsilon}_p = E \dot{\epsilon}_p$$

Note the following:

i) The maximum range of specimen plastic (creep) extension during relaxation is ΔL_i^e, i.e., the elastic extension of the specimen on loading to the initial stress.

ii) The cross head movement required to keep L constant at L_i increases as k decreases.

Therefore, the cross head rate must be greater than the specimen creep rate in order to "keep up".

An effort was made to run strain-control stress relaxation by following the strain output from an electromechanical extensometer and manually decreasing the load to maintain the total strain constant. This was generally unsuccessful for the stresses and temperatures employed because the load could not be reduced fast enough with accuracy during the initial portion of the test. The results of a few strain-control tests on beryllium are shown in Figures 20 and 21 of the text. However, it is noted that unless otherwise specified, the stress relaxation plots in Section 4 refer to constant cross head displacement and represent the load on the load cell divided by the initial specimen diameter. Since the spring constant of the machine was much less than that of the specimen, these curves should be corrected as discussed in Part D of this Appendix. In addition, some of the data should be corrected for the relaxation of the system according to the data given in Tables D1 and D2 of Appendix IV.

C. Alternative Derivations of Stress Relaxation Equations

By leaving out the details, the stress relaxation equations of the previous sections can be derived in a much more direct manner as shown below:

i) Constant Cross Head Displacement

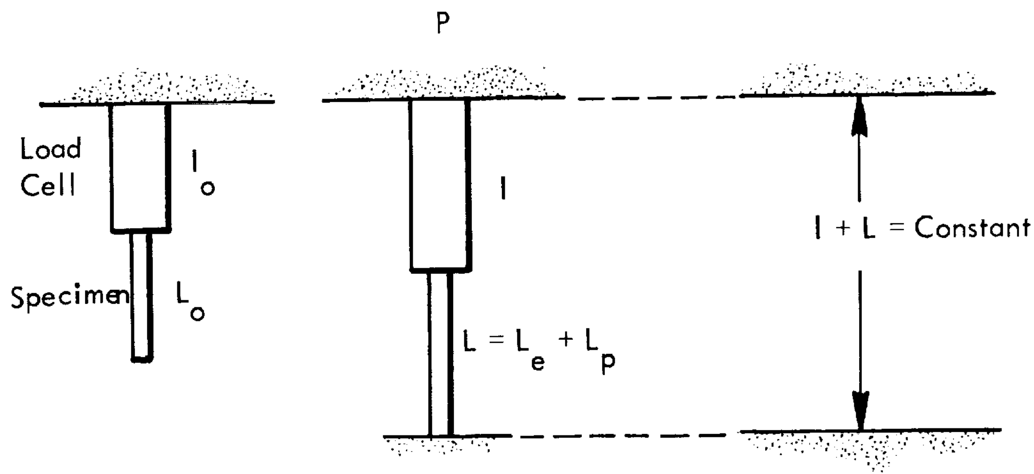

$$L + l = L_e + L_p + l$$

$$d(L + l) = 0 = dL_e + dL_p + dl$$

$$0 = dL_e + dL_p + \frac{P}{k} \quad \ldots\ldots \qquad P = k(l - l_o)$$

$$= \frac{dL_e}{L_o} + \frac{dL_p}{L_o} + \frac{A_o \sigma}{L_o k} \qquad P = K(L_e - L_o)$$

$$= \epsilon_e + \epsilon_p + \frac{A_o}{L_o} \frac{\sigma}{k} \qquad K = \frac{A_o}{L_o} E$$

$$= \frac{\sigma}{E} + \epsilon_p + \frac{A_o}{L_o} \frac{\sigma}{k}$$

or,

$$\sigma \left[\frac{1}{E} + \frac{A_o}{L_o k} \right] = - \epsilon_p$$

or

$$\sigma = - \frac{L_o}{A_o} \left[\frac{k\,K}{k + K} \right] \epsilon_p$$

And in terms of rates,

$$\dot{\sigma} = - \frac{L_o}{A_o} \left[\frac{k\,K}{k + K} \right] \dot{\epsilon}_p$$

ii) Constant Specimen Length

$$L = L_e + L_p$$

$$dL = 0 = dL_e + dL_p$$

$$= \frac{dL_e}{L_o} + \frac{dL_p}{L_o}$$

$$= \epsilon_e + \epsilon_p$$

$$= \frac{\sigma}{E} + \epsilon_p$$

$$\therefore \quad \sigma = - E\,\epsilon_p = - \frac{L_o}{A_o} K\,\epsilon_p$$

And in terms of rates,

$$\dot{\sigma} = - E\,\dot{\epsilon}_p = - \frac{L_o}{A_o} K\,\dot{\epsilon}_p$$

D. Relationship Between Stress Relaxation at Constant Cross Head Displacement and at Constant Strain

Let c denote cross head control and s denote strain control. Then,

$$\dot{\sigma}_c = - \frac{L_o}{A_o} \frac{k\,K}{k+K} \dot{\epsilon}_p \qquad \ldots\ldots \text{ from Part A or C}$$

and $$\dot{\sigma}_s = - \frac{L_o}{A_o} K \dot{\epsilon}_p = - E \dot{\epsilon}_p \qquad \ldots\ldots \text{ from Part B or C}$$

Now, for given ϵ_p, σ_i, σ_o, etc., it follows that:

$$\dot{\sigma}_c < \dot{\sigma}_s \qquad \ldots\ldots \text{ for all } k$$

$$\dot{\sigma}_c = \frac{10}{11} \dot{\sigma}_s \qquad \ldots\ldots \text{ for } k = 10\,K$$

$$\dot{\sigma}_c = \frac{1}{2} \dot{\sigma}_s \qquad \ldots\ldots \text{ for } k = K$$

$$\dot{\sigma}_c = \frac{1}{11} \dot{\sigma}_s \qquad \ldots\ldots \text{ for } k = \frac{1}{10} K$$

$$\dot{\sigma}_c = \frac{k}{K} \dot{\sigma}_s \qquad \ldots\ldots \text{ for } k << K$$

These comparisons are shown graphically in the schematic plot of Figure AIII-3. Thus, the actual shape of the stress relaxation curve, σ vs t, depends on the method of testing. For constant cross head control, the curve can fall anywhere between that for constant strain control and that for creep at constant stress, depending on the elasticity of the machine (load cell, loading bars, etc.) relative to that of the specimen.

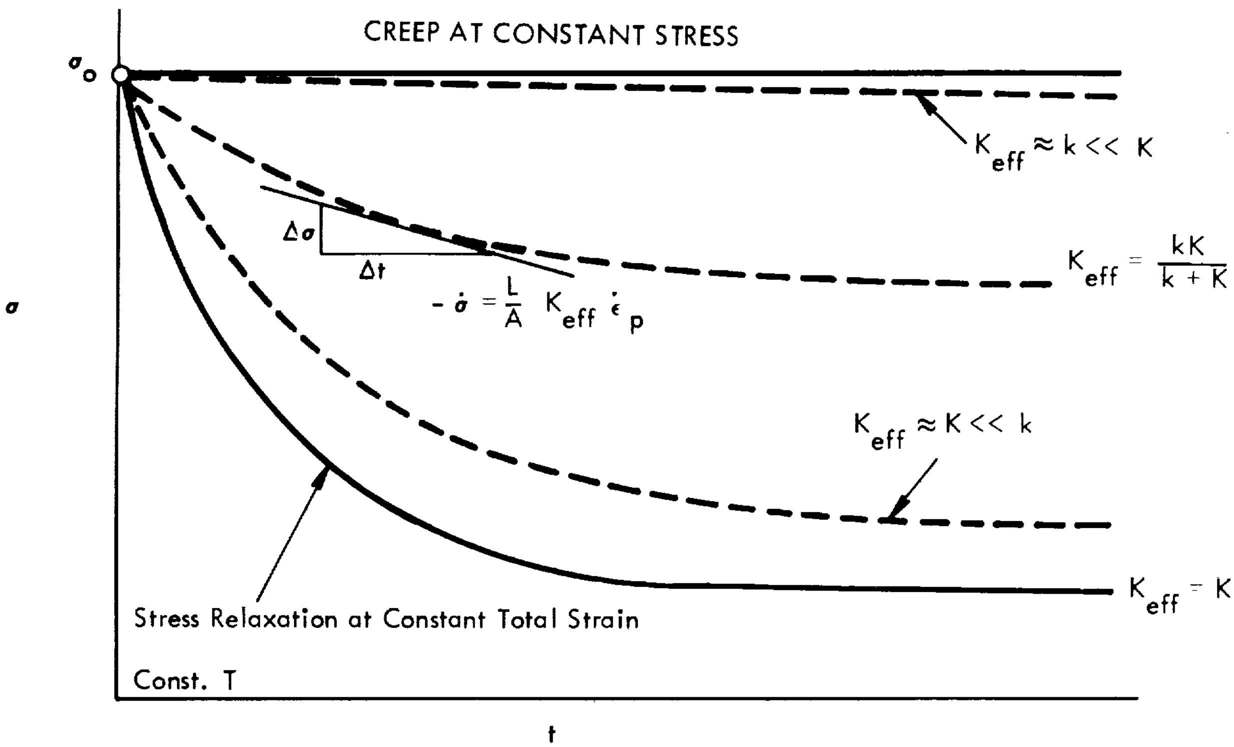

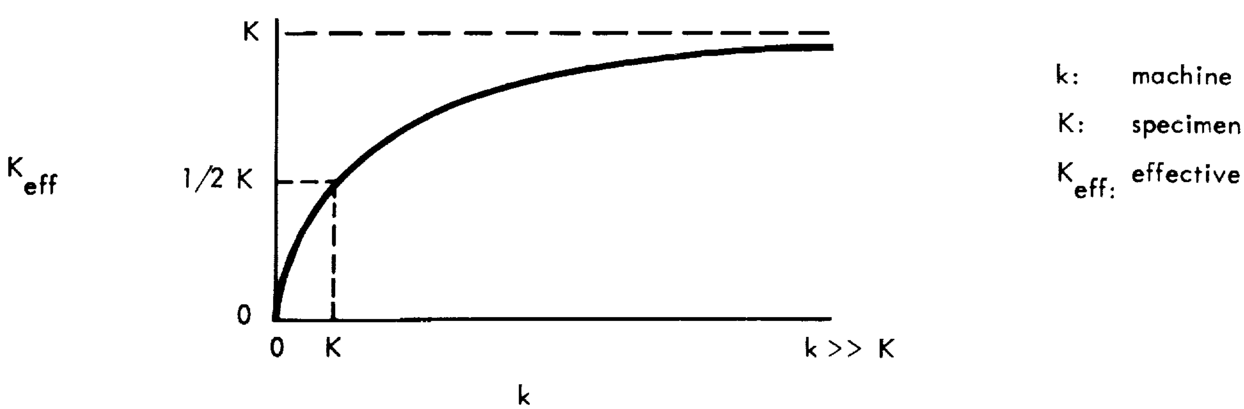

FIGURE AIII-3. Comparison of Stress Relaxation at Constant Crosshead Displacement and Constant Specimen Length (Total Strain)

E. Relationship Between Creep and Stress Relaxation

The stress relaxation curve can be predicted, in principle, if the specimen plastic strain rate $\dot{\epsilon}_p$ is known. In correlating stress relaxation with creep, the plastic strain rate $\dot{\epsilon}_p$ is identified with a creep rate $\dot{\epsilon}_c$. If $\dot{\epsilon}_c$ is further associated with a steady-state creep rate $\dot{\epsilon}_{ss}$ then reasonably simple empirical expressions for the stress and temperature dependence of $\dot{\epsilon}_{ss}$ can be used to predict stress relaxation. Since the creep behavior in the present tests was mostly nonsteady-state, identification of the appropriate creep rate is problematical. This complication in the formulation of mathematically tractable expressions for the time dependent deformation behavior makes correlation of creep and stress relaxation difficult. No correlation was established using the experimental data developed in this program. However, the general approach that would be followed is outlined below.

From the previous sections the stress relaxation equation is

$$\dot{\sigma} = - \frac{L_o}{A_o} K_{eff} \dot{\epsilon}_p$$

and for any given experimental setup there results a stress relaxation curve like that shown in Figure AIII-4a. From this curve, get, for each value of σ, a value for $\dot{\sigma}$, and for each value for $\dot{\sigma}$ calculate a value for $\dot{\epsilon}_p$ from the above equation. Then plot $\dot{\epsilon}_p$ vs σ and get a curve as shown in Figure AIII-4b. The argument now runs that one should get the same curve of $\dot{\epsilon}_p$ vs σ for all K_{eff} (Figure AIII-4c) if $\dot{\epsilon}_p$ is a unique function of σ. Thus, in Figure AIII-4c, $\dot{\epsilon}_p$ for K_{eff}, 2 is less than $\dot{\epsilon}_p$ for K_{eff}, 1 for const. $\dot{\sigma}$ because σ_2 is lower than σ_1 (see again Figure AIII-4b).

The analysis at this point is straightforward. It says that stress relaxation is due to creep and, conversely, should be predictable from creep data. Thus,

$$\dot{\sigma} = - \frac{L_o}{A_o} K_{eff} \dot{\epsilon}_p$$

$$- \dot{\sigma} = E \dot{\epsilon}_p \text{ for strain control or true stress relaxation.}$$

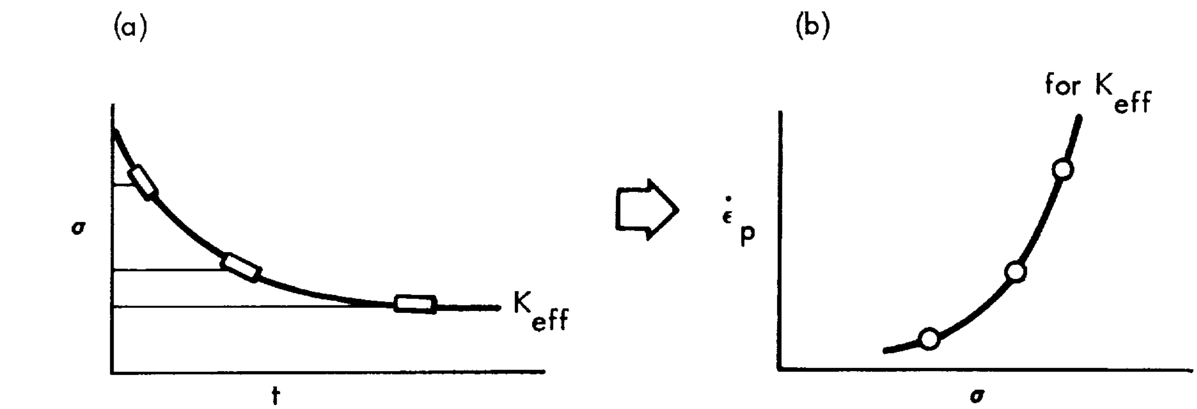

For each $\dot{\sigma}$ get $\dot{\epsilon}_p$

Plot $\dot{\epsilon}_p$ vs σ; should get the same curve for all K_{eff} if $\dot{\epsilon}_p$ is a unique function of σ.

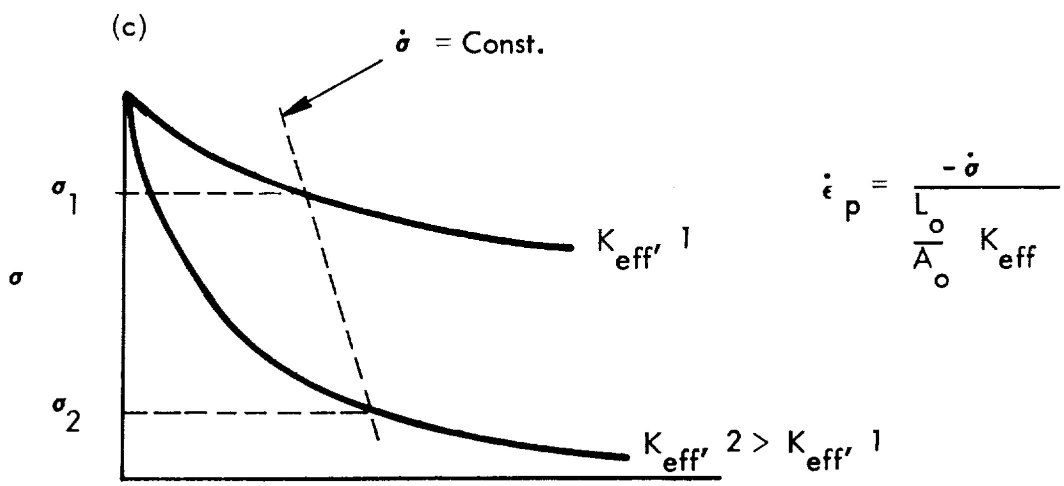

FIGURE AIII-4. Correlation of Stress Relaxation with Creep Rate for Various Values of K_{eff}

To get σ as a function of t we must integrate the above differential equation, and to do this we must know how $\dot{\epsilon}_p$ varies with σ, t, and T in creep tests. For simplicity, we assume constant temperature T. (Even for const. T the analysis is difficult, and for variable T it is very difficult.) Creep curves at constant T and σ (in text book fashion) are of the form shown in Figure AIII-5a, and the steady-state creep rate is a function of σ as shown in AIII-5b. If $\dot{\epsilon}_p$ of the above equation is associated with $\dot{\epsilon}_{ss}$ then integration of the above equation can be carried out in closed-form solution to yield σ as a function of t, i.e., the stress relaxation curve, as was first done by Robinson (E. L. Robinson, "A Relaxation Test on 0.35C Steel K20", Trans. ASME, Vol. 59, p. 451, 1937; and also Trans. ASME Vol. 61, p. 551, 1939).

If $\dot{\epsilon}_p$ is associated with primary creep then $\dot{\epsilon}_p$ is a function of time as well as σ. Gittus (Phil. Mag. 9, p. 749, 1964) has discussed stress relaxation for the case where

$$\dot{\epsilon}_p = (\text{constant})\ \sigma^n\ t^m.$$

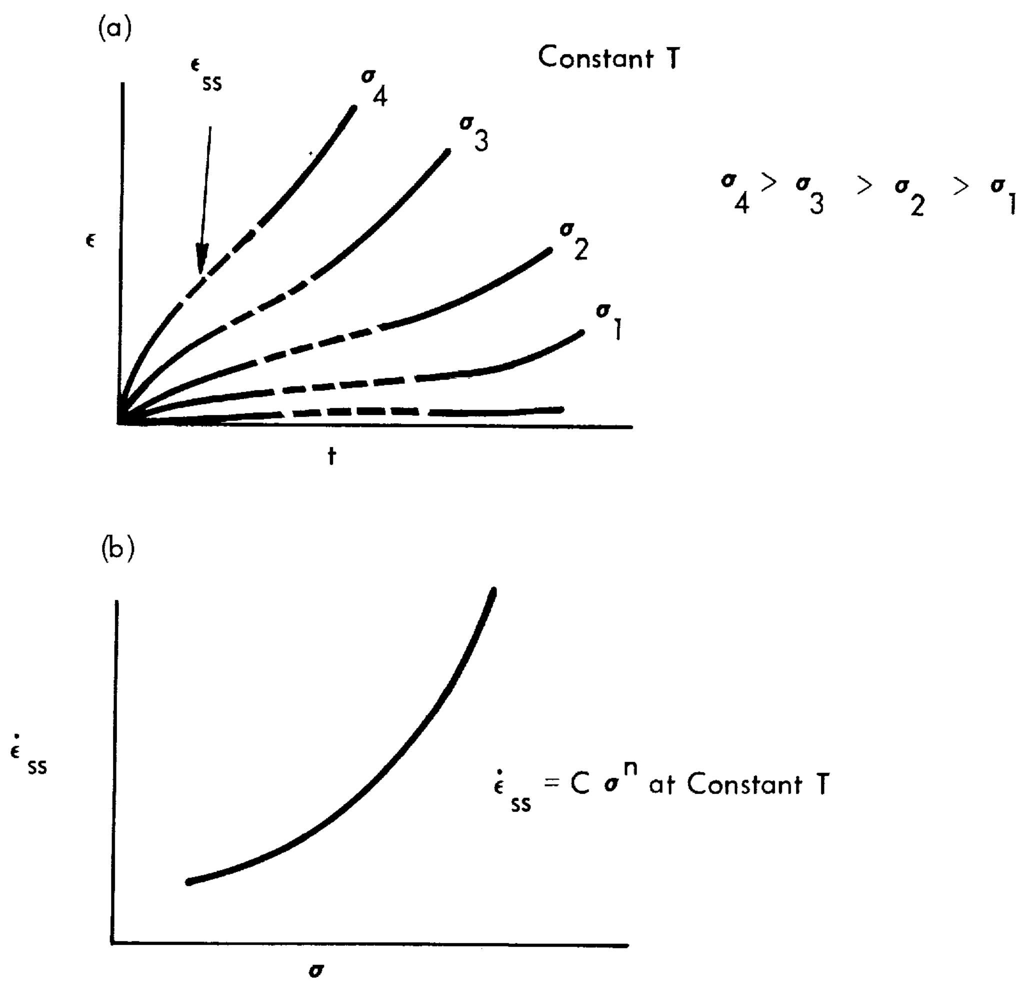

FIGURE AIII-5. Illustrating Creep Curves and Power Law Stress Dependence of Steady State Creep Rate

APPENDIX IV

TABULATION OF TEST DATA

APPENDIX IV

TABULATION OF TEST DATA

This appendix contains a tabulation of the "raw" test data. It is hoped that the tabulation is sufficiently complete to allow replotting of the data according to whatever method is desired. The beryllium data is tabulated in Tables A-1 through A-8, the pure copper data are in Tables B-1 through B-8, and the beryllium-copper Alloy 10 data are in Tables C-1 through C-8. Tables D-1 and D-2 contain correction data for machine relaxation. The symbols employed in these tables are defined as follows: *

P	=	Load in pounds
A_o	=	Initial cross sectional area in $inches^2$
L_o	=	Initial gage length in inches (as-machined or effective, see Appendix II and footnotes to Tables)
δ	=	Plastic deflection, inches
E	=	Elastic modulus, psi x 10^6
G	=	Shear modulus, psi x 10^6
ν	=	Strain ratio

Other abbreviations used are:

PtS. G.	=	Platinum strain gages
A7 S. G.	=	Constantan strain gages
AFX7 S. G.	=	Biaxial constantan strain gages
E-M Ext.	=	Electromechanical extensometer

* Also see Figures AIV-1 and AIV-2 for illustration definition.

Tables A-1, B-1, and C-1 give conventional engineering properties of yield and ultimate strengths based on A_o and % elongation and reduction in area based on A_o and L_o.

Tables A-2, B-2, and C-2 (Tension Tests) and Tables A-3, B-3, and C-3 (Compression Tests) give the raw data for the constant strain rate tests where δ is the plastic deflection as illustrated in Figure AIV-1. Thus, the first load listed corresponds to the proportional limit, the highest load is the ultimate load, and the final load listed is the load at fracture.

Tables A-4, B-4, and C-4 (Tension) and Tables A-5, B-5, and C-5 (Compression) give the raw creep data in terms of the terms defined in Figure AIV-2. Thus, δ is the plastic component of the deformation. The first value of δ given at time $t = 0$ corresponds to the plastic deformation on loading to the creep stress (load) and the subsequent values give the additional deformation due to loading plus time dependent or creep deformation. Tables A-6, B-6, and C-6 (Tension) and Tables A-7, B-7, and C-7 (Compression) give the raw data from stress relaxation tests.

Tables A-8, B-8, and C-8 give the elastic property measurements.

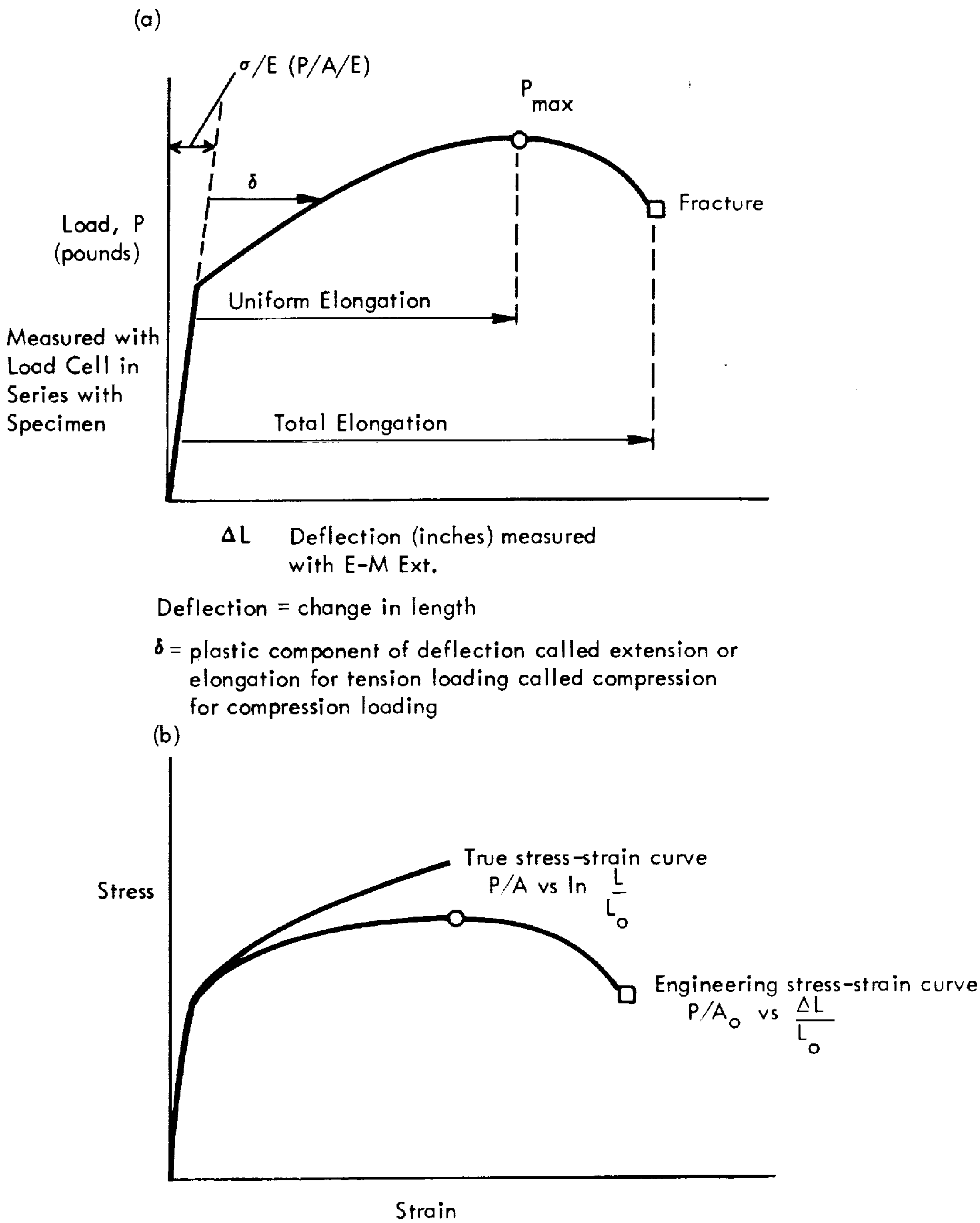

FIGURE AIV-1. Illustrating Terms Used in Connection with Constant Strain Rate Tests

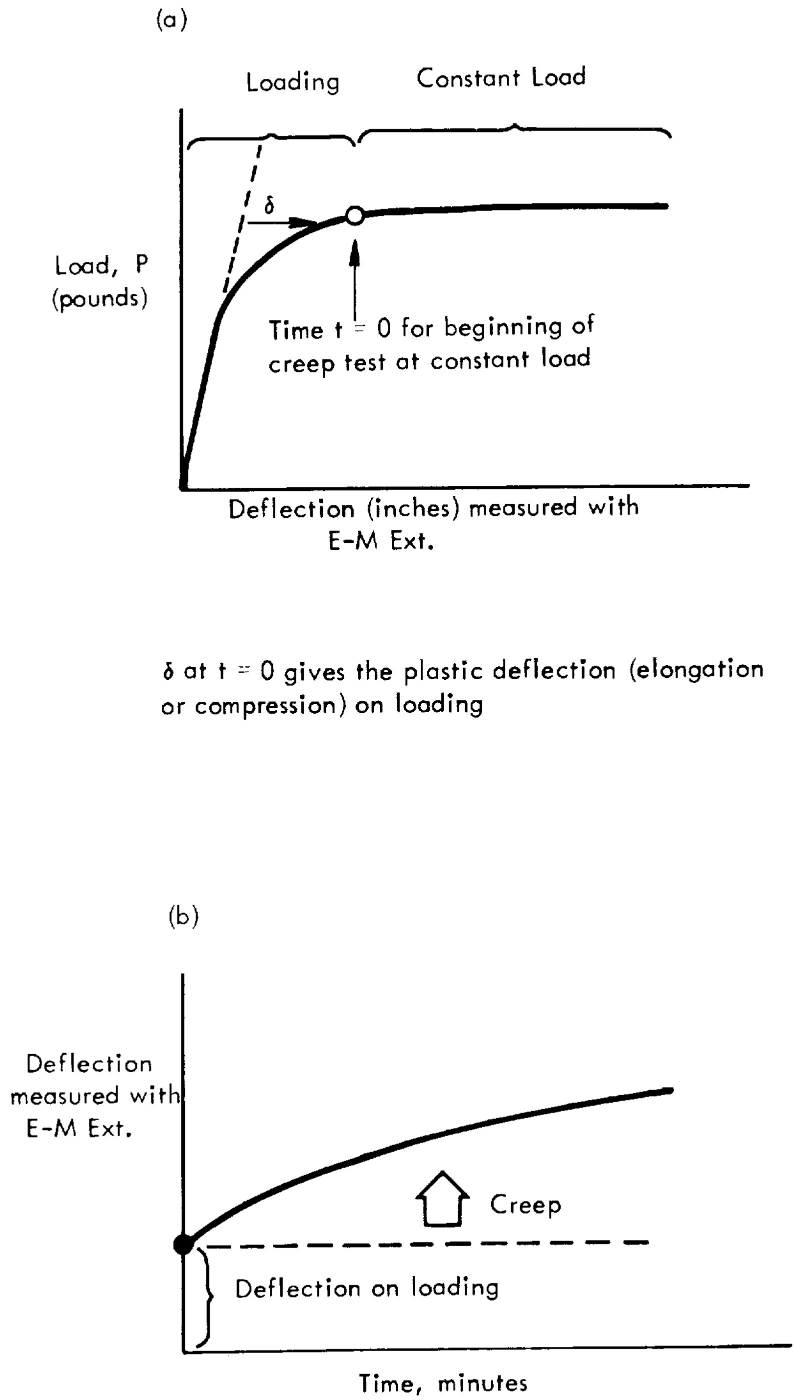

FIGURE AIV-2. Illustrating Terms Used in Connection with Creep Tests

Table A-1. Engineering Constant Strain Rate Data on Be***

	Tension									
Test Temp, °F	75	75	250	500	500	750	1000	1000	1250	1600
Specimen No.	1	2	3	4	5	6	7	8	11	12
Upper Yield Stress, psi	45400	44000	46100	42600	46200	3400				
Lower Yield Stress, psi	41900	41300	41600	36100	37800	29200				
0.2% Offset Stress, psi				*	*	*	21700	23100	8860	1190
Ultimate Tensile Stress, psi	54600	52700	52600	42600/40000	46200/40600	34000/33000	25600	27400	9260	1190
Reduction in Area, %	2.1	3.2	9.4	39.6	48.1	49.1	22.8	30.3	5.0	11.0
% Elongation**										
Uniform	2.29	2.16	11.0	9.2	8.0	4.8	5.9	6.1	0.52	---
Total	2.29	2.16	11.0	21.6	23.6	14.1	12.38	15.1	7.96	9.45
	Compression									
Temp., °F	75	75	250	500	750	750	1000	1250	1250	1600
Specimen No.	1	30	19	4	5	9	7	6	8	10
0.2% Yield Stress, psi	37100	38100	36100	35400	26700	28000	21500	9350	8000	360

* Ultimate load attained at yield, subsequent highest load also reported

** Gage length = 2.12 inches for tension and 1.0 inches for compression (both as-machined) = Effective Gage Length

*** 0.01 and 0.005 inches per minute cross head rate for tension and compression respectively.

Yield stresses and ultimate tensile stresses based on P/A_o

Elongations based on $\Delta L/L_o$

Table A-2. Beryllium Tensile Constant Strain Rate Data

75°F				250°F		500°F				750°F		1000°F				1250°D	
Spec. T-1		Spec. T-2		Spec. T-3		Spec. T-4		Spec. T-5		Spec. T-6		Spec. T-7		Spec. T-8		Spec. T-11	
P,lbs	δ,in	P, lbs	δ,in	P,lbs	δ,in	P,lbs	δ,in	P,lbs	δ,in	P,lbs	δ,in	P,lbs	δ,in	P,lbs	δ,in	P,lbs	δ,in
3800	0.0000	4240	0.000	3210	0.000	3000	0.000	4200	0.000	2400	0.000	1795	0.000	2000	0.000	600	0.000
4380	0.0012	3980	0.000	4480	0.002	4120	0.002	4500	0.002	3295	0.003	2125	0.005	2255	0.005	865	0.005
4030	0.0012	4040	0.010	4050	0.002	3520	0.002	3630	0.011	2900	0.003	2470	0.066	2500	0.035	825	0.050
4200	0.0154	4580	0.025	4280	0.030	3700	0.025	3950	0.150	3010	0.050	2500	0.125	2675	0.132	675	0.100
5000	0.0356	4960	0.038	4680	0.060	3900	0.286	3940	0.300	3200	0.150	2430	0.200	2575	0.254	375	0.169
5280	0.0485	5080	0.046	4980	0.132	3760	0.459	3230	0.500	2650	0.299	2085	0.262	2330	0.320		
Ao=0.0965in^2		Ao=0.0963		4990	0.192	Ao=0.9069		Ao=0.0972in^2		Ao=0.0963in^2		Ao=0.0980in^2		Ao=0.0976in^2		Ao=0.0976in^2	
				5120	0.233												
				Ao=0.0973													

* Gage length = 2.12 inches (as-machined) = Effective Gage Length

δ = plastic elongation measured on the load-deflection (E-MExt) curve.

Table A-3. Beryllium Compressive Constant Strain Rate Data*

75°F				250°F		500°F		750°F				1000°F		1250°F				1600°F	
C-1		C-30		C-19		C-4		C-5		C-9		C-7		C-6		C-8		C-12	
P, in	δ, in	P, lbs	δ, in	P, lbs	δ, in	P, lbs	δ, in	P, lbs	δ, in	P, lbs	δ, in	P, lbs	δ, in	P, lbs	δ, in	P, lbs	δ, in	P, lbs	δ, in
2800	0.000	3150	0.000	2700	0.000	3430	0.000	2290	0.000	2500	0.000	1750	0.000	800	0.000	500	0.000	10	0.000
3710	.002	3810	.002	3710	.002														
5400	.015	5000	.010	4000	.012	3540	.002	2670	.002			2150	.002	935	.002	800	.002	36	.002
7000	.039	6400	.0230	5400	.036	4000	.030	2800	.011	2800	.002	2250	.004	1075	.039	900	.030	40	.104
9000	.085	8000	.053	6400	.064	4600	.056	3000	.016	3000	.014	2500	.016	1175	.117	900	.211	49	.213
11650	.155	9700	.092	7400	.102	5000	.080	3600	.039	3500	.034	3000	.064	1250	.200				
		11000	.121	8500	.158	5600	.135	4000	.168	4000	.075	3500	.116	1295	.208				
		12000	.148	10000	.238	6000	.172	4500	.110	4500	.119	4000	.201						
				12000	.296			5100	.157	5000	.163	4060	.223						
								5700	.212	5500	.212								
								6200	.242	5740	.230								
A_o=0.0968 in^2		A_o=0.1002 in^2		A_o=0.0969 in^2		A_o=0.0971 in^2		A_o=0.0962 in^2		A_o=0.0968 in^2		A_o=0.0969 in^2		A_o=0.0978 in^2		A_o=0.0968 in^2		A_o=0.0969 in^2	

* Gage length = 1.0 inches (as-machined) = Effective Gage Length

δ = Plastic compression measured on the load-deflection (E-M Ext)curve.

Table A-4. Tension Creep Data on Beryllium

Spec. No.	15	16	20	17	18	19	21	22	32
Gage Length, Lo., in	2.12	2.12	2.12	2.12	2.12	2.12	2.12	2.12	2.12
Cross Section Area, Ao, in^2	0.09754	0.09775	0.09731	0.09719	0.09731	0.09649	0.09754	0.09676	0.09655
Applied Load, P., Lbs.	3660	3544	3410	1942	1752	1834	39.0	24.2	48.3
Initial Stress, P/Ao, KSI	37.5	36.25	35.0	20.0	18.0	19.0	0.40	0.250	0.50
Test Temp., °F	500	500	500	1000	1000	1000	1600	1600	1600
Time, minute	δ = Plastic Elongation, inches								
0	0.0000	0.0000	0.0000	0.0000	0.0000	0.0000	0.0000	0.0000	0.0000
1	0.0010	0.0011	0.0011	0.0055	0.0021	0.0023	0.0028	0.0013	0.0049
3	.0016	.0015	.0015	.0127	.0041	.0043	.0065	.0024	.0090
6	.0353	.0017	.0020	.0215	.0061	.0070	.0107	.0034	.0142
12	.0776	.0017	.0025	.0369	.0097	.0121	.0182	.0042	.0215
18	.0918	.0020	.0027	.0539	.0132	.0170	.0251	.0047	.0286
24	.1025	.0024	.0030	.0705	.0175	.0200	.0307	.0055	.0341
30	.1120	.0024	.0033	.0900	.0198	.0234	.0366	.0060	.0393
36	.1212	.0666	.0035	.1133	.0224	.0270	.0412	.0062	.0445
42	.1305	.0868	.0038	.1456	.0255	.0308	.0455	.0066	.0495
48	.1397	.0988	.0040	Broke at 42 min.	.0281	.0349	.0485	.0070	.0548
54	.1490	.1079	.0042		.0306	.0385	.0524	.0073	.0586
60	.1583	.1159	.0044		.0335	.0427	.0559	.0076	.0638

Gage Length = 2.12 inches (as-machined) = Effective Gage Length

Table A-5. Compression Creep Data on Beryllium

Spec. No.	13	12	14	15	16	17	18	31	20
Gage Length, Lo., in	0.9992	0.9982	0.9999	0.9987	0.9985	0.9983	0.9903	0.9937	0.9963
Cross Section Area, Ao., in^2	0.09720	0.90720	0.09665	0.09627	0.90599	0.09687	0.09665	0.09643	0.09687
Applied Load, P., Lbs.	3888	3644	3384	1926	1824	1744	48.3	38.6	24.2
Initial Stress, P/Ao, KSI	40.0	37.5	35.0	20.0	19.0	18.0	0.50	0.40	0.25
Test Temp., °F	500	500	500	1000	1000	1000	1600	1600	1600
Time, minute	δ = Plastic Compression, in.								
0	0.0170	0.0055	0.0000	0.0000	0.0000	0.0000	0.0000	0.0000	0.0000
1	.0215	.0165	.0029	.0017	.0014	.0016	.0008	.0013	.0004
3	.0257	.0202	.0059	.0033	.0022	.0027	.0026	.0028	.0008
6	.0278	.0207	.0089	.0056	.0031	.0035	.0037	.0043	.0009
12	.0302	.0214	.0130	.0100	.0050	.0045	.0053	.0057	.0013
18	.0317	.0217	.0182	.0124	.0062	.0055	.0065	.0059	.0022
24	.0329	.0220	.0191	.0146	.0075	.0064	.0077	.0061	.0023
30	.0338	.0228	.0195	.0165	.0087	.0070	.0087	.0063	.0023
36	.0345	.0239	.0198	.0179	.0101	.0075	.0097	.0065	.0024
42	.0351	.0246	.0200	.0196	.0112	.0081	.0106	.0068	.0026
48	.0356	.0246	.0200	.0211	.0123	.0088	.0112	.0070	.0027
54	.0361	.0246	.0200	.0222	.0132	.0095	.0125	.0071	.0026
60	.0364	.0247	.0200	.0236	.0142	.0101	.0136	.0072	.0025

Gage Length = 1.0 inches (as-machined) = Effective Gage Length

Table A-6. Tension Stress Relaxation Data on Beryllium

Spec. No.	T-23	T-24	T-25	T-26	T-27	T-28	T-29	T-33*
Gage Length, Lo., in.	2.12	2.12	2.12	2.12	2.12	2.12	2.12	2.12
Cross Section Area, Ao., in^2	0.09692	0.09649	0.09689	0.09709	0.09731	0.09725	0.09731	0.0969
Initial Stress, P/Ao, KSI	36.35	35.15	34.25	19.42	17.50	18.45	0.52	17.50
Test Temp., ^{o}F	500	500	500	1000	1000	1000	1600	1000
Time, minute	Tensile Stress, KSI, P/A_o							
0	36.35	35.15	34.25	19.42	17.50	18.45	0.522	17.50
1		33.60	32.75	17.75	16.38	16.75	0.190	7.50
2								6.05
3	34.75	33.10	32.25	16.98	15.75	15.95	0.156	5.18
6	34.40	32.90	32.10	16.25	15.18	15.30	0.146	3.75
12	34.00	32.40	31.75	15.30	14.70	14.50	0.144	2.32
18	30.00	32.10	31.15	15.05	14.52	14.22	0.144	1.58
24	28.75	31.90	30.95	14.85	14.45	14.02	0.143	1.30
30	28.30	31.65	30.80	14.62	14.30	13.78	0.142	1.10
36	28.10	31.55	30.50	14.48	14.22	13.60	0.140	0.95
42	27.90	31.50	30.45	14.42	14.15	13.38	0.138	0.80
48	27.80	31.50	30.40	14.30	13.95	13.25	0.136	0.65
54	27.70	31.50	30.35	14.20	13.82	13.12	0.135	0.58
60	27.60	31.50	30.35	14.12	13.68	12.85	0.134	0.55

*Strain controlled, see text.
Gage Length = 2.12 inches (as-machined) = Effective Gage Length

Table A-7. Compression Stress Relaxation Data on Beryllium

Spec. No.	21	22	23	24	25	26	27	28	29
Gage Length, Lo., in.	0.9972	1.0035	0.9972	0.9990	1.0018	0.9932	0.9967	1.0013	0.9943
Cross Section Area, Ao., in^2	0.09693	0.09687	0.09720	0.09720	0.09726	0.09687	0.09610	0.09621	0.09676
Initial Stress, P/Ao, KSI	37.60	36.25	35.30	50.96	19.05	18.00	0.520	0.440	0.250
Test Temp., ^{o}F	500	500	500	1000	1000	1000	1600	1600	1600
Time, minute	Compression Stress, KSI, P/A_o								
0	37.60	36.25	35.30	50.96	19.05	18.00	0.520	0.440	0.250
1				34.58	17.50	16.60	.220	.180	.188
3	34.10	31.85	31.50	29.99	17.02	16.05	.202	.168	.172
6	33.85	31.20	30.90	26.94	16.60	15.70	.192	.162	.170
12	33.75	30.90	30.00	23.95	15.85	15.12	.184	.160	.160
18	33.50	30.50	29.45	22.35	15.45	14.70	.176	.160	.156
24	33.45	30.25	29.10	20.82	15.03	14.32	.170	.160	.156
30	33.40	30.20	28.90	19.66	14.70	14.05	.162	.160	.154
36	33.40	30.00	28.80	18.93	14.50	13.80	.158	.160	.150
42	33.10	30.00	28.60	18.00	14.30	13.50	.150	.158	.144
48	32.90	30.00	28.50	17.33	14.20	13.22	.150	.150	.140
54	32.80	30.00	28.50	16.90	14.10	13.08	.148	.148	.140
60	32.65	30.00	28.50	16.45	14.03	13.05	.144	.148	.138

Gage Length = 1.0 inch (as-machined) = Effective Gage Length

Table A-8. Elastic Property Data on S-200 Beryllium

	R.T.			250°F			500°F			750°F			1000°F			1250°F			1600°F		
	E	G	ν	E	G	ν	E	G	ν	E	G	ν	E	G	ν	E	G	ν	E	G	ν
Dynamic	54.5	25.2	.068	51.7	25.2	.029	50.7	24.5	.038	48.5	23.2	.049	47.7	22.9	.043	45.9	22.9	.034	44.0	21.2	.038
Tension																					
Pt SG (No. 9)	42.1		.02	41.2		.04	41.4		.04	41.5		.05									
(No. 10)	42.4		.02				42.3		.04	41.2		.03	41.2		.05	32.6		.06			
A7SG (No. 9)	49.3																				
A7SG (No. 10)	40.3																				
A7SG (Round)	44.9																				
Dentronic SG (Round)	42.2																				
E-M Ext (CSR)	37.5 36.7			42.4			44.2			45.3			36.4			23.1					
(GL 2.12) =$GL_{eff.}$	44.1 45.5						44.2						31.1								
	43.2 40.3																				
	42.5 36.4																				
	37.4																				
Compression																					
Pt SG (No. 2)	44.1		.01	43.2		.03	42.7		.02	41.3		.06	39.5		.07	36.3		.17			

Table B-1. Copper Engineering Constant Strain Rate Data**

Tension											
Test Temp., °F	75	75	250	500	500	750	1000	1000	1250	1600	1600
Specimen No.	1	2	3	4	5	6	7	8	31	11	30
0.2% Offset Stress, psi	6720	8670	6960	7040	6720	5480	4570	5020	2950	1510	1610
Ultimate Tensile Stress, psi	29000	29100	25000	19600	19500	13900	7230	8870	4210	2080	2110
Reduction in Area, %	88.1	88.8	85.3	42.3	42.1	28.9	28.9	32.1	12.9	8.7	15.5
% Elongation*											
Uniform	31.0	32.2	23.4	20.3	22.2	16.5	9.4	12.3	6.6	3.5	4.8
Total	43.6	47.1	43.3	27.0	29.4	19.2	18.3	26.1	12.3	10.6	11.3
Compression											
Temperature, °F	75	75	250	500	750	750	1000	1250	1250	1600	1600
Specimen No.	1	30	3	4	5	6	7	8	9	10	11
0.2% Yield Stress, psi	6800	6400	6200	5700	4900	5100	5250	2700	2100	1470	1700

* Gage Length = 2.50 inches (effective) for tension and 1.0 inch (as-machined) for compression

** 0.01 and 0.005 inches per minute cross head speed for tension and compression respectively.

Yield and ultimate stresses based on P/A_o

Elongations based on $\Delta L/L_o$

Table B-2. Copper Tensile Constant Strain Rate Data

75°F				250°F		500°F				750°F		1000°F				1250°F		1600°F			
1		2		3		4		5		6		7		8		31		11		30	
P,lbs	δ,in	P,lbs	δ,in	P,lbs	δ,in	P,lbs	δ,in	P,lbs	δ,in	P,lbs	δ,in	P,lbs	δ,in	P,lbs	δ,in	P,lbs	δ,in	P,lbs	δ,in	P,lbs	δ,in
1100	0.0000			1220	0.0000	1150	0.0000	1100	0.0000	700	0.0000	660	0.0000								
1350	.0045	1600	0.0000	1390	.0045	1400	.0045	1350	.0045	980	.0020	800	0.0015	870	0.0000	500	0.0000	220	0.0000	230	0.0000
1500	.0059	1740	.0045	1990	.0320	1530	.0120	1570	.0190	1100	.0045	920	.0045	1000	0.0045	590	0.0045	250	0.0005	243	.0015
2000	.0260	1960	.0185	2490	.0706	1930	.0396	1970	.0495	1230	.0100	1200	.0380	1198	.0180			300	.0045	293	.0020
2500	.0561	2460	.0430	2990	.1066	2330	.0695	2370	.0855	1480	.0260	1400	.1420	1398	.0545	700	.0410	350	.0290	320	.0045
3000	.0982	2960	.0840	3490	.1586	2730	.1450	2770	.1395	1730	.0540	1444	.2120	1598	.1350	800	.1060	400	.0810	343	.0115
3500	.1520	3460	.1865	3990	.2326	3130	.2310	3170	.2215	1980	.0900	1000	.4120	1766	.3450	842	.1865	417	.1390	393	.0045
4000	.2160	3960	.1975	4490	.3446	3530	.3130	3570	.3495	2230	.1420	600	.4540	1000	.6200	400	.3850	200	.2970	421	.1305
4500	.2925	4460	.2750	5000	.6526	3930	.5990	3905	.6195	2480	.2200	43	.5152	100	.7335					200	.3172
5000	.3940	4960	.3750	2970	1.2195	3250	.7582	3300	.8258	2730	.3680										
5500	.5480	5460	.5280							2780	.4680										
5830	.8750	5840	.9065							2400	.5400										
3150	1.2262	3220	1.3252																		
A_o=0.201in^2		A_o=0.201in^2		A_o=0.200in^2		A_o=0.199in^2		A_o=0.200in^2		A_o=0.200in^2		A_o=0.200in^2		A_o=0.199in^2		A_o=0.200in^2		A_o=0.200in^2		A_o=0.199in^2	

Gage Length = 2.0 inches (as-machined), Effective Gage Length = 2.5 inches

δ = plastic elongation measured on the load-deflection (E-M Ext) curve.

Table B-3. Copper Compressive Constant Strain Rate Data*

75°F				250°F		500°F		750°F				1000°F		1250°F				1600°F			
C-1		C-30		C-3		C-4		C-5		C-6		C-7		C-8		C-9		C-10		C-11	
P,lbs	δ,in	P,lbs	δ,in	P,lbs	δ,in	P,lbs	δ,in	P,lbs	δ,in	P,lbs	δ,in	P,lbs	δ,in	P,lbs	δ,in	P,lbs	δ,in	P,lbs	δ,in	P,lbs	δ,in
500	0.000	550	0.000	500	0.000	400	0.000	380	0.000	420	0.000	370	0.000	240	0.000	200	0.000	130	0.000	145	0.000
680	.002	640	.002	620	.002	570	.002	490	.002	510	.002	525	.002	270	.002	210	.002	147	.002	170	.002
1000	.010	1000	.010	1500	.036	1500	.052	1000	.026	1000	.026	750	.029	400	.032	400	.026	200	.023	200	.023
2500	.030	2000	.048	2500	.091	2500	.134	2000	.144	2000	.133	1000	.081	600	.109	600	.088	250	.058	250	.063
4000	.110	4000	.144	3500	.162	3500	.230	3000	.289	3000	.269	1250	.143	700	.192	800	.440	300	.150	300	.147
5000	.200	5000	.200	5000	.270	4000	.280	4000	.432	4000	.392	1410	.248	800	.332					325	.208
A_o=0.1005in^2		A_o=0.1007in^2		A_o=0.1000in^2		A_o=0.1003in^2		A_o=0.1000in^2		A_o=0.1004in^2		A_o=0.1005in^2		A_o=0.0998in^2		A_o=0.1003in^2		A_o=0.1004in^2		A_o=0.0995in^2	

*Test stopped before fracture.

Gage Length = 1.0 inch (as-machined) = $GL_{eff.}$

δ = plastic compression measured on the load-deflection (E-MExt) curve.

Table B-4. Tension Creep Data on Copper

Spec. No.	12	13	14	15	16	17	18	19	20
Gage Length, Lo., in.*	2.0	2.0	2.0	2.0	2.0	2.0	2.0	2.0	2.0
Cross Section Area, Ao., in^2	0.1997	0.1997	0.1998	0.2001	0.1999	0.2001	0.2004	0.1997	0.2007
Applied Load, P., Lbs.	1400	2400	3000	1000	597	800	241	200	221
Initial Stress, P/Ao, KSI	7.0	12.0	15.0	5.0	3.0	4.0	1.20	1.00	1.10
Test Temp., ^{o}F	500	500	500	1000	1000	1000	1600	1600	1600
Time, minute	Plastic Elongation, in.								
0	.0106	.0912	.1650	.0100	0.0000	0.0000	0.0000	0.0000	0.0000
1	.0118	.0940	.1720	.0182	.0002	.0002	.0022	.0002	.0000
3	.0120	.1000	.1832	.0306	.0002	.0004	.0056	.0004	.0010
6	.0122	.1054	.1948	.0438	.0002	.0011	.0104	.0011	.0025
12	.0141	.1120	.2108	.0624	.0003	.0024	.0184	.0024	.0056
18	.0142	.1144	.2228	.0770	.0003	.0038	.0260	.0038	.0090
24	.0144	.1160	.2304	.0896	.0003	.0046	.0338	.0046	.0126
30	.0148	.1174	.2352	.1006	.0004	.0058	.0420	.0058	.0170
36	.0150	.1182	.2382	.1102	.0004	.0066	.0496	.0066	.0214
42	.0151	.1190	.2404	.1188	.0004	.0082	.0580	.0082	.0258
48	.0153	.1194	.2418	.1272	.0005	.0092	.0696	.0092	.0304
54	.0154	.1202	.2426	.1358	.0005	.0102	.0864	.0102	.0354
60	.0156	.1204	.2440	.1444	.0005	.0112	Spec. broke at 0.95 hrs. .1175	.0114	.0404

* Gage length = 2.0 inches (as-machined), Effective Gage Length = 2.5 inches

Table B-5. Compression Creep Data on Copper

Spec No.	12	13	14	15	16	17	18	19	20	21
Gage Length, Lo., in.	1.0035	1.0030	1.0024	1.0027	1.0019	0.9990	1.0034	1.0033	1.0032	1.0158
Cross Section Area, Ao., in^2	0.10037	0.10060	0.09992	0.10027	0.10049	0.10038	0.10043	0.10049	0.09982	0.09982
Applied Load, P., Lbs.	1483	1193	700	500	600	400	110	100	120	110
Initial Stress P/Ao., KSI	14.83	11.93	7.0	5.0	6.0	4.0	1.1	1.0	1.2	1.1
Test Temp., °F	500	500	500	1000	1000	1000	1600	1600	1600	1600
Time, minute	δ = Plastic Compression, inches									
0	0.0412	0.0260	0.0030	0.0046	0.0080	0.0011	0.0000	0.0000	0.0000	0.0000
1	.0461	.0302	.0043	.0101	.0182	.0016	.0003	.0004	.0006	.0002
3	.0483	.0317	.0047	.0156	.0262	.0027	.0008	.0006	.0015	.0004
6	.0498	.0328	.0053	.0203	.0329	.0037	.0012	.0010	.0026	.0006
12	.0516	.0338	.0056	.0261	.0418	.0057	.0020	.0018	.0044	.0012
18	.0527	.0345	.0057	.0305	.0478	.0072	.0026	.0026	.0059	.0018
24	.0535	.0351	.0059	.0340	.0522	.0088	.0032	.0034	.0076	.0022
30	.0541	.0355	.0060	.0366	.0560	.0105	.0038	.0042	.0092	.0025
36	.0548	.0359	.0060	.0390	.0592	.0121	.0042	.0050	.0106	.0030
42	.0552	.0362	.0061	.0412	.0617	.0137	.0047	.0058	.0019	.0033
48	.0556	.0365	.0061	.0430	.0641	.0143	.0052	.0066	.0131	.0038
54	.0561	.0368	.0062	.0446	.0664	.0151	.0057	.0074	.0144	.0042
60	.0563	.0371	.0062	.0463	.0684	.0157	.0063	.0082	.0155	.0046

Gage Length = 1.0 inches (as-machined) = Effective Gage Length

Table B-6. Tension Stress Relaxation Data on Copper

Spec. No.	21	22	23	25	26	32	27	29
Gage Length, Lo., in.*	2.0	2.0	2.0	2.0	2.0	2.0	2.0	2.0
Cross Section Area, Ao., in^2	0.1997	0.1998	0.2001	0.2005	0.1999	0.2004	0.1997	0.1995
Initial Stress, P/Ao., KSI	7.0	12.0	15.0	6.0	4.0	5.0	1.20	1.00
Test Temp., ^{o}F	500	500	500	1000	1000	1000	1600	1600
Time, minute	Tensile Stress, KSI, P/A_o							
0	7.00	12.00	15.00	6.00	4.00	5.00	1.20	1.03
1	6.60	11.30	13.92	5.13	3.88	4.47	.86	.79
3	6.55	11.00	13.40	4.72	3.76	4.22	.81	.72
6	6.50	10.92	13.19	4.43	3.66	4.00	.74	.66
12	6.45	10.82	13.10	4.12	3.51	3.80	.67	.58
18	6.42	10.78	13.03	3.91	3.41	3.65	.60	.50
24	6.41	10.71	12.97	3.75	3.32	3.56	.56	.45
30	6.41	10.69	12.93	3.63	3.26	3.48	.54	.40
36	6.41	10.68	12.90	3.53	3.22	3.40	.50	.36
42	6.40	10.62	12.90	3.45	3.15	3.32	.50	.35
48	6.40	10.62	12.87	3.40	3.12	3.26	.50	.34
54	6.40	10.61	12.86	3.34	3.09	3.22	.50	.33
60	6.40	10.60	12.86	3.28	3.06	3.19	.50	.32

* Gage Length = 2.0 inches (as-machined), Effective gage length = 2.5 inches

Table B-7. Compression Stress Relaxation Data on Copper

Spec. No.	29	27	28	25	26	24	22	21	23
Gage Length, Lo., in	1.0004	1.0039	1.0021	1.0032	1.0012	1.0031	1.0010	1.0035	1.0030
Cross Section Area, Ao., in^2	0.10055	0.10049	0.10049	.10039	.09971	0.10060	0.10043	0.10032	0.10043
Initial Stress, P/Ao., KSI	7.0	12.0	15.0	4.0	5.0	5.98	1.0	1.08	1.20
Test Temp., $^{\circ}F$	500	500	500	1000	1000	1000	1600	1600	1600
Time, minute	Compression Stress, KSI, P/A_o								
0	7.00	12.00	15.00	4.00	5.00	5.98	1.00	1.08	1.20
1	6.85	11.40	14.10	3.75	4.55	5.17	0.60	0.81	0.88
3	6.80	11.29	13.92	3.61	4.37	4.83	.51	.76	.85
6	6.79	11.22	13.80	3.54	4.22	4.57	.45	.74	.83
12	6.79	11.17	13.71	3.44	4.07	4.27	.40	.72	.70
18	6.78	11.11	13.65	3.33	3.94	4.13	.34	.71	.64
24	6.77	11.06	13.60	3.26	3.87	4.02	.34	.70	.60
30	6.76	11.00	13.54	3.22	3.80	3.91	.32	.67	.56
36	6.76	10.98	13.48	3.15	3.76	3.87	.31	.64	.54
42	6.76	10.98	13.44	3.12	3.73	3.83	.29	.64	.52
48	6.76	10.97	13.40	3.10	3.70	3.80	.26	.63	.50
54	6.76	10.97	13.39	3.07	3.67	3.76	.25	.63	.48
60	6.76	10.96	13.38	3.03	3.65	3.75	.24	.61	.46

Gage Length = 1.0 inch (as-machined) = Effective Gage Length

Table B-8. Elastic Property Data on OFHC Copper

	R.T.			250°F			500°F			750°F			1000°F			1250°F			1600°F		
	E	G	ν	E	G	ν	E	G	ν	E	G	ν	E	G	ν	E	G	ν	E	G	ν
Dynamic Run 1	15.6	7.6	.025	15.9	7.9	.024	15.6	7.6	.027	15.3	7.4	.041	14.5	6.9	.048	13.2	5.7	.16			
Run 2	16.5	7.9	.036	14.7	7.6	.049	14.8	7.1	.040	13.9	6.9		13.8	6.5	.065	12.7	5.7	.13			
Tension																					
Pt SG (No. 9)	18.9		.41	15.5			16.5		.32	15.1		.30									
A7 SG (No. 9)	18.0		.32																		
Au SG (No. 1)	17.9																				
E-M Ext.(No. 9) Up	17.4			16.7			13.9			9.7			11.6			11.9					
(GL 2.0") Down	17.0						14.0			12.9			11.8						7.1		
E-M Ext. (CSR)	17.8			17.6			15.9			10.2			12.4			9.8			7.0		
(GL 2.5") (CSR)	18.1						12.6						11.5						8.0		
Compression																					
Pt SG (OC3)Air Cured	17.2																				
Pt SG (OC2) Up	15.0		.018	14.2		.014	12.1		.04												
(Vac Cured) Down	15.2			14.7																	
A7 SG (OC3)	19.0																				
AFX7 SG (OC3)	18.0		.32																		
A7 SG (OC2)	15.9																				
E-M Ext (OC2)																					
(GL 1.0")	12.0			10.2			8.9														
E-M Ext (CSR)	15.7			10.1			8.6			13.4			8.3						7.5		
(GL 1.0")	14.9																				

Table C-1. Beryllium-Copper Alloy 10 Engineering Constant Strain Rate Data***

Tension											
Test Temp., °F	75	75	250	500	500	750	1000	1250	1250	1600	1600
Specimen No.	T-1	T-2	T-3	T-4	T-5	T-6*	T-7*	T-8	T-30	T-31	T-11
0.2% Offset Stress, psi	87700	85800	87200	80800	76000			19630	20950	2700	3320
Ultimate Tensile Stress, psi	112700	111700	111300	93800	90000			20130	21590	3300	3750
Reduction in Area, %	37.1	38.9	24.7	7.7	8.6	*	*	33.9	29.2	92.1	91.9
%Elongation**											
Uniform	12.6	10.6	12.1	4.0	4.3			0.60	0.44		
Total	17.6	15.5	14.1	4.0	4.3	*	*	13.3	12.2	61.2	38.4
Compression											
Temperature, °F	75	75	250	500	750	750	1000	1000	1250	1600	1600
Specimen No.		30	31	4	5	6	7	8	9	10	11
Yield Stress, psi	75700	70500	65000	87000	77400	78600	50300	48800	20900	3700	3300

*Specimen Broke in Threads. T-6 at 50,000 psi and T-7 at 34,800 psi stress on gage section.

**Gage Length = 2.50 inches (effective) for tension and 1.0 inch (as-machined) for compression.

***0.01 and 0.005 inches per minute cross head rate for tension and compression respectively.

Yield and ultimate stresses based on P/A_o

Elongations based on $\Delta L/L_o$

Table C-2. Beryllium Copper Tensile Constant Strain Rate Data

75°F				250°F		500°F				1250°F				1600°F			
T-1		T-2		T-3		T-4		T-5		T-8		T-30		T-31		T-11	
P, lbs	δ, in	P, lbs	δ, in	P, lbs	δ, in	P, lbs	δ, in	P, lbs	δ, in	P, lbs	δ, in	P, lbs	δ, in	P, lbs	δ, in	P, lbs	δ, in
15300	0.0000	15200	0.0000	16000	0.0000	13600	0.0000	13000	0.0000	3380	0.0000	3650	0.0000	200	0.0000	555	0.0000
16800	.0020	16200	.0015	17000	.0035	14100	.0010	14000	.0020	3480	.0005	3750	.0005	300	.0003	580	.0005
17600	.0045	17200	.0045	17400	.0045			15200	.0045	3680	.0015	3950	.0010	400	.0019	605	.0010
18800	.0150	19200	.0295	19000	.0215	15200	.0045	16000	.0100	3950	.0045	4150	.0040	500	.0053	630	.0015
19800	.0380	20200	.0620	20000	.0500	17100	.0125	17000	.0305	4040	.0540	4210	.0045	600	.0270	655	.0025
20300	.0600	21200	.1260	21000	.1075	18100	.0380	18000	.0975	2580	.3330	4340	.0400	670	.0517+	705	.0085
20800	.0875	22400	.2990	22000	.1975	18800	.0920	18000	.1064			650	.3060			730	.0150
21300	.1150	20100	.3870	22200	.3025	18700	.1006									750	.0500+
21800	.1655			22200	.3532												
22300	.2300																
22600	.3180																
20000	.4388																
$A_o=0.201 in^2$		$A_o=0.200 in^2$		$A_o=0.200 in^2$		$A_o=0.200 in^2$		$A_o=0.200 in^2$		$A_o=0.201 in^2$		$A_o=0.201 in^2$		$A_o=0.201 in^2$		$A_o=0.200 in^2$	

Gage Length = 2.0 inches (as-machined) = 2.5 inches effective gage length

δ = plastic elongation measured on the load-deflection (E-M Ext) curve.

Table C-3. Beryllium Copper Compressive Constant Strain Rate Data

75°F				250°F		500°F		750°F				1000°F				1250°F		1600°F			
1		30		31		4		5		6		7		8		9		10		11	
P,lbs	δ,in	P,lbs	δ,in	P,lbs	δ,in	P,lbs	δ,in	P,lbs	δ,in	P,lbs	δ,in	P,lbs	δ,in	P,lbs	δ,in	P,lbs	δ,in	P,lbs	δ,in	P,lbs	δ,in
6400	0.0000	6000	0.0000	5870	0.0000	7450	0.0000	7160	0.0000	7350	0.0000	4250	0.0000	4440	0.0000	1940	0.0000	325	0.0000	280	0.0000
6800	.0004	6400	.0008	6270	.0010	7750	.0006	7460	.0010	7650	.0015	4450	.0005	4640	.0010	2040	.0010	340	.0010	300	.0010
7570	.0020	6800	.0016	6500	.0020	8050	.0008	7740	.0020	7860	.0020	4650	.0010	4880	.0020	2090	.0020	370	.0020	330	.0020
7600	.0024	7050	.0020	6670	.0030	8350	.0012	8060	.0050	7950	.0035	4850	.0015	5040	.0060	2140	.0030	385	.0055	360	.0050
8000	.0046	7200	.0026	7070	.0060	8650	.0018	8360	.0085	8250	.0070	5030	.0020	5240	.0135	2240	.0125	400	.0110	380	.0105
8400	.0076	7600	.0040	7470	.0104	8700	.0020	8660	.0140	8550	.0120	5250	.0045	5440	.0220	2340	.0390	415	.0245	400	.0210
8800	.0124	8000	.0074	7870	.0150	8950	.0032	8960	.0215	9150	.0280	5450	.0055	5640	.0345	2440	.1200	430	.0375	420	.0370
9200	.0212	8400	.0130	8270	.0210	9250	.0042	9260	.0280	9450	.0385	5650	.0080	5840	.0485	2460	.1750	445	.0575	440	.0565
9350(1)	.0270	8800	.0190	8670	.0280	9550	.0064	9560	.0400	9750	.0500	5850	.0120	6040	.0750			460	.0870	460	.0805
8800	.0280	9200	.0264	9070	.0350	9850	.0104	9860	.0525	10000	.0595	6050	.0185	6240	.1350			475	.1475	480	.1160
9200	.0294	9600	.0334	9470	.0430	10000(2)	.0124	10000(2)	.0610			6250	.0450	6120	.1670			490	.2125	500	.1575
9350	.0300	10000(2)	.0406	9870	.0520	9000	.0128					6650	.0950							508	.2060
9600	.0316	9500	.0416	10000(2)	.0540	9500	.0132					6400	.1300								
10000(2)	.0360	10000	.0436	9000	.0548	10000	.0140					Ao=0.1004in^2		Ao=0.1005in^2		Ao=0.1004in^2		Ao=0.1002in^2		Ao=0.1005in^2	
9540	.0366	10500	.0550	9500	.0558	10500	.0198														
9940	.0380	11000	.0666	1000	.0592	11000	.0306														
10440	.0472	12400	.1076	10500	.0690	12000	.0654														
10940	.0586			11000	.0812	14700	.1984														
11440	.0720			11500	.0954																
11940	.0852			11900	.1088																
1370	.1580			12000	.1270																
13700	.1730																				
Ao 0.1005in^2		Ao 0.1001in^2		Ao=0.1003in^2		Ao=0.1005in^2		Ao=0.1002in^2		Ao 0.1005in^2											

(1) Grip broke
(2) Limit of compression fixture

Gage length = 1.0 inch (as-machined) = effective gage length

δ = plastic compression measured on the load-deflection (E-M Ext) curve.

Table C-4. Tension Creep Data on Cu Be

Spec. No.	12	13	14	33	16	17	18	19	20
Gage Length, Lo., in*	2.0	2.0	2.0	2.0	2.0	2.0	2.0	2.0	2.0
Cross Section Area Ao., in^2	0.2003	0.1993	0.2010	0.0999	0.1003	0.1004	0.2002	0.2004	0.1999
Applied Load, P., Lbs.	16016	12950	12060	2248	4012	3012	320	421	240
Initial Stress, P/Ao, KSI	70.8	65.0	60.0	22.5	40.0	30.0	1.60	2.10	1.20
Test Temp., ^oF	500	500	500	1000	1000	1000	1600	1600	1600
Time, minute	δ = Plastic Elongation, in								
0	0.0061	0.0041	0.0003	0.0001	0.0015	0.0003	0.0000	0.0039	0.0000
1	.0074	.0047	.0005	.0005	.0044	.0009	.0041	.0080	.0015
2	.0079	.0049	.0006	.0008	.0059	.0014	.0058	.0112	.0020
3	.0083	.0050	.0007	.0011	Broke at 2.4 min	.0017	.0071	.0140	.0025
6	.0090	.0052	.0008	.0015		.0027	.0111	.0254	.0039
12	.0092	.0053	.0008	.0020		.0042	.0192	.0511	.0061
18	.0110	.0055	.0009	.0024		.0057	.0270	.0766	.0079
24	Broke in threads at 18.5 min	Broke in threads at 22.0 min	.0009	.0027	.00	.0073	.0348	.1065	.0095
30			.0009	.0030		.0091	.0429	.1433	.0111
36			.0009	.0033		.0106	.0515	.1877	.0130
42			.0009	.0035		.0128	.0608	.2327	.0146
48			.0009	.0037		.0174	.0696	.2776	.0161
54			Broke in threads at 51.5 min	.0039		Broke at 49 min.	.0790	.3256	.0180
60				.0041			.0882	.3994	.0196

* Gage Length = 2.0 inches (as-machined) = 2.5 inches effective gage length

Table C-5. Compression Creep Data on Beryllium Copper

Spec. No.	12	13	14	15	16	20	17	19	32
Gage Length, Lo., in.	1.0034	1.0043	1.0037	1.0045	1.0032	1.0040	1.0035	1.0030	1.0040
Cross Section Area, Ao., in^2	0.1005	0.1004	0.1003	0.1000	0.1004	0.1003	0.1004	0.1003	0.1004
Applied Load, P., Lbs.	7115	6526	7522	4000	3012	3510	1205	2106	1606
Initial Stress, P/Ao, KSI	70.80	65.00	75.00	40.00	30.00	35.00	1.20	2.10	1.60
Test Temp., ^oF	500	500	500	1000	1000	1000	1600	1600	1600
Time, minute	δ = Plastic Compression, in.								
0	0.0000	0.0000	0.0005	0.0000	0.0000	0.0000	0.0000	0.0010	0.0000
1	.0009	.0005	.0010	.0026	.0011	.0010	.0017	.0060	.0037
3	.0013	.0012	.0015	.0044	.0017	.0016	.0035	.0121	.0079
6	.0016	.0014	.0022	.0057	.0027	.0022	.0047	.0205	.0136
12	.0020	.0016	.0032	.0085	.0040	.0041	.0067	.0350	.0235
18	.0023	.0016	.0037	.0120	.0041	.0051	.0084	.0463	.0316
24	.0025	.0016	.0041	.0156	.0041	.0053	.0103	.0555	.0395
30	.0026	.0016	.0043	.0197	.0039	.0054	.0120	.0638	.0476
36	.0026	.0016	.0045	.0245	.0040	.0056	.0128	.0715	.0554
42	.0026	.0016	.0045	.0287	.0048	.0059	.0129	.0791	.0630
48	.0027	.0016	.0045	.0328	.0055	.0063	.0138	.0860	.0703
54	.0027	.0016	.0046	.0373	.0069	.0069	.0144	.0929	.0772
60	.0027	.0016	.0046	.0407	.0073	.0078	.0156	.0994	.0835

Gage Length = 1.0 inch (as-machined) = effective gage length

Table C-6. Tension Stress Relaxation Data on Beryllium Copper

Spec. No.	21	22	23	24	25	26	27	28	29
Gage Length, Lo., in. *	2.0	2.0	2.0	2.0	2.0	2.0	2.0	2.0	2.0
Cross Section Area, in^2	0.1000	0.1003	0.1005	.1000	0.1004	0.1003	0.2008	0.2006	0.2004
Initial Stress, P/Ao KSI	70.80	65.00	60.00	40.00	30.00	22.70	2.11	1.65	0.62
Test Temp., °F	500	500	500	1000	1000	1000	1600	1600	1600
Time, minute	Tensil Stress, KSI, P/A_o								
0	70.80	65.00	60.00	40.00	30.00	22.70	2.11	1.65	0.62
1				Broke at 1.2 min 37.8 KSI			1.25	1.08	.42
3							1.04	.87	.38
6	68.60_T	64.00	58.90		27.90	20.80	.90	.74	.37
12	68.10	63.80	58.60		27.50	19.20	.75	.61	.29
18	67.70	63.50	58.00		27.20	18.70	.65	.53	.28
24	67.50	63.20	57.90		26.80	18.20	.58	.49	.26
30	67.20	63.10	57.90		26.50	18.00	.54	.46	.23
36	66.80	62.90	57.90		26.20	17.80	.50	.44	.21
42	66.70	62.80	57.90		25.90	17.50	.48	.42	.19
48	66.40	62.70	57.90		25.40	17.30	.46	.40	.18
54	66.30	62.50	57.90		25.10	17.10	.45	.38	.18
60	66.20	62.50	57.90		24.80	17.00	.45	.35	.17

* Gage Length = 2.0 inches (as-machined) = 2.5 inches effective gage length

Table C-7. Compression Stress Relaxation Data on Beryllium Copper

Spec No.	21	22	23	24	25	26	27	28	29
Gage Length, Lo., in.	1.0040	1.0034	1.0034	1.0031	1.0031	1.0045	1.0040	1.0031	1.0031
Cross Section Area, Ao., in^2	0.1001	0.1003	0.1004	0.1001	0.1003	0.1003	0.1002	0.1004	0.1004
Initial Stress, P.Ao. KSI	64.97	54.00	75.00	40.00	30.00	35.00	2.092	1.600	1.227
Test Temp., °F	500	500	500	1000	1000	1000	1600	1600	1600
Time, minute	Compression Stress, KSI, P/A_o								
0	64.97	54.00	75.00	40.00	30.00	35.00	2.092	1.600	1.227
1							1.310	.953	.805
3							1.090	.815	.702
6	63.72	54.00	72.30	37.80	27.50	32.20	.975	.718	.628
12	63.47	54.00	71.80	37.50	26.80	31.00	.865	.625	.560
18	63.14	54.00	71.40	37.00	26.50	30.30	.800	.578	.505
24	62.89	54.00	71.40	36.50	26.00	29.80	.740	.548	.472
30	62.64	54.00	71.40	36.00	25.50	29.20	.710	.518	.438
36	62.31	54.00	71.40	35.80	24.90	29.00	.690	.498	.425
42	62.14	54.00	71.40	35.00	24.50	28.80	.676	.482	.412
48	62.14	54.00	71.40	34.80	24.20	28.50	.670	.475	.400
54	62.14	54.00	71.40	34.60	23.90	28.30	.670	.475	.392
60	62.14	54.00	71.40	34.40	23.50	28.20	.670	.475	.380

Gage Length = 1.0 inch (as-machined)

Table C-8. Elastic Property Data for Beryllium-Copper Alloy No. 10

	R.T.			250°F			500°F			750°F			1000°F			1250°F			1600°F		
	E	G	ν	E	G	ν	E	G	ν	E	G	ν	E	G	ν	E	G	ν	E	G	ν
Dynamic	16.8	6.1	.38	16.9	6.1	.38	16.7	6.1	.38	15.9	5.8	.37	14.2	5.2	.32	14.1	5.2	.32	12.5	4.6	.36
Tension																					
Pt SG (No. 9)	17.2		.22	16.1		.23	14.8		.23	13.8		.25	11.3		.28	9.9		.33			
A7 SG	19.5																				
E-M Ext (No. 9)	13.8			14.1			12.6			11.3			9.3			6.4					
(GL 2.0")																					
E-M Ext (CSR)	18.1 19.0			18.0			12.6			12.6			12.3			9.8			7.0		
(GL = 2.5")	15.7 16.7						17.1									11.9			5.2		
	17.8 17.9																				
	18.6 18.3																				
	16.5 16.3																				
Compression																					
Pt SG (No. 2)	14.9		.31	13.6		.30	11.7		.24	10.2		.24									
A7 SG(No. 7)	20.9																				
A7 SG(No. 8)	20.4																				
E-M Ext (No. 2)							14.5			13.9			12.8								
(GL 1.0")																					
E-M Ext (CSR)	14.4 14.8			15.0			13.5			11.9			10.5			7.3			3.9		
(GL 1.0")	15.1 14.4									12.3			12.5						4.1		
	14.0 15.1																				
(No. 7 & 8)	15.7 13.8																				
(GL = 1.0")	15.9 12.5																				
	10.2																				

Table D-1. Machine Relaxation in Tension

Time, Min	Room Temp. Load, lbs.			500°F Load, lbs.			1000°F Load, lbs.			1600°F Load, lbs.		
0	3000	2000	1000	2400	1400	3000	1200	1000	800	240	220	200
1	2970	1960	990	2370	1370	2970	1190	970	780	230	210	180
2	2960	1960	990	2360	1365	2960	1180	970	780	220	200	180
3	2960	1960	990	2360	1365	2960	1180	970	730	220	200	170
6	2960	1960	990	2360	1365	2960	1180	970	780	220	200	160
12	2960	1960	990	2360	1365	2960	1180	970	780	200	180	150
18	2960	1960	990	2360	1365	2960	1180	970	780	190	170	140
24	2960	1960	990	2360	1365	2960	1180	970	780	180	160	140
30	2960	1960	990	2360	1365	2960	1180	970	780	170	150	130
36	2960	1960	990	2360	1365	2960	1180	970	780	170	140	120
42	2960	1960	990	2360	1365	2960	1180	970	730	170	140	120
48	2960	1960	990	2360	1365	2960	1180	970	780	170	140	120
54	2960	1960	990	2360	1365	2960	1180	970	780	170	140	120
60	2960	1960	990	2360	1365	2960	1180	970	780	170	140	120

Table D-2. Machine Relaxation in Compression

Time, min.	500°F Load, lbs.	1000°F Load, lbs.	1600°F Load, lbs.
0	7000	4000	210
1	7000	4000	204
2	7000	4000	202
3	7000	4000	200
6	7000	4000	199
12	7000	4000	199
18	7000	4000	199
24	7000	4000	199
30	7000	4000	199
36	7000	4000	199
42	7000	4000	199
48	7000	4000	199
54	7000	4000	199
60	7000	4000	199

APPENDIX V

CALCULATION OF TRUE STRESSES AND TRUE STRAINS

APPENDIX V

CALCULATION OF TRUE STRESSES AND TRUE STRAINS

Conventional engineering stress and strain are based on initial cross sectional area A_o and gage length, L_o, whereas true stress and true strain are based on the actual or instantaneous values of A and L. Now at small strains, say, less than 1-2%, the magnitude of the difference between engineering and true values of stress and strain are quite small, and generally considered to be insignificant. At larger strains, say, greater than 1-2%, the elastic component is small compared to the plastic component, and hence can be neglected. Since plastic deformation occurs at constant volume, at least to an approximation which is excellent in terms of stress analysis, we can calculate true stress and strain from the engineering values. (This is equivalent to assuming that the material is incompressible, which is equivalent to assuming that Poisson's ratio is 1/2. Usually, by the time the strain reaches 1-2%, Poisson's ratio will have changed from its elastic value to the fully plastic value of 1/2.) The calculations proceed as follows:

P	=	load
A_o	=	initial area
A	=	actual area
L_o	=	initial (effective) length
L	=	instantaneous (effective) length
V	=	volume = constant = $A_oL_o = AL$ . . . for plastic flow
δ	=	plastic elongation

Engineering stress $\equiv \sigma = P/A_o$

$$\text{Engineering strain} \equiv e = \frac{L - L_o}{L_o} = \frac{\Delta L^*}{L_o} = \frac{L}{L_o} - 1$$

---

* ΔL (total elongation) $= \Delta L_{elastic} + \Delta L_{plastic} = \frac{\sigma}{E} L_o + \delta$

True stress* $\equiv \sigma_t = \frac{P}{A} = \frac{P}{\frac{A_o L_o}{L}} = \frac{P}{A_o} \frac{L}{L_o} = \sigma (1 + e)$

True strain** $\equiv \epsilon = \ln \frac{L}{L_o} = \ln (1 + e)$

These calculations are good so long as the deformation is uniform. Thus, they are good out to the point of instability, i.e., out to the maximum load in tension tests and out to the onset of barrelling in compression tests.

Note that the above definitions of true stress and strain are always correct, i.e., the true values, even in the elastic range. Again, at small strains the difference between true and engineering values (ficticuous values based on constant A_o and L_o) are insignificant and at larger strains the true values can be calculated assuming constant volume deformation with an accuracy exceeding what is required for stress analysis in the elastic-plastic and elastic-plastic-creep regimes.

In the present test program, the quantities measured experimentally were the load P (from a load cell in series with the specimen) and deflection ΔL (from an electro-mechanical extensometer). These quantities were recorded simultaneously on an x-y plotter. The engineering stresses and strains were calculated from the P- ΔL curve and the true stresses and strains were calculated from the engineering stresses and strains.

It should be noted that the calculated true creep strains for the latter portion of the curves, particularly for copper, could be in error due to necking of the specimen.

---

* $\sigma_t = \sigma \left(1 + \frac{\sigma}{E} + \frac{\delta}{L_o}\right) = \frac{P}{A_o} \left(1 + \frac{P/A_o}{E} + \frac{\delta}{L_o}\right)$

** $\epsilon = \ln \left(1 + \frac{\sigma}{E} + \frac{\delta}{L_o}\right) = \ln \left(1 + \frac{P/A_o}{E} + \frac{\delta}{L_o}\right)$

DISTRIBUTION LIST

NASA Ames Research Center
Moffett Field, Calif. 94035
Attn: Patents and Contract Mgmt.

NASA Headquarters
Washington, D. C. 20546
Attn: Contracting Officer (1)
Patent Office (1)

NASA Lewis Research Center
21000 Brookpark Road
Cleveland, Ohio 44135
Attn: Office of Technical Information (1)

NASA Manned Spacecraft Center
Houston, Texas 77058
Attn: Office of Technical Information (1)

NASA Marshall Space Flight Center
Huntsville, Alabama 35812
Attn: Office of Tech. Information, MS-IP (2)
Technical Library (1)
Dale Burrows, S&E-ASTN-PJ (1)
Tech. Utilization Office, MS-T (1)

Jet Propulsion Laboratory
4800 Oak Grove Dr.
Pasadena, Calif. 91103
Attn: W. B. Powell (4)
Mgr., Liquid Rocket Propulsion
Tech., Code RPT (3)

Mgr., Space Storable Propulsion
Tech., Code RPI (1)
Office of R&D

NASA Headquarters
Washington, D. C. 20546
Attn: Director, Tech. Util. Div. (1)

NASA Scientific & Tech. Infor. Facility
P. O. Box 33
College Park, Maryland 20740 (25)

Office of Space Science & Applications
NASA Headquarters
Washington, D. C. 20546
Attn: Director, Launch Vehicles & Propulsion, SV (1)

Ames Research Center
Moffett Field, Calif. 94035
Attn: Hans M. Mark (2)

Goddard Space Flight Center
Greenbelt, Maryland 20771
Attn: Merland L. Moseson, Code 620 (1)

Jet Propulsion Laboratory
California Institute of Technology
4800 Oak Grove Dr.
Pasadena, Calif. 91103
Attn: Henry Burlage, Jr.
Propulsion Div. 38 (2)

John F. Kennedy Space Center, NASA
Cocoa Beach, Florida 32931
Attn: Dr. Kurt H. Debus (2)

Langley Research Center
Langley Station
Hampton, Virginia 23365
Attn: Ed Cortwright, Director (2)

Lewis Research Center
21000 Brookpark Road
Cleveland, Ohio 44135
Attn: Bruce Ludin, Director (1)
H. Douglass (1)
Gary Halford (1)

Marshall Space Flight Center
Huntsville Alabama 35812
Attn: Hans G. Paul, Code R-P+VED (2)

Manned Spacecraft Center
Houston, Texas 77058
Attn: J. G. Thibodaux, Jr.,
Chief, Prop. + Power Div. (1)
H. Pohl, (1)
Charles Yodzis, (1)

Headquarters, U. S. Air Force
Washington, D. C. 20546
Attn: Col. C. K. Stambaugh, AFRST (1)
Alan Eaffey (1)

Arnold Engineering Development Center
Arnold Air Force Station
Tullahoma, Tenn. 37388
Attn: Dr. H. K. Doetsch (1)

Air Force Rocket Propulsion Laboratory
Research & Technology Div.
Air Force Systems Command
Edwards, Calif. 93523
Attn: RPRPD/H. Main (1)
F. Forbes, FTRPL (1)
D. Penn, LKCE, (1)

Air Force Missile Test Center
Holloman Air Force Base, N.M. 45433
Attn: Library (1)

Air Force Missile Test Center
Patrick Air Force Base, Florida
Attn: L. J. Ullian (1)

Aeronautical Systems Div.
Air Force Systems Command
Wright Patterson Air Force Base
Dayton, Ohio 45433
Attn: D. L. Schmidt Code ASRCNC-2 (1)

Space & Missile Systems Organization
Air Force Unit Post Office
Los Angeles, Calif. 90045
Attn: Col. Clark, Tech. Data Center (1)

Defense Documentation Center Headquarters
Cameron Station, Bldg. 5
5010 Duke Street
Alexandria, Virginia 22314
Attn: TISIA (1)

Bureau of Naval Weapons
Dept. of the Navy
Washington, D. C. 20546
Attn: J. Kay, RIMS-41 (1)

U. S. Naval Ordnance Test Station
China Lake, Calif. 93557
Attn: Code 4562, Chief, Missile Propulsion Div. (1)

Picatinny Arsenal
Dover, N. J. 07801
Attn: I. Forsten, Chief, Liquid Propulsion Lab. (1)

Chemical Propulsion Information Agency
Applied Physics Lab.
8621 Georgia Ave.
Silver Spring, Maryland 20910
Attn: Tom Reedy (1)

Aerojet Liquid Rocket Co.
P. O. Box 13222
Sacramento, Calif. 95813
Attn: Dave Kors (1)

Aerojet General Corporation
P. O. Box 1947
Tech. Library, Bldg. 2015, Dept. 2410
Sacramento, Calif. 95809
Attn: R. Stiff

Aerojet General Corp.
Space Div.
9200 East Flair Dr.
El Monte, Calif. 91734
Attn: S. Machlawski

Aerospace Corp.
2400 East El Segundo Blvd.
P. O. Box 95085
Los Angeles, Calif. 90045
Attn: John G. Wilder, MS 2293 (1)

Beech Aircraft Corp.
Boulder Div.
Box 631
Boulder, Colorado
Attn: J. H. Rodgers (1)

Bell Aerosystems Company
P. O. Box 1
Buffalo, N. Y. 14240
Attn: W. M. Smith (1)

Bellcomm
955 L-Enfant Plaza, S.W.
Washington, D. C.
Attn: H. S. London (1)

Bendix Systems Div.
Bendix Corp.
3300 Plymouth Road
Ann Arbor, Mich. 48105
Attn: John M. Brueger (1)

Boeing Co.
P. O. Box 3999
Seattle, Wash. 98124
Attn: Library (1)

Boeing Company
1625 K Street N. W.
Washington, D. C. 20006
Attn: Library (1)

Boeing Company
P. O. Box 1680
Huntsville, Alabama 35801
Attn: Ted Snow (1)

Missile Div.
Chrysler Corp.
P. O. Box 2628
Detroit, Mich. 48231
Attn: John Gates (1)

Wright Aeronautical Div.
Curtiss-Wright Corp.
Wood Ridge, N. J. 07075
Attn: G. Kelley (1)

Research Center
Fairchild Hiller Corp.
Germantown, Maryland
Attn: Ralph Hall (1)

Republic Aviation Corp.
Fairchild Hiller Corp.
Farmingdale, L. I., N.Y.
Attn: Library (1)

General Dynamics, Convair Div.
P. O. Box 1128
San Diego, Calif.
Attn: Library (1)

Missile & Space Systems Center
General Electric Co.
Valley Forge Space Technology Center
P. O. Box 8555
Philadelphia, Pa.
Attn: F. Mezger/F. E. Schultz (1)

Grumman Aircraft Engineering Corp.
Bethpage, L. I., N.Y. 11714
Attn: Joseph Gavin (1)

Huges Aircraft Co.
Aerospace Group
Centinela and Teale Streets
Culver City, Calif. 90230
Attn: E. H. Meier, V.P. & Div. Mgr.
Research and Dev. Div. (1)

Walter Kidde and Co., Inc.
Aerospace Operations
567 Main Street
Belleville, N. J.
Attn: R. J. Hanville, Dir.
Research Engr. (1)

Ling-Temco-Vought Corp.
P. O. Box 5907
Dallas, Texas 75222
Attn: Library (1)

Arthur D. Little, Inc.
20 Acorn Park
Cambridge, Mass. 02140
Attn: Library

Lockheed Missiles and Space Co.
Attn: Technical Infor. Center
P. O. Box 504
Sunnyvale, Calif. 94088
Attn: J. Guill (1)

Lockheed Propulsion Co.
P. O. Box 111
Redlands, Calif. 92374
Attn: Library (1)

The Marquardt Corp.
16555 Saticoy Street
Van Nuys, Calif. 91409
Attn: Library

Baltimore Div.
Martin Marietta Corp.
Baltimore, Maryland 21203
Attn: Mr. John Calathes (3214) (1)

Denver Div.
Martin Marietta Corp.
P. O. Box 179
Denver, Colorado 80201
Attn: Dr. Morganthaler/A. J. Kullas (1)

Orlando Div.
Martin Marietta Corp.
Box 5837
Orlando, Florida
Attn: J. Ferm (1)

McDonnell Douglas Corp.
P. O. Box 516
Municipal Airport
St. Louis, Missouri 63166
Attn: R. A. Herzmark (1)

Space & Information Systems Div.
North American Rockwell
12114 Lakewood Blvd.
Downey, Calif. 90241
Attn: Library (1)

Rocketdyne (Library 586-306) (2)
6633 Canoga Ave.
Canoga Park, Calif. 91304
Attn: Dr. R. J. Thompson
S. F. Iacobellis
Jack Lewis

Northrop Space Laboratories
3401 West Broadway
Hawthorne, Calif. 90250
Attn: Dr. Wm. Howard (1)

Aeroneutronic Corp.
Philco Corp.
Ford Road
Newport Beach, Calif. 92663
Attn: Library

Rocket Research
York Center
Redmond, Washington 98052
Attn: F. McCullough, Jr. (1)

Scientific Service Bureau Inc.
P. O. Box 375
Morrisplains, N. J. 07950
Attn: T. F. Seamans

Stanford Research Institute
333 Ravenswood Ave.
Menlo Park, Calif. 94025
Attn: Dr. Gerald Marksman (1)

Sunstrand Aviation
2421 11th St.
Rockford, Illinois 61101
Attn: R. W. Reynolds (1)

TRW Systems Group
TRW Inc.
One Space Park
Redondo Beach, Calif. 90278
Attn: G. W. Flverum (2)

TAPCO Div.
23555 Euclid Ave.
Cleveland, Ohio 44117
Attn: P. T. Angell (1)

Research Laboratories
United Aircraft Corp.
400 Main St.
East Hartford, Conn. 06108
Attn: Erle Martin (1)

United Technology Center
587 Methilda Ave.
P. O. Box 358
Sunnyvale, Calif. 94088
Attn: Dr. David Altman (1)

Florida Research & Development
Pratt & Whitney Aircraft
United Aircraft Corp.
P. O. Box 2691
West Palm Beach, Florida 33402
Att: R. J. Coar (1)